
Masters Theses

Student Theses and Dissertations

1969

Thermal fatigue testing of die casting die steels

Kulwant Singh Sabharwal

Follow this and additional works at: https://scholarsmine.mst.edu/masters_theses



Part of the [Metallurgy Commons](#)

Department:

Recommended Citation

Sabharwal, Kulwant Singh, "Thermal fatigue testing of die casting die steels" (1969). *Masters Theses*. 6967.

https://scholarsmine.mst.edu/masters_theses/6967

This thesis is brought to you by Scholars' Mine, a service of the Missouri S&T Library and Learning Resources. This work is protected by U. S. Copyright Law. Unauthorized use including reproduction for redistribution requires the permission of the copyright holder. For more information, please contact scholarsmine@mst.edu.

THERMAL FATIGUE TESTING OF
DIE CASTING DIE STEELS

BY

2248

KULWANT SINGH SABHARWAL, 1944 -

A

THESIS

submitted to the faculty of

THE UNIVERSITY OF MISSOURI - ROLLA

in partial fulfillment of the requirements for the

Degree of

MASTER OF SCIENCE IN METALLURGICAL ENGINEERING

Rolla, Missouri

1969

T2301

c. I

145 pages

183271

Approved by

183271

Carl V. Wall

(Advisor)

J. B. Remington

Fred Kissinger

ABSTRACT

Thermal fatigue is a form of surface failure produced by repeated thermal stresses and is the main cause of die retirement in the die casting industry. A general review of the fundamental and practical aspects of thermal fatigue as encountered in the dies, based on earlier published work, is given and preliminary experiments in an effort to set up a suitable method of testing to study this phenomenon are then described.

In the present technique developed to create the thermal conditions experienced by a die steel in aluminum die casting, a small portion of one face of a cylindrical test-piece is intermittantly heated by H.F. induction whilst the main body of the test-piece is kept at a lower temperature by means of a copper jig. Air under pressure is used as a cooling medium during the cooling part of the cycle. Thermal fatigue resistance of various die steels and prospective die materials for aluminum die casting is determined on the basis of number of cycles for crack initiation, propagation, frequency and severity of cracking supported by graphs and series of photographs. Photographic evidence presented gives a detailed look into the mechanism of thermal fatigue.

Present investigations reveal that 18% nickel maraging steel is the most suitable steel for aluminum die casting dies, followed by H-21, H-13 and H-11 respectively.

ACKNOWLEDGEMENT

The author wishes to express his gratitude to Professor R.V. Wolf for his faithful guidance and assistance throughout this research.

The author is greatly indebted for financial assistance to Rotary International and University of Missouri - Rolla, without which this work could not be pursued.

The author wishes to acknowledge sincere thanks to the following steel companies for supplying the die steels and related information for the present investigation:

1. Ladish Company
2. The Carpenter Steel Company
3. Latrobe Steel Company
4. Universal-Cyclops Steel Corporation

Thanks to the various members of the faculty for their help and suggestions from time to time during the course of the investigation.

TABLE OF CONTENTS

	PAGE
LIST OF FIGURES	vii
LIST OF TABLES	xi
I. INTRODUCTION	1
II. REVIEW OF LITERATURE	4
A. Types of Die Failure	4
B. Mechanism of Thermal Fatigue	5
C. Die Temperatures	8
D. Thermal Stresses	10
E. Appearance of Thermal Fatigue Cracks	12
F. Physical and Mechanical Properties Affecting Thermal Fatigue	15
G. Methods of Thermal Fatigue Evaluation	17
III. EXPERIMENTAL PROCEDURE	30
A. Selection of Steels Used	30
1. AISI 4340 H	31
2. Ladish D-11	31
3. AISI H-11 and H-13	32
4. AISI H-21	33
5. Maraging Steel	35
B. Preliminary Experiments	40
C. Present Experimental Methods	43
1. Test-piece and Inductor	43
2. Cooling Arrangement	44
3. Temperature Measurement	47
4. Heat Treatment	51

	PAGE
5. Heating and Cooling Cycling	52
6. Experimental Procedure	58
IV. EXPERIMENTAL RESULTS AND DISCUSSION	60
A. Observations and Results on 4340 Steel	60
1. Heat Treatment	60
2. Hardness	60
3. Thermal Cycling	60
4. Results	60
5. Discussion of Results	61
B. Ladish D-11 Steel	68
1. Heat Treatment	68
2. Hardness	68
3. Thermal Cycling	68
4. Results	68
5. Discussion of Results	70
C. H-11 Die Steel	79
1. Heat Treatment	79
2. Hardness	79
3. Thermal Cycling	79
4. Results	80
5. Discussion of Results	81
D. H-13 Die Steel	87
1. Heat Treatment	87
2. Hardness	87
3. Thermal Cycling	87

	PAGE
4. Results	90
5. Discussion of Results	90
E. H-21 Die Steel	98
1. Heat Treatment	98
2. Hardness	98
3. Thermal Cycling	98
4. Results	98
5. Discussion of Results	100
F. Maraging Steel	104
1. Heat Treatment	104
2. Hardness	109
3. Thermal Cycling	109
4. Results	109
5. Discussion of Results	110
G. Some General Features of Cracks Observed . .	117
V. CONCLUSIONS	124
VI. SUGGESTED FURTHER RESEARCH	131
VII. BIBLIOGRAPHY	132
VIII. VITA	134

LIST OF FIGURES

FIGURES	PAGE
1. Die exposure to molten metal	7
2a. Diagram of simplified die-casting die	9
2b. Temperatures of points A,B,C,D and E in die as Fig. 2a with continuous feeding	9
2c. Temperatures of points A,B,C,D and E in die as Fig. 2a with metal fed at regular time intervals	9
3a. Thermo-element used by Mickel	11
3b. Positions 1-5 of thermocouples in Mickel's die	11
3c. Changes in temperatures at points 1-5 (Fig. 3b) during the die casting process	11
4a. Large heat checks in aluminum die casting die	13
4b. Severe heat checking in H-21 die after 3000 brass casting cycles.	13
4c. The start of a heat check or narrow pit in a die.	13
5. Test-pieces and inductors used in preliminary experiments by Northcott and Baron	24
6. Appearance of macrocracks due to thermal fatigue in En 25 steel	26
7. Influence of maximum temperature and no. of cycles on depth of cracks	27
8. Thermal fatigue of medium carbon steel	28
9. Appearance of microstructure and a thermal fatigue crack in En 25 steel	28
10. Tempering temperature vs hardness data for various steels	34
11. Comparative oxidation resistance of H-13 die steel and maraging steels at 1000°F	38
12. Arrangement of the test-piece and inductor used in present investigation	46

FIGURES	PAGE
13a. Temperature profile in radial direction of the test-piece	50
13b. Temperature profile in axial direction of the test-piece	50
14. Apparatus setup for thermal fatigue testing of die steels	54
15. Induction heating and air cooling cycle for thermal fatigue of die steels	56
16. Heat affected pattern on a thermal fatigued specimen of 4340 steel after 100 cycles, in air, top face	57
17. Oxide scale and cracks formed on the side of the cylindrical test-piece of 4340 steel, in air, after 1200 cycles	62
18. An oxide filled thermal fatigue crack in 4340 steel after 900 cycles	63
19. Stress raising effect of a thermocouple hole only 0.04 inch below the top surface; 4340 steel, 400 cycles	63
20. Sequence of crack propagation in 4340 steel, in air, 250-670°C	64
21. Propagation of the longest crack with thermal cycling in AISI 4340 steel	67
22. Crack propagation in Ladish D-11 steel samples of hardness Rc 48	71
23. Crack propagation in Ladish D-11 steel samples of hardness Rc 40	72
24. Propagation of the longest crack with thermal cycling in Ladish D-11 steel samples of hardness Rc 48 and 40	74
25. Cumulative number of cracks vs crack length at different stages of thermal cycling in Ladish D-11 samples of hardness Rc 48	76
26. Cumulative number of cracks vs crack length at different stages of thermal cycling in Ladish D-11 samples of hardness Rc 40	78

FIGURES	PAGE
27a. A thin, adherent oxide film formed in H-11 after 1200 cycles	82
27b. Brittle oxide scale and cracking in 4340 steel after 800 cycles	82
28. (a) Initiation of a microcrack; (b) propagation of microcrack; (c) large macrocrack formed in H-11. Note the sharp tip of crack in (a)-(c). All these photographs are of the same crack after different number of cycles	83
29. Propagation of thermal fatigue cracks with further cycling in H-11	84
30. Propagation of the longest crack with thermal cycling in AISI H-11 steel	86
31. Cumulative number of cracks vs crack length at different stages of thermal cycling in AISI H-11 steel	89
32. (a) Initiation of a microcrack; (b) propagation of the microcrack; (c) a large macrocrack formation and its branching at an impurity or an inclusion	91
33. A sequence of crack initiation and propagation on macroscale in H-13	93
34. Propagation of the longest crack with thermal cycling in AISI H-13 steel	95
35. Cumulative number of cracks vs crack length at different stages of thermal cycling in AISI H-13 steel	97
36. (a)-(c) Crack-like streaks are formed in oxide film during early stages of cycling in H-21 but disappear on polishing; (d) shows the actual crack formed in the metal which propagates on further cycling as in (e)	101-2
37. Propagation of thermal fatigue cracks in H-21	103
38. Propagation of the longest crack with thermal cycling in AISI H-21 steel	106
39. Cumulative number of cracks vs crack length at different stages of thermal cycling in AISI H-21 steel	108

FIGURES	PAGE
40. (a) Initiation of microcracks near the specimen edge; (b)-(c) propagation of the same microcrack with further thermal cycling in 18% nickel maraging steel	111
41. Propagation of macrocracks with thermal cycling in maraging steel	112
42. Propagation of the longest crack with thermal cycling in 18% nickel maraging steel	114
43. Cumulative number of cracks vs crack length at different stages of thermal cycling in 18% nickel maraging steel	116
44. Two adjacent cracks propagate simultaneously and finally join together on further cycling, causing the small chunk of metal to drop off and form a pit or heating check in maraging steel	118
45. Initiation of a crack at an inclusion or an impurity, away from the specimen and its propagation in both directions with thermal cycling in H-13	120
46. Appearance of a thermal fatigue crack at different depths from the top surface in H-21 .	121
47. Microstructures of die steels after thermal cycling	122
48. Bar chart showing the comparison of number of cycles at the initiation of thermal fatigue cracking in different steels tested in the present study	127

LIST OF TABLES

TABLES	PAGE
I. COMPOSITION OF VARIOUS STEELS TESTED	30
II. PROPERTIES OF DIE STEELS TESTED BY THERMAL FATIGUE CYCLING	32
III. FATIGUE ENDURANCE LIMITS OF MARAGING STEEL COMPARED WITH H-13 DIE STEELS	36
IV. HARDNESS AND TENSILE PROPERTIES OF MARAGING STEELS COMPARED WITH CONVENTIONAL DIE STEELS .	36
V. PROPAGATION OF THE LONGEST CRACK IN 4340 STEEL .	60
VI. CRACK PROPAGATION WITH THERMAL CYCLING IN LADISH D-11 STEEL	69
VII. CRACK PROPAGATION WITH THERMAL CYCLING IN H-11 STEEL	80
VIII. CRACK PROPAGATION WITH THERMAL CYCLING IN H-13 STEEL	90
IX. CRACK PROPAGATION WITH THERMAL CYCLING IN H-21 STEEL	99
X. CRACK PROPAGATION WITH THERMAL CYCLING IN MARAGING STEEL	109

I. INTRODUCTION

The rapid modern technological developments taking place throughout industry in the twentieth century have consistently put pressure on die casters to get increasing length of runs and greater efficiency from every die casting machine. This demand for more rapid production can be achieved only by more drastic cooling of the dies coupled with a longer die life. Such severe conditions of fast cyclic heating and cooling as encountered in a die casting die, result in a die failure variously known as thermal fatigue, craze cracking or heat checking. Thus there is presently an urgent need to carry out research work in the area of thermal fatigue failure of die steels so as to get the best possible die materials.

Thermal fatigue is defined as "Fracture resulting from the presence of temperature gradients which vary with time in such a manner as to produce cyclic stresses in a structure"⁽¹⁾ It is the most frequent mode of failure encountered in die casting dies although mechanical erosion and chemical attack also contribute to the degradation of dies to some extent. In die casting, die pressures are not as high as in forging, so research is mainly concerned with the factors which influence the die materials' resistance to thermal stress for a given alloy and die temperature. The important die material properties are those that limit

surface stresses and those that resist surface stresses.

Two primary reasons for die retirement in the die casting industry are:

1. Surface imperfections in the production parts because of cracks in the die formed by thermal fatigue.
2. The catastrophic failure of the die itself because of propagation of these cracks.

The thermal fatigue resistance of a die material at the required hardness determines resistance to crack initiation and crack propagation. The crack frequency and severity determine at what production count surface roughness, and parts sticking as a result of hot metal flowing on to these cracks are sufficiently severe to cause the die to be removed from service.

Although some research work has been done about thermal fatigue testing of low alloy steels, cast iron, etc. in the past, very little work has been done about die casting die steels. The object of the present investigation was therefore to develop a suitable test equipment and procedure to study the thermal fatigue cracking obtained in die steels, and to evaluate different commercially available and the potential candidate die steels for their tendency to resist thermal fatigue.

The test method developed in this study is simple, efficient and comprehensive as it simulates the actual

service conditions encountered in die casting dies fairly closely over a wide controlled range of temperature. The procedure adopted takes a relatively short time to test a given die steel and the test conditions are uniform and reproducible. The steels selected are mainly those which are of interest to aluminum die casting industry. The author's interest in this project developed from over two years of industrial experience with aluminum die casting problems.

II. REVIEW OF LITERATURE

Theoretical and experimental investigations have been carried out by several authors in the general area of thermal fatigue failure of steels. A detailed review of the information available from the last three decades of work is as follows:

A. Types of Die Failure

There are three distinct modes of failure, though not completely independent of each other, which are mainly seen in die casting dies. They are mechanical erosion, chemical attack and thermal fatigue. However, heat checking, sometimes referred to as "fire cracking" or "craze-cracking" is the most frequent manifestation of die failure and is caused directly by thermal fatigue.

Mechanical erosion is of two types. The first is the wearing erosion caused by the abrasive action of flow of heterogeneous phases over the die surface (gas bubbles or solidified crystallites in the casting metal). The second type of erosion is caused by the cavitation of the liquid metal and the subsequent collapse of the vapor filled bubbles near the die surface.⁽²⁾ This collapse causes extremely high pressures at the die surface. The repeated surface straining causes mechanical fatigue and is additive to any thermally induced fatigue that occurs in die casting dies.

Chemical attack also manifests itself in a number of

ways; first, through compositional changes in the die surface and second, by adhesion of cast metal to the die surface. The latter is known as "soldering", which results in immediate damage to the cast part rather than to the die, since the rupture strength of the die material at its operating temperature is always much greater than that of the hot die cast part.

Compositional changes in the die alloys have the effect of degrading the strength and ductility of the die surfaces and result in accelerated thermal fatigue failure. Decarburization of steel die surfaces during heat treatment or use, and the replacement of carbon in steel with aluminum during aluminum die casting⁽³⁾ to form brittle compounds are two examples of chemical attack which lower the strength and ductility. In contrast, Williams⁽⁴⁾ et. al. found that oxidation had little if any, effect on the fatigue life of H-21 or H-23 hot work die-steels.

Another source of die failure, gross cracking, may frequently occur early in the life of the die, starting at stamp marks, changes of section or other discontinuities. It usually happens very early in the expected die life and is related to poor heat treatment or incorrect die design rather than to service conditions.

B. Mechanism of Thermal Fatigue

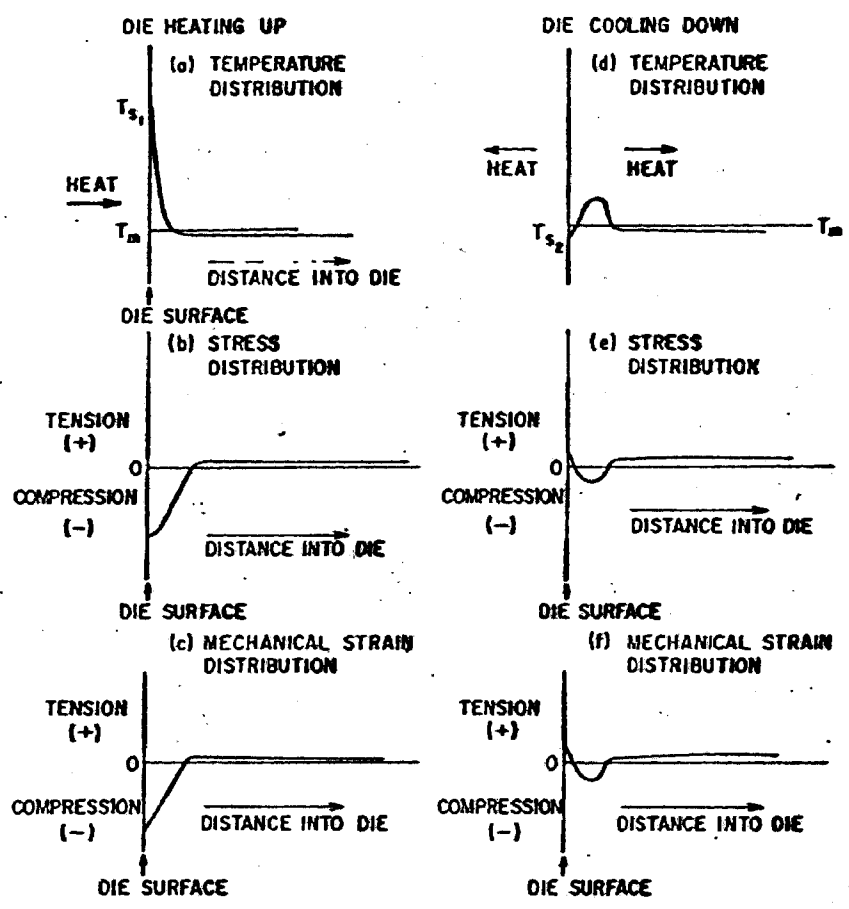
The mechanism by which die surfaces fail as a result of temperature cycling is illustrated qualitatively in

Fig. 1. (5) Each half of the cycle is portrayed by three schematic drawings. Drawings 1a through 1c show the effect of increased surface temperature on the stress and strain distribution from the surface to the interior of the die material. And drawings 1d through 1f illustrate the subsequent stress and strain conditions which exist during the second half of the casting cycle, the cooling-down half.

During heating (the injection half of the die casting cycle), the surface attempts to expand, putting it in compression with respect to the die interior, as shown in Fig. 1b. The corresponding compression strain is shown in Fig. 1c. The combination of the temperature gradient and the coefficient of thermal expansion of the die material determines the magnitude of the die surface stress.

Initially, the surface deformation strain is within the elastic capabilities of the die material. However, if the combination of the temperature gradient and the prevailing thermal expansion is high enough, the compressional stress developed will exceed the elastic limit of the die material and plastic deformation will take place after the initial elastic strain has occurred.

During cooling (the ejection half), the elevated die surface temperature T_{s1} declines and reaches some minimum value T_{s2} which varies widely with specific die casting



DIE EXPOSURE TO MOLTEN METAL
FIGURE 1

practice. Fig. 1d shows T_{s2} at a lower temperature than basic mold temperature T_m . As the surface metal cools with respect to adjacent metal further into the die block, it attempts to contract more rapidly than the warmer adjacent metal and is put in tension. If the product of temperature change and coefficient of thermal expansion (thermal strain) causes stresses larger than the elastic limit of the material in its prevalent condition, reversed plastic deformation will occur. Exceeding the elastic limit even by an infinitesimal amount will ultimately result in a fatigue failure after a sufficiently large number of cycles have occurred. (5)

C. Die Temperatures

Nicolson⁽⁶⁾ says, "Any die at work is a complex of pulsating temperature gradients." Fig. 2a shows a die in which he assumes that heat only enters at the cylindrical portion marked F, and leaves at the outer surface G, which is water cooled. If metal were poured continuously into F, points A, B, C, D and E would have temperatures as shown in Fig. 2b, and isotherms would be circular, and concentric with F. If, however, metal were injected at regular intervals, the points A, B, C, D and E would have pulsating temperatures as shown by the curves of Fig. 2c, and the maxima would occur gradually later and become less as the outside of the die was approached. Isotherms remain circular and concentric with F and may be regarded as concentric waves of decreasing amplitude as they approach G.

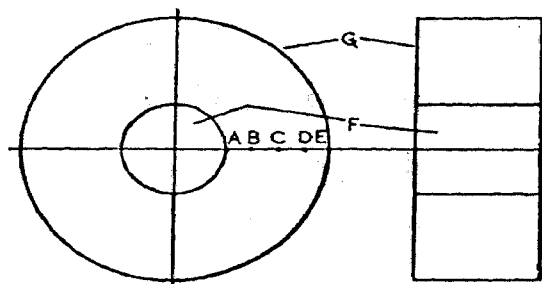


Fig. 2a-Diagram of simplified die-casting die

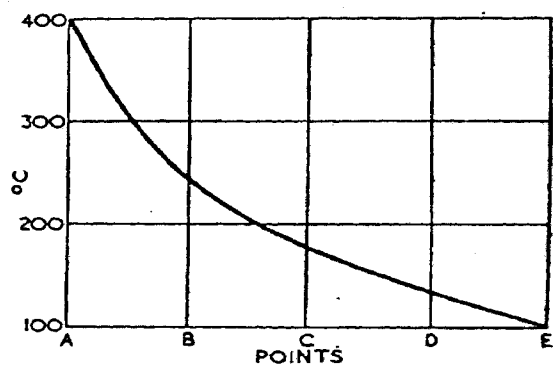


Fig. 2b-Temperatures of points A, B, C, D and E in die as Fig. 2a with continuous feeding

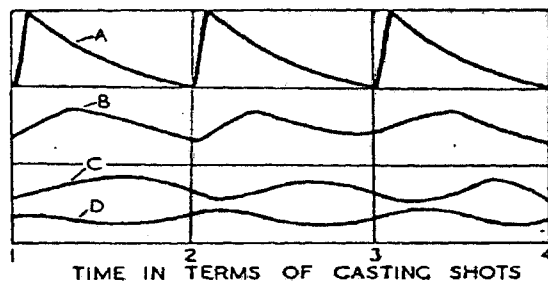


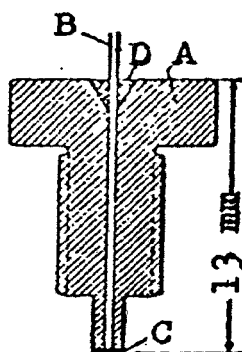
Fig. 2c-Temperatures of points A, B, C, D and E in die as Fig. 2a with metal fed at regular time intervals

In the case of an actual die the same thermal waves are obtained but, of course, the shape of the die introduces complexities.

To get a very close idea about temperature distributions in a die casting die, Mickel⁽⁷⁾ used specially designed thermo elements (Fig. 3a) and placed these at the locations shown in Fig. 3b in an actual production die. He obtained a temperature distribution of the type shown in Fig. 3c. The temperature measured at the surface of the die in some cases exceeded the casting temperature by 40 to 70°C. This temperature excess is explained by the fact that the molten metal is forced (through the relatively narrow injection gate) under a high pressure and very high speed, the frictional forces developed in the course of injection raise the temperature of both the metal and the die.

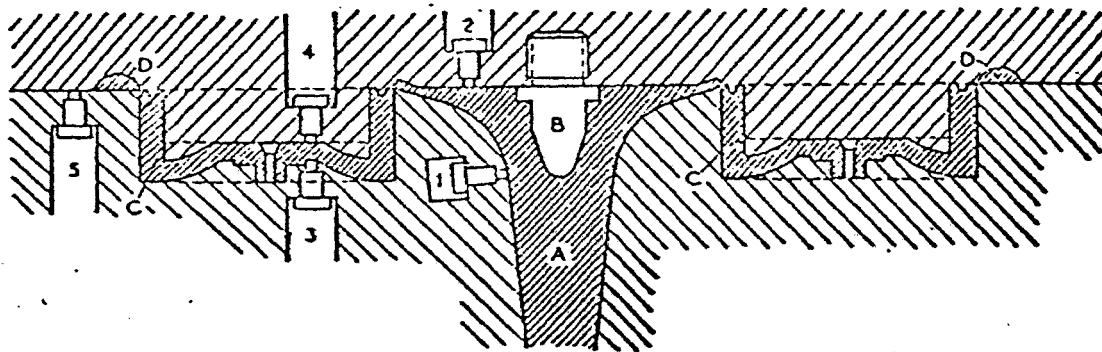
D. Thermal Stresses

The subject of thermal stresses is a very difficult one from a mathematical point of view, and it is possible to deal with it only if considerable simplifying assumptions are made. Such simplifications, however, are permissible in estimating the order of magnitude of the stresses. Mickel⁽⁷⁾ derived a formula for the stress developed after having assumed that the surface is a plane of infinite extent, the die extending to an infinite distance in a direction normal to that plane. It results in a completely balanced state of



A—Body of die-steel; B—Pure nickel wire with insulating oxide film; C—Electrodeposited pure nickel coating of $10 \pm 2\mu$ thickness; D—Insulating material

Fig. 3a-Thermo-element used by Mickel



A—Gate; B—Distributor plug; C—Casting; D—Air pocket

Fig. 3b-Positions 1-5 of thermocouples in Mickel's die

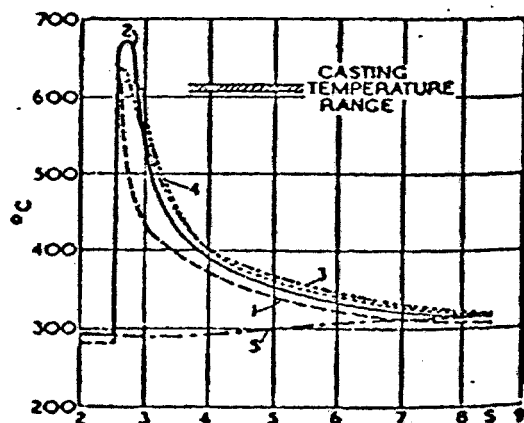


Fig. 3c-Changes in temperatures at points 1-5

(Fig. 3b) during the die-casting process

affairs with a variability only in one direction, namely, normal to the surface.

With these assumptions, he derived that the stress developed in the surface of the die is given by

$$\sigma = - \frac{m E}{m-1} \alpha (T_2 - T_1)$$

Where E = Elastic moduli

$$m = \frac{1}{\text{Poisson's Ratio}} = \frac{10}{3} \text{ for steel}$$

α = coefficient of linear thermal expansion

T_2, T_1 are the upper and lower temperature limits

If the stresses involved in raising the very thin surface layer of die steel from about 600°F, to about 1100°F are calculated, and elevated temperature properties of steel are taken into account, it is found that stresses of the order of magnitude to 100,000 psi are attained. To these must be added the casting pressures of the machine, notch effects due to die design, etc.

Since most steels have a fatigue strength in the vicinity of 100,000 to 150,000 psi, it is apparent that thermal gradients and stresses of die casting are adequate to produce thermal fatigue in the manner described.

E. Appearance of Thermal Fatigue Cracks

Roberts and Grobe⁽⁸⁾ studied a number of dies to determine the mechanisms of die failure in die casting. The dies shown in Figs. 4a-b are good examples of heat checking. The checks filled with aluminum in Fig. 4a are in marked contrast to the oxidized steel background.

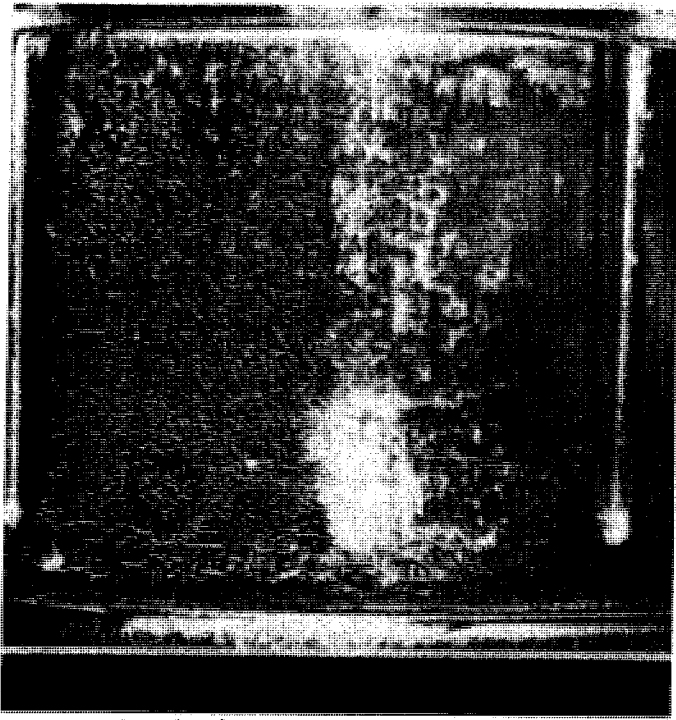


Fig. 4-(a) Large heat checks in aluminum die casting die



Fig. 4-(b) Severe heat checking in H-21 die after 3000 brass casting cycles



Fig. 4-(c) The start of a heat check or narrow pit in a die

2% Nital Etch, 500X

Micro-examination of cross sections through the heat checks and through some pits not apparent in Fig. 4a indicates that the two types of defect are due to stress-corrosion and differ only in size. The alternating stress (due to a combination of thermal and mechanical stresses) combined with the oxidizing attack of the air cause cracks to form at grain boundaries. The cracks continue to grow until a whole grain or several grains are completely cracked out. If round or oval holes are formed when the grains come out, then the defects are called heat checks. The beginning of such a heat check or pit is shown in Fig. 4c.

Roberts and Grobe further found that almost all heat checks in the die were filled with aluminum but in the metallographic examination there was no evidence of aluminum attacking, alloying with, or dissolving the die steel. In every instance there was an oxide film or an air gap which prevented direct contact between the aluminum and die steel.

Impingement soldering is another defect observed in aluminum die casting dies. It is nothing but mechanical holding of the aluminum by very small pits or scratches.⁽⁸⁾ Aluminum is not welded to the steel. The pits due to impingement soldering differ in appearance from the heat checks and result from scratching or breaking of the semi-protective oxide surface that is built up on a die when it is broken in. When the scale is broken, the steel

reoxidizes and if the cycle is repeated several times, a broad shallow pit develops.

F. Physical and Mechanical Properties Affecting Thermal Fatigue

In order to resist thermal fatigue in dies, a proper combination of certain desirable mechanical and physical properties of the die steel and the cast metal is essential. Following is a brief discussion of such properties:

1. Thermal gradient is a function of the thermal conductivity of the die material. Increased thermal conductivity will result in a lower thermal gradient and thus lower stresses and strains.
2. The combination of the temperature gradient and the coefficient of thermal expansion of the die material determines the magnitude of the die surface stress. Hence a good die material should have a low coefficient of thermal expansion.
3. To produce thermal fatigue in a metal, plastic deformation must occur cyclically, and it is only after a material has been stressed beyond its elastic limit that plastic deformation can occur. It becomes obvious therefore that a high yield strength material is desirable.
4. Increased ductility, as measured by the reduction of cross sectional area during tensile testing to failure, decreases the detrimental effect of each cycle of plastic deformation, thus lengthening

fatigue life.

5. It is desirable for a die material to have a low modulus of elasticity, since the thermally-induced strain (expansion or contraction as during die casting) will produce a minimum elastically-computed stress in the die material, all other factors being equal.
6. The physical properties of specific heat, density and melting point also have an effect on thermal fatigue life. In general, a prospective die material should have high values of each of these three physical properties.
7. The actual value of the temperatures, within limits, is less important than the difference between them, since the magnitude of the temperature change $T_{s1} - T_{s2}$ is directly related to the maximum strain that the die surface undergoes. The maximum temperature may not exceed the temperature at which the yield point of the metal is reduced to very low levels.

There are two additional physical characteristics of crystalline solids which influence thermal fatigue life. They are the presence or absence of phase transformations and crystalline isotropy. In cubic metals which are relatively isotropic, the phenomenon of anisotropy is probably unimportant. Allotropic phase transformations in die materials result in a change in contraction or expansion

in areas exposed to a sufficiently high temperature for a sufficiently long time to cause transformation; and secondly, the transformation will result in an altered metallurgical structure which changes the mechanical properties of the die material in the affected zone. A complete discussion of the phenomenon as it affects the die casting dies is outside the scope of present work. It is generally agreed that phase transformations which occur in the operating temperature range of structural parts are detrimental to the successful function of such parts. (9)

G. Methods of Thermal Fatigue Evaluation

1. Noesen and Williams (5) have developed a mathematical computer program using "Coffin's modified low cycle fatigue equation" to predict the thermal fatigue life of candidate materials. Coffin expresses the number of cycles to failure (N_f) as a function of the change in the cyclic plastic strain ($\Delta\epsilon_p$)

$$N_f^{\frac{1}{2}} = \frac{C}{\Delta\epsilon_p}$$

If $\Delta\epsilon_p = 0$, infinite die life is predicted.

It has been shown that $C = \frac{\epsilon_f}{2}$, where ϵ_f is the true fracture ductility in pure tension, since $\Delta\epsilon_p = \epsilon_f$ at $N_f = \frac{1}{2}$ cycle. The fracture ductility is defined as

$$\epsilon_f = \ln \frac{A_0}{A_f} \text{ or } \ln \left(\frac{100}{100 - \% \text{ R.A.}} \right)$$

where A_0 is the initial specimen area and A_f is the fracture area.

Coffin⁽¹⁰⁾ describes a model illustrating how cyclic plastic strain is produced as a consequence of cyclic temperature. The cyclic plastic strain is defined as

$$\Delta\epsilon_p = \Delta\epsilon_t - \Delta\epsilon_e = \frac{\alpha\Delta T}{1-\nu} - \frac{2X \text{ endurance limit}}{E}$$

where endurance limit is defined as that stress which gives a fracture life of at least 10^7 cycles.

$$\Delta\epsilon_t \text{ is the cyclic thermal strain} = \frac{\alpha\Delta T}{1-\nu}$$

$$\Delta\epsilon_e \text{ is the cyclic elastic strain} = \frac{2X \text{ endurance limit}}{E}$$

Also, ΔT is defined as

$\Delta T = T_s - T_m$ where T_s is the surface temperature of the die and T_m is assumed to equal the die operating temperature.

ν = Poisson's Ratio

A log log plot of $\Delta\epsilon_p$ vs N_f is a straight line with a slope of $(-\frac{1}{2})$; with ϵ_f , the fracture ductility, a point on the curve for N_f equal to $\frac{1}{2}$ cycle. Therefore an entire curve can be obtained by just the knowledge of the fracture ductility, ϵ_f .

Noesen and Williams used 0.1% yield stress instead of the endurance limit in the calculation of $\Delta\epsilon_e$ because of scarcity of published fatigue data.

Some metals have been verified experimentally to agree with "Modified Coffin's low cycle equation"⁽⁵⁾ but unfortunately in many other cases of die steels, the predicted life is far in excess of the actual die life. For example, for casting aluminum in H-13 die steel or in maraging steel,

this method predicts infinite value of N_f . But in actual die casting operations, H-13 dies have been found to show fatigue cracks much earlier. Also, Ladish Company's Research Laboratory has reported (personal communication)(20) thermal fatigue cracking of maraging steel after a certain finite number of cycles for similar ΔT (700°F). Hence this method of theoretical prediction is not very satisfactory.

2. D.N. Williams⁽⁴⁾ et. al. examined two hotwork die steels, H-21 and H-23, by means of elevated temperature mechanical fatigue studies to determine the relative importance of oxidation and fatigue loading on corrosion fatigue (or heat checking) failures in die steels. They found that sample life in the range of 1100° to 1400°F. was relatively independent of oxidation. Variations in heat treatments, test conditions or other material properties were found to affect the sample life in direct proportion to their effect on plastic strain imposed on the sample during cyclic loading. They derived that sample life could be calculated by use of the equation

$$N = \frac{1000}{s^2}$$

where N = sample life in cycles
 s = plastic strain in percent imposed on the sample each half cycle

Above formula holds good for an annealed material only.

As this method uses a cyclic load applied at a constant high temperature, it does not exactly follow the physical conditions of alternate heating and cooling that a die casting die undergoes in actual production. Further, the authors themselves indicate in their paper that plastic strain values of the heat treated samples were very uncertain. Thus they could not develop the equations relating sample life to strain, strain rate and temperature. This method therefore does not seem to be very helpful in predicting the thermal fatigue life of a fully hardened die steel.

3. Glenny^(11, 12) et. al. developed a laboratory testing technique by immersion of the test specimen in a bed of powdered refractory substance supported on a permeable plate and fluidized by a stream of air. These fluidized beds were used for alternate heating and cooling to study thermal fatigue of Nimonic alloys. Recently, I.I.T. Research Institute, Illinois and some industries are using this technique for thermal fatigue of steels.

Glenny et. al. found by experimental study that a higher upper temperature in the cycle and a higher holding time at an upper constant temperature result in lower number of cycles to cause fatigue failure. Also, a higher ΔT (at a constant upper temperature) results in lower number of cycles to failure. Argon gas atmosphere resulted in higher number of cycles to failure than in air for the same sample. The

criterion for failure was taken as first appearance of a radial crack at the periphery of a tapered disc specimen.

Number of cycles to failure, N , was defined as

$$N = \frac{N_1 + N_2}{2}$$

where N_2 = No. of cycles when cracks first seen at 60X
 N_1 = No. of cycles when specimen was last examined without showing any cracks.

4. Wollering and Oertle⁽¹³⁾ of Ladish Company have developed a cyclic thermal fatigue testing machine in which polished die steel samples are mounted on a wheel rotating at a controlled speed. Heating source is an oxy-acetylene torch which raises the temperature of a small central portion of the top surface of the specimen to 680-700°F in about 4.3 seconds. The specimen is then water quenched by rotation of the mounted wheel into a water bath kept at 66°F. An air blast dries the surface of the specimen, as it emerges out of the water bath, before being heated again. Specimens are removed from the machine at intervals of 10 to 15 cycles during the early stages of the testing, surfaces are metallographically polished and photographs taken at 25X. After the cracks have initiated, during the later stages of testing, this procedure is repeated less frequently.

Using this method, Wollering and Oertle were able to make a bar chart for different die steels, showing the number of cycles per specimen at the initiation of surface fissures. They have also presented photographs showing the

fatigue crack propagations after initiation at different cycles for various die steels.

5. Coffin⁽¹⁴⁻¹⁶⁾ used a thin walled cylindrical test-piece which was alternately heated by passing a heavy current through the wall, then cooled by a flow of cold gas through the bore. The thermal cycle was continued until a crack developed. The test is closely related to conventional push pull fatigue tests, but perhaps the chief advantage is that the stress in the test piece can be measured throughout the cycle and therefore useful information can be derived about stress strain behavior. Coffin used an 18/8 Cr-Ni austenitic steel. The main disadvantage of this method is the lack of uniformity of temperature along the gage length of the test piece; the center attains a higher temperature than the radiused shoulders and consequently there is probably some degree of strain concentration near the center.

6. Northcott and Baron⁽⁹⁾ presented a valuable review of "Craze-cracking" in die casting dies, ingot molds, hot rolls, forging tools and dies, brake drums and railway wheels, as an introduction to their work on thermal fatigue of low alloy steels.

After a few tests with different methods of heating, Northcott and Baron decided that induction heating was the most convenient and versatile method. Initially they tried to heat a flat surface using a spiral pan-cake inductor as

shown in Fig. 5a but they found the efficiency of the coil to be low and a steep temperature gradient could not be obtained. The efficiency of coupling was found to be much better when cylindrical shaped specimens were tested as in Fig 5b. The base was cooled by a continuous water flow to control the temperature gradient and decrease the cooling time. They could not attain a high enough maximum temperature with a high frequency generator of 7kw power output for the cylindrical specimens. To concentrate the available power into a small volume of metal, the test piece and inductor shown in Fig. 5c were then tried. Thermal stresses set up in such a specimen were found to be uniaxial which was undesirable. The type of cracking produced did not bear any obvious resemblance to ordinary craze cracking and since the heated layer was quite deep there was a tendency for the edge to buckle. This design was modified by machining a flat 0.050 inch wide along the sharp edge and using the inductor shown in Fig. 5d. A copper shield kept the base of the test piece cool. The narrow edge was intermittently heated whilst the bore was continuously water cooled. This form of test piece gave satisfactory results for their experiments.

Later, most of their work was carried out with a standard H.F. generator with a maximum power output of 25kw and a high frequency of about 500 kc/s. Temperature measurements were taken by means of standard chromel/alumel thermocouples,

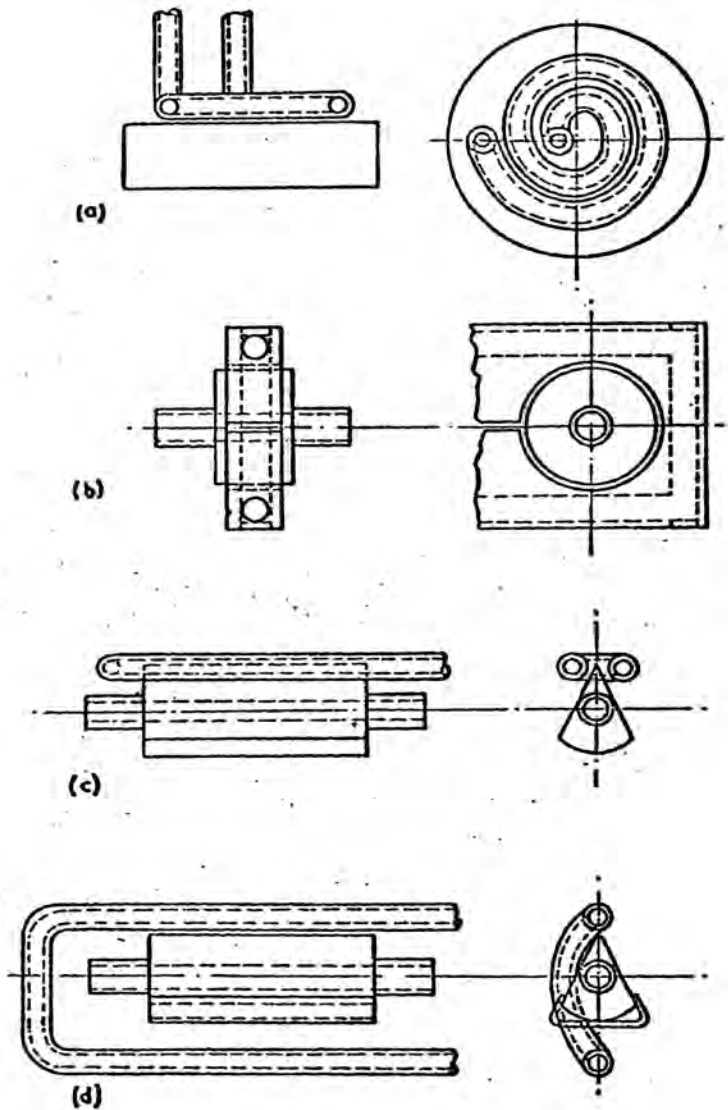


Fig. 5 Test-pieces and inductors used in preliminary experiments by Northcott and Baron.

each wire being spot welded to the test-piece.

Most of their experiments were directed towards the behavior of low-alloy steels, using maximum temperatures in the cycle which exceeded the A_{c3} temperature for steel. The surface then undergoes ferrite to austenite transformation on heating, but the rate of subsequent cooling is so fast that the reverse transformation is suppressed until the temperature reaches the M_s point. The cracks obtained in this case were not very sharp. They also tried lower maximum temperatures between 40-700°C where no phase transformation occurs as A_{c3} temperature is not exceeded. Much sharper cracks were reported for such a temperature range (Fig. 6).

The effect of maximum temperature in the cycle on the rate of cracking in various steels is shown in Fig. 7. They further found that stress concentration plays an important part in the development of these cracks and when transverse notches were cut into the surface, the rate of cracking was greatly accelerated even when the notch was only a few thousandths of an inch deep.

Northcott and Baron also carried out a few tests on the influence of various atmospheres and their results suggest that the nature of the atmosphere does not have a marked effect on the rate of cracking. However, in oxidizing atmospheres a fine network of cracks developed in the brittle scale as shown in Fig. 8a. The metal sur-

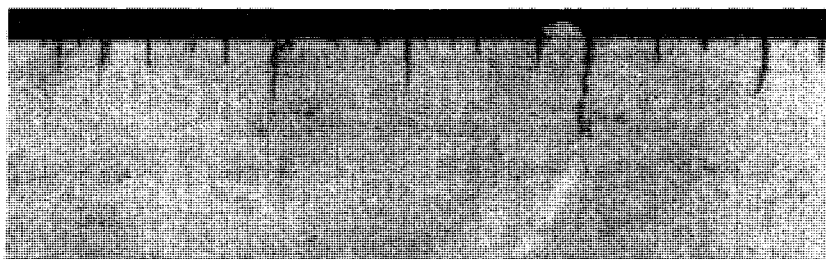
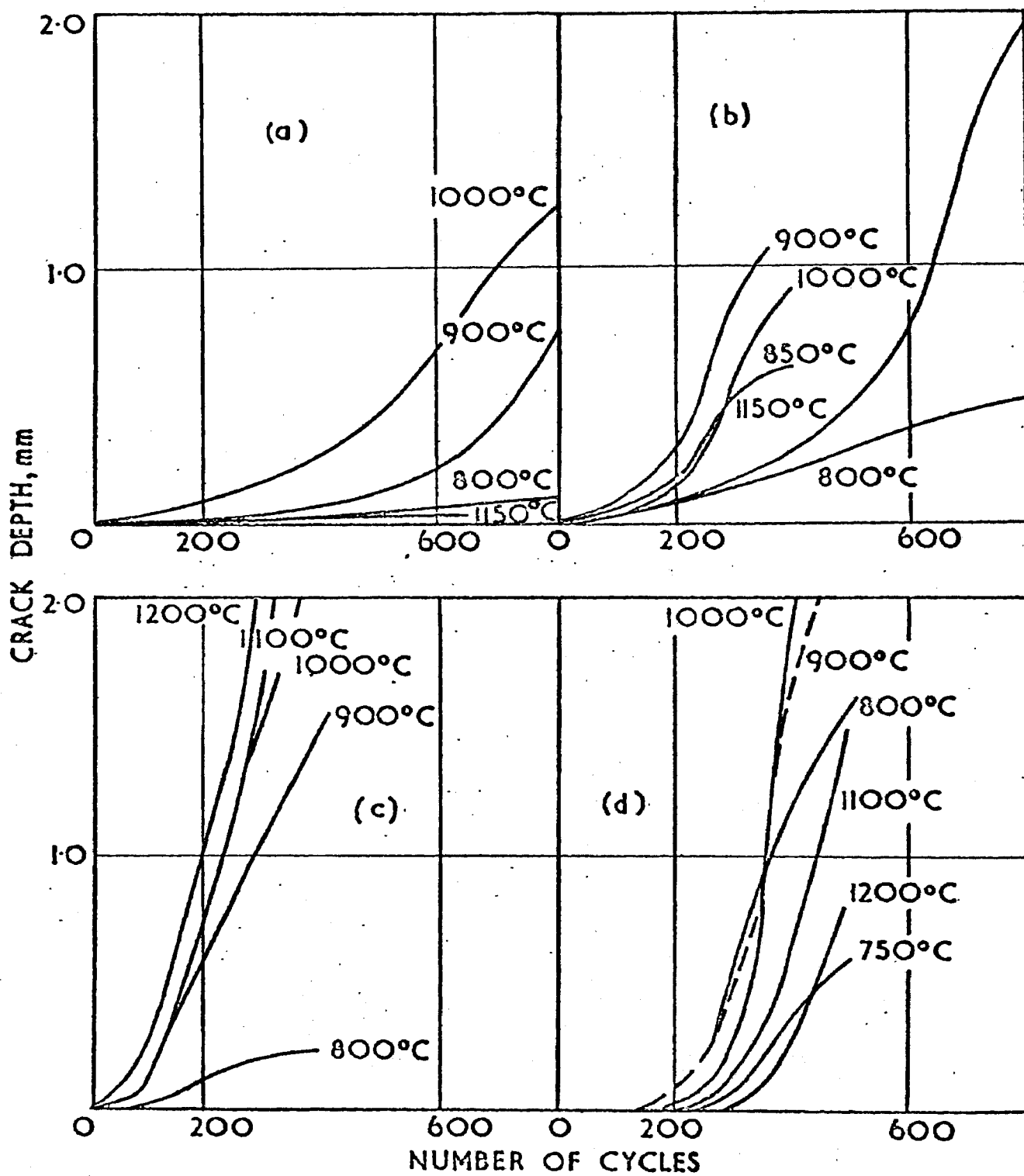


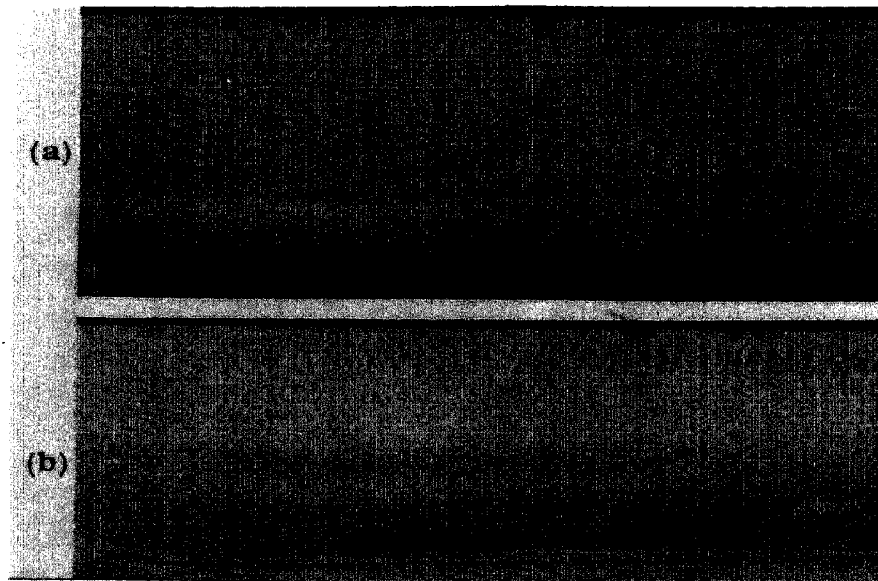
Fig. 6-Appearance of macrocracks due to
thermal fatigue in En. 25 steel,
1700 cycles, 40-700°C in air 10X



(a) 0.34% carbon steel
 (b) 0.89% carbon steel

(c) 1.24% carbon steel
 (d) Ni-Cr-Mo steel Ea. 25

Fig. 7—Influence of maximum temperature and no. of cycles on depth of cracks. Test-pieces cycled between temperatures shown and 40°C, in argon



(a) 200 cycles, 40-850°C in air

(b) 200 cycles, 40-850°C in hydrogen

Fig. 8-Thermal fatigue of medium carbon steel 5X

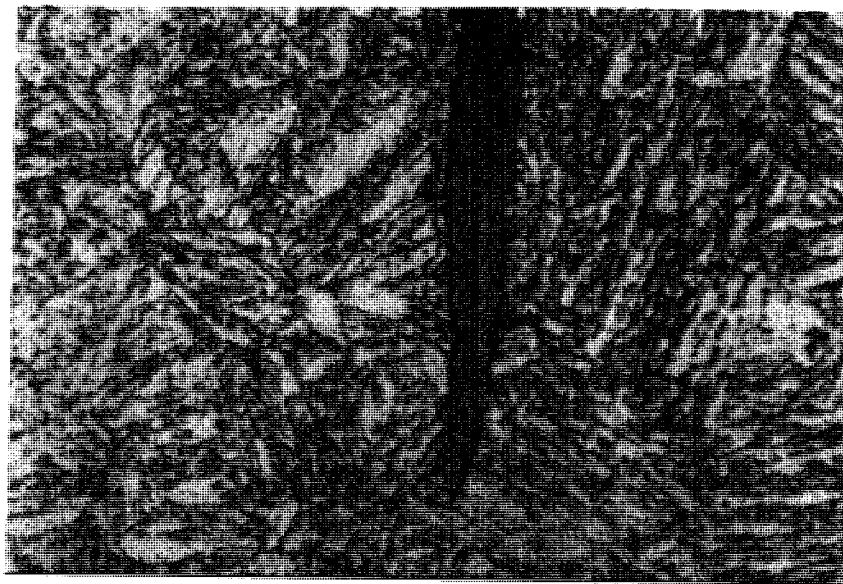


Fig. 9-Appearance of microstructure and a thermal fatigue crack in En. 25 steel, tested for 4000 cycles in air, 40-600°C 800X

face is oxidized more rapidly beneath these cracks than in positions shielded by scale, and hence the pattern is reproduced on the metal surface. Fig. 8b shows the effect of hydrogen atmosphere.

When a thermal cycle of 40-700°C. was used with a hardened and tempered En 25 steel (C 0.34, Ni 2.54, Cr 0.65, Mo 0.6), at higher magnification the cracks were seen to be fairly straight transcrystalline (Fig.9) and oxide filled. When a hydrogen atmosphere was used the cracks showed some tendency to follow shear planes and the number of cracks was reduced although the number of cycles to first evidence of a crack was not very different.

III. EXPERIMENTAL PROCEDURE

A. Selection of Steels Used

The compositions of the steels used in the present study are given in Table I.

TABLE I
COMPOSITION OF VARIOUS STEELS TESTED

Material	AISI 4340H	Ladish D-11	AISI H-11	AISI H-13	AISI H-21	Maraging UM-300
Element						
C	.40	.46	.40	.39	.35	.03
Mn	.76	.75	.29	.36	.25	.10
Si	.25	.25	1.00	1.06	.35	.10
Ni	1.71	.50	.06	.17	--	18.50
Cr	.81	1.00	5.00	5.23	3.50	--
Mo	.22	2.00	1.50	1.35	--	4.80
V	--	.50	.40	1.04	.50	--
W	--	--	--	--	9.50	--
Co	--	--	--	--	--	9.00
Al	--	--	--	--	--	.10
Ti	--	--	--	--	--	.60
B	--	--	--	--	--	.003
Zr	--	--	--	--	--	.02
Ca	--	--	--	--	--	.05
Cu	--	--	.04	.11	--	--

1. AISI 4340H

This steel was used in preliminary work for developing the experimental techniques. It was selected primarily because it had a low alloy composition range of the order of Ladish D-11 steel and was readily available in the stock room.

The remaining five steels were selected as they showed promising physical and mechanical properties (mentioned earlier in the literature review section) which are necessary for aluminum die casting dies.

2. Ladish D-11

Ladish Company had claimed its D-11 steel to be very suitable for aluminum die casting industry.⁽¹³⁾ It was therefore decided to test this steel for its suitability on the basis of present experimental techniques.

Table II shows a comparison of some of the physical and mechanical properties of interest of the die steels used.

TABLE II

PROPERTIES OF DIE STEELS TESTED BY THERMAL FATIGUE CYCLING

Material	Room Temp. Ultimate Strength	Thermal Expan- sion	Thermal Conduc- tivity	Elastic Modulus at Room Temp.	Ultimate Strength at 1000°F
	ksi			psi x10 ⁶	ksi
L D-11	274	7.25	17.7	30.7	162
AISI H-11	217	7.40	16.6	30.0	140
AISI H-13	217	7.50	16.6	30.0	145
AISI H-21	243	7.60	17.9	--	163
Maraging UM300	294	5.60	16.7	27.5	165

Ladish D-11 steel bars of 23/32 inch diameter were supplied by Ladish Company in two different lots at different times on the basis of requirement for the present study. These bars were in annealed condition and were machined to the required specimen sizes of $\frac{1}{2}$ inch diameter X $\frac{3}{4}$ inch length.

Heat treatment parameters were decided from the Fig. 10a supplied by Ladish Company and samples were heat treated in sealed stainless steel envelopes, in a manner indicated in the general procedure.

3. AISI H-11 and H-13

Consumable vacuum re-melted H-11 steel bars of 0.770 inch diameter were supplied by The Carpenter Steel Company. H-13 steel was obtained from three different sources, namely,

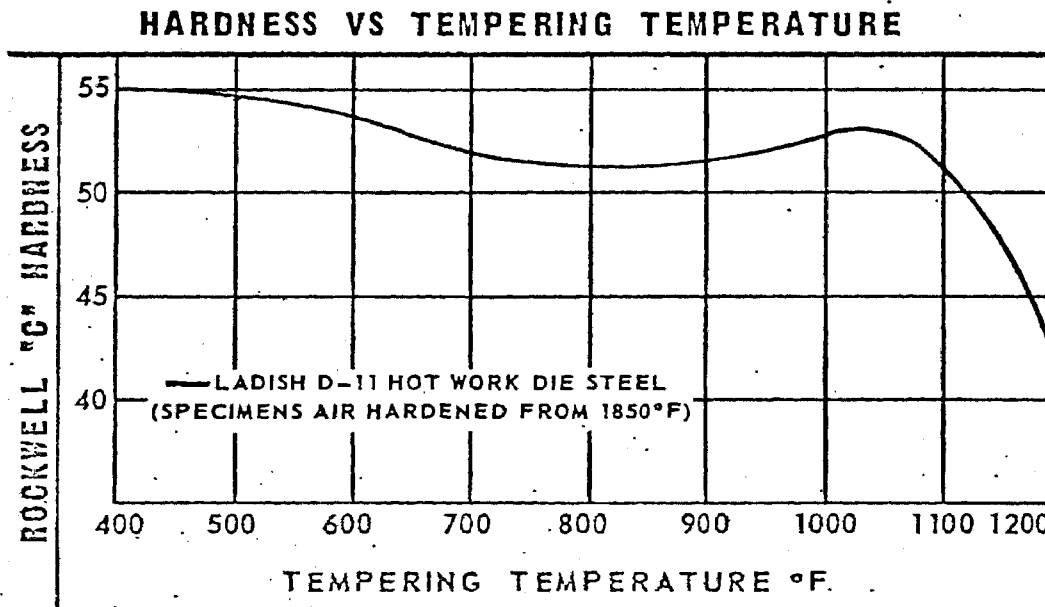
The Carpenter Steel Company, Universal-Cyclops Steel Corporation and Latrobe Steel Company.

H-11 and H-13 are both chromium type hot work steels and have basically the same chemical composition with the exception that vanadium content is increased from 0.5 to 1.0 percent in H-13. Both the steels have high ductility and toughness. The 1.5% molybdenum imparts very high hardenability to these two grades, enabling them to harden throughout large sections using still air quench. Both the steels have a good resistance to softening at elevated temperatures. Higher vanadium content imparts higher hot hardness and better wear resistance to H-13. Typical applications of H-11 include die casting dies, punches, piercing tools, extrusion tooling and forging dies. H-13 is presently widely being used as die steel for aluminum and magnesium die castings and for long run zinc die castings.

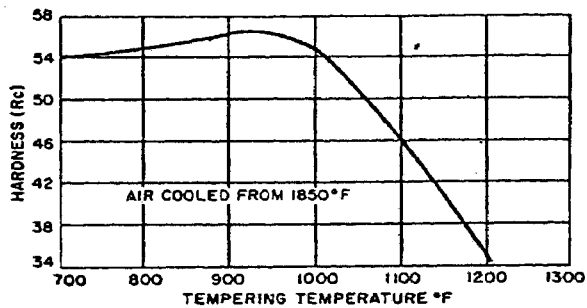
Heat treatment parameters for these two steels were selected from Figs. 10b-c supplied by Latrobe Steel Company.

4. AISI H-21

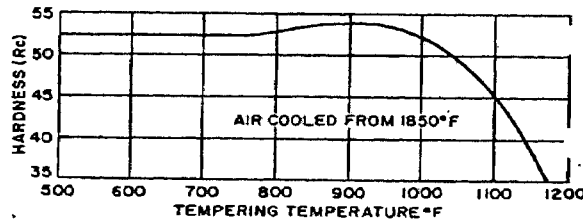
This steel shows better wear resistance and higher hot hardness than H-11 and H-13 die steels. It has higher strength properties at elevated temperature (Table II) and better thermal conductivity than other steels discussed earlier. Because of these reasons, it is frequently used for applications where resistance to softening at elevated temperatures is important. It has been used in industry for dies for die-casting brass⁽¹⁸⁾, permanent molds for



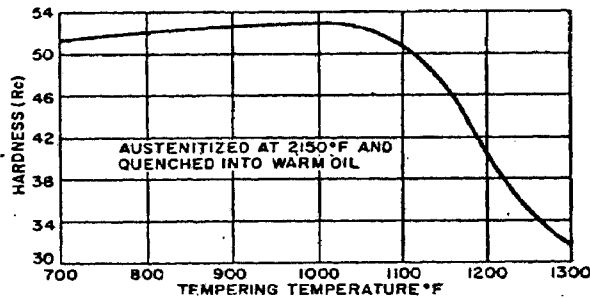
(a) Ladish D-11



(b) H-11



(c) H-13



(d) H-21

Fig. 10-Tempering temperature vs hardness data for various steels

gravity die casting, brass extrusion dies, hot punches etc.

H-21 was selected to find its suitability for the temperature range normally employed for aluminum die casting. As it shows good results for brass die-casting dies, it was reasoned that it might prove better than H-11 and H-13 die steels for aluminum die casting.

Latrobe Steel Company could supply a minimum size of 1 5/8 inch diameter rods of H-21 steels. These rods were therefore machined to $\frac{1}{2}$ inch diameter to get test specimens of required dimensions. Heat treatment parameters were selected on the basis of Fig. 10d as supplied by Latrobe Company.

5. MARAGING STEEL

Maraging steel is one of the latest developments in the alloy steel industry and it has some very promising properties which make it a potential candidate for die casting dies. It has maximum room temperature strength and elevated temperature strength among all steels listed in Table II. Thermal conductivity of maraging steels is comparable to that of H-13 but their coefficient of thermal expansion is about 12% lower. Thus maraging steels are superior in two properties of importance in resistance to heat checking. The maraging steels show a higher fatigue endurance limit⁽¹⁹⁾ in comparison with conventional H-13 as shown in Table III.

TABLE III

FATIGUE ENDURANCE LIMITS OF MARAGING STEEL COMPARED WITH H-13 DIE STEELS

Steel	Rc	10^8 cycles, psi
Vasco Max 300 CVM	54	125,000
H-13	47	110,000

Sufficient hardness and strength are needed if the die is to resist deformation, peening or brinelling of flash into the steel, and other abuses of the casting operation. The higher hardness and tensile properties of the maraging steels in comparison with some of the conventional die steels are shown in Table II and IV.

TABLE IV

HARDNESS AND TENSILE PROPERTIES OF MARAGING STEELS COMPARED WITH CONVENTIONAL DIE STEELS

Type	Rockwell Hardness	Yield Strength	Elongation %	Reduction in Area %
	Rc	(0.2% off-set, psi)		
H-11	46	190,000	11	39
H-13	46	190,000	10	35
H-21	50	215,000	12	37
Maraging 300	54	270,000	11	57

In addition, for an equivalent hardness and strength level, the maraging steels are generally tougher than conventional die steels and show considerably more ductility. This makes maraging steel more resistant to gross cracking. Also, because of higher hardness levels permitted by its toughness, the maraging steel should exhibit good resistance to washing. The oxidation resistance of maraging steel is considerably better than that of H-13 die steel, as shown in Fig. 11.

All the above desirable properties of maraging steels for dies are attributable to a precisely controlled composition and structure achieved by high purity alloys, consumable vacuum melting and special hot working techniques. Table I shows the nominal analysis of 18% Ni maraging steel based upon yield strength of about 300,000 psi. Large percentages of nickel, cobalt, and molybdenum are important contributors to the unique maraging hardening mechanism. Unlike H-13 or H-21, which are hardened by the effect of heat treatment on the carbon in steel, the maraging alloys are essentially carbon-free and derive their strength by an aging process in iron-nickel martensite.

In order to retain maximum toughness in large steel die block sizes, normal steelmaking impurities must be kept at extremely low levels. The element titanium is a very potent strengthener on maraging (each 0.1% increases yield strength about 10,000 psi). Boron, zirconium and

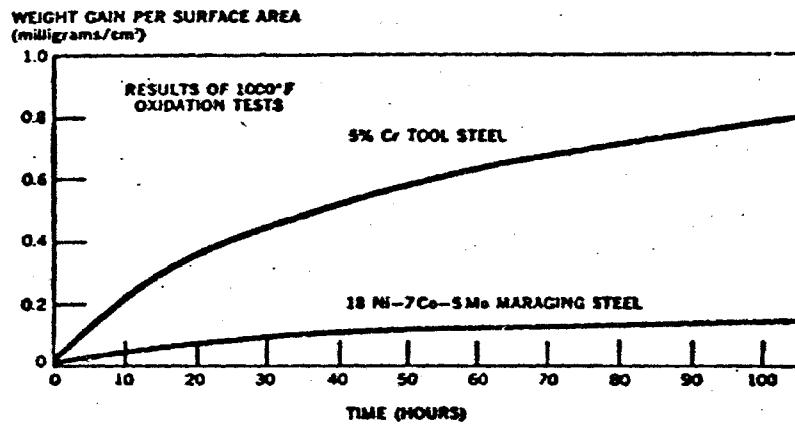


Figure 11. Comparative oxidation resistance of H-13 die steel and maraging steels at 1000°F.

calcium are added to retard grain boundary precipitation and improve toughness.

Maraging steel Unimar 300 was supplied in $\frac{1}{2}$ inch diameter rod form by Universal-Cyclops Steel Corporation in the solution annealed condition and it needed only to be aged at 900°F for 3 hours to develop full properties.

Another interesting characteristic of 18% nickel maraging steel is its small dimensional change on aging. After a proper mill anneal, the block contracts about 0.0005 inch per inch during aging. (19)

As not much detailed work in the area of suitability of maraging steels for aluminum die casting had been reported in literature, the author decided to carry out detailed investigations about maraging steel.

B. Preliminary Experiments

The initial phase of present project involved the selection of a suitable method of heating. It was intended to choose a method of heating which would closely simulate the actual temperatures experienced by a die in comparable production times on an aluminum die casting machine.

Fluidized bed type of arrangement involves too many variables to be controlled. A proper size and type of powder material has to be selected because below a critical size the fluidization becomes non-uniform and the heat transfer coefficient decreases. Also, a critical air flow (or gas flow) rate has to be used to get the maximum heat transfer. Transfer of specimen from hot bed to cold bed (and vice versa) takes some time during which the specimen temperature can change appreciably. This results in a non-uniform heating or cooling conditions of the specimen. It needs 72 to 96 hours cooling time if the furnace is to be repaired.

Gas torch flame heating and water quenching method, as adopted by Ladish Steel Company⁽¹³⁾, involves too severe a quench which is actually not experienced by the top surface of a die in production. Also, the heating times involved for 250 to 700°C temperature range are comparatively longer there.

Induction heating provides a convenient and versatile method and thus it was decided to use an induction heating unit for the present work.

In aluminum die casting, the die surfaces are normally preheated to about 250°C before the molten metal is injected. Injection may raise the temperature of the die surface up to 670°C as shown earlier in Fig. 3c. It was therefore the object of the preliminary experiments to achieve this temperature range in the minimum possible time with the available induction heating unit. The available induction unit was a single phase, 220 volt, 1½ kw output unit with current being variable from 0 to 500 mA.

In the first experiments, just to set up the proper experimental procedure, 4340H steel was used as die steels were not immediately available in stock. Initially cylindrical shaped specimens were tested as in Fig. 5b. To control the temperature gradient and decrease the cooling time, the bore was cooled by a continuous water flow. All the cylindrical test-pieces could be heated only up to 600°C in about 2½ minutes. Attempts to increase the heating rate by altering diameters of test-pieces and coil were not very successful because when the wall thickness was increased to lower the rate of dissipation of heat to the bore, the surface area to be heated was increased. Also, steep temperature gradients between outer periphery and the center of the specimen could not be obtained.

Another type of trials were carried out so as to heat the surface of the steel specimen (placed outside the heating coil) by placing it in contact with one flat end of a

cylindrical core piece of a different metal of higher thermal conductivity (e.g. Ni, Cu, W etc.) which was surrounded by the induction coil. To improve the physical contact, the cylindrical core and the bottom steel piece were gripped between insulated faces of a vertical C-clamp. A spring was attached between the cylindrical core and upper face of the C-clamp so as to allow for the expansion of the core during heating without increasing the pressure at the point of contact of the steel piece and the core.

A temperature increase from 250 to 670°C on the surface of steel piece was obtained in 35 and 30 seconds with nickel and copper cores respectively. Attempts to increase the heating rates by varying the sizes of the core, steel test-piece and coil did not result in any appreciable advantage. Further, attempts to attain any temperatures higher than 670°C resulted in melting away of the copper and nickel cores. Also, copper core showed slight diffusion tendency into the steel surface.

Cylindrical cores of tungsten were tried so as to overcome the above melting problem as it has a very high melting point. It took about 40 seconds to get the required increases in temperature from 250 to 670°C in the beginning. But after few cycles, tungsten cores were very badly oxidized and heating times increased still more due to the oxide layer.

To prevent copper diffusion into steel surfaces, some

copper cores were electro-coated with nickel and gold as these two metals have very low diffusion tendency in steel at the operating temperature of interest. To make the coatings adherent, the electro-coated cores were annealed in neutral atmosphere. When these nickel and gold coated copper cores were used for the above heating purpose, the coatings spalled off during the cooling part of the cycle.

Molybdenum and tantalum foils (0.003 inch thick) were then tried as separation media between copper cores and steel pieces. It did prevent the diffusion problem but no improvement in heating time was achieved.

During the final trials, to utilize the maximum power available out of the induction unit, air gap between the steel test-piece and the copper inductor coils and also the number of turns of the coil were varied. Maximum efficiency was obtained by using a circular coil with an inside diameter of $5/8$ inch for a $1/2$ inch diameter cylindrical test-piece with one complete turn of the coil only around its top end. As quite short heating times resulted from this, it was therefore decided to use this arrangement for the actual experiments.

C. Present Experimental Methods

1. Test-piece and Inductor

A cylindrical test-piece of $1/2$ inch diameter and $3/4$ inch long is used. Top $1/16$ inch high portion of the sample is surrounded by one complete turn of a copper inductor coil made from $1/8$ inch outside diameter tubing with cold water

continuously flowing through its 1/16 inch diameter bore. The test-piece is located in a copper jig which extracts heat from the base of the specimen thus giving a vertical temperature gradient (Fig. 12).

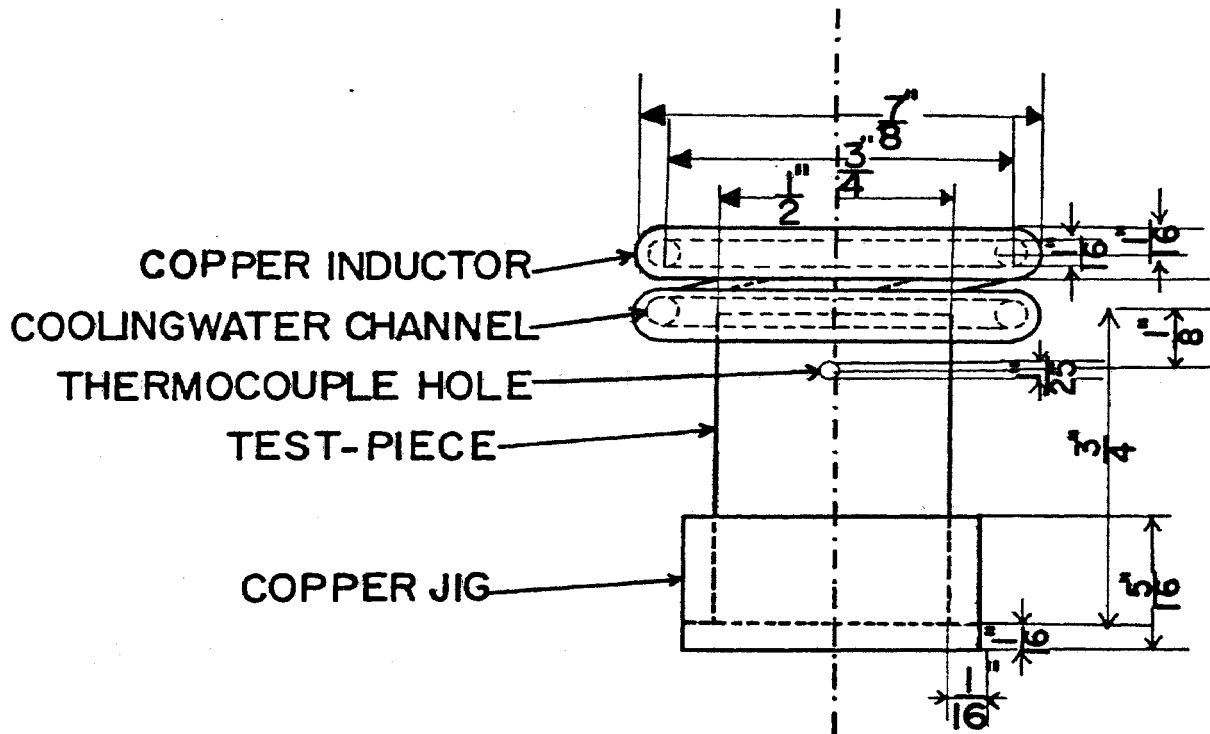
Measurements have been taken of the temperature distribution radially on top face and down the vertical side. The results are plotted in Fig. 13a-b. A specimen of 4340H was used and temperature at the top periphery was cycled between 250-670°C. The graphs show the maximum temperatures recorded at other positions.

2. Cooling Arrangement

It was decided to use pressurized air for cooling part of the thermal cycling of the specimen. In actual production, die-casting die surface is not cooled by water. Water cooling channels are made much below the surface of the massive dies. Use of water quenching on the surface of a test-piece causes quench cracking and the thermal fatigue cracking data so obtained can be misleading and erroneous. In fact, in industry, air blowers are used to cool the die surface during the ejection half of the casting cycle. For these reasons, air cooling was incorporated in the present experiments.

A solenoid operated valve of $\frac{1}{2}$ inch size, with a capacity of operating up to 100 psi was connected in the air supply line. The pressurized air is passed through a set of filters to remove any dust or moisture before entering

Fig. 12-Arrangement of the test-piece and inductor used
in present investigation.



ARRANGEMENT OF TEST PIECE AND INDUCTOR.

SCALE- 2" TO 1"

FIGURE 12

the air valve. The solenoid valve is connected in such a manner to the OFF timer of the timer unit, that the air valve supplies air for cooling only when the induction unit is off. A nozzle is fitted about $\frac{1}{2}$ inch above the top edge of the test-piece so as to cool the specimen surface by pressurized air supplied by the air valve.

The timers do not require resetting after each cycle and the sequence is therefore completely automatic. An electric clock incorporated in the circuit of the induction unit gives the total time for which the unit is run and thus the total number of cycles are known. The clock incorporated has further advantage of indicating the exact time of run if accidentally the unit stops functioning at any hour of the day or night.

3. Temperature Measurement

Standard chromel/alumel thermocouple wires of 0.012 inch diameter are used. To determine the accurate temperatures on the surface, trials were carried out on dummy samples. One 0.04 inch diameter hole was drilled on the side of the cylindrical test-piece, with its center being just 0.04 inch below the top surface and up to a depth of only 0.03 inch. The thermocouple wires were welded to form a bead of just the size which will push fit into the above drilled hole. The specimen was heated in the induction unit and the temperature recorded by means of a sensitive galvanometer. Further, 0.04 inch diameter holes were

drilled at close spacing radially on the top surface and along the vertical side so as to get the temperature profile of the whole test-piece. These temperature profiles were found to be similar in all the steels.

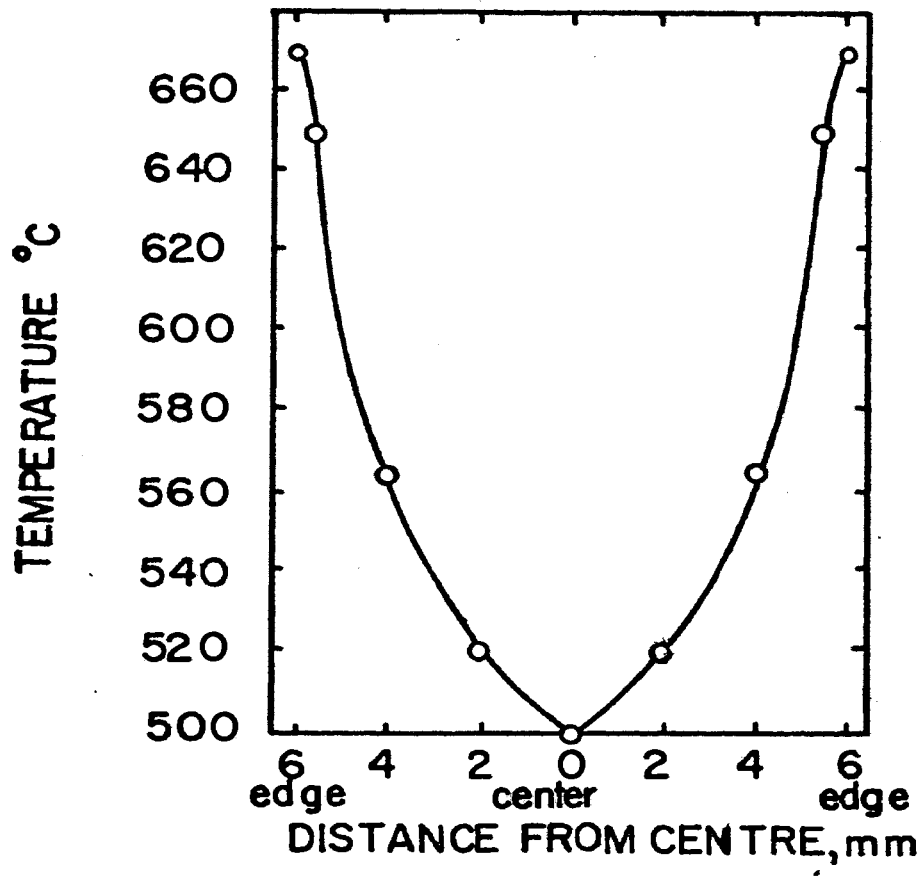
Once the temperature profile of the dummy test-piece in each steel was mapped out (Fig. 13), only one hole of 0.04 inch diameter was drilled (1/8 inch below the top surface) in further test samples. The top surface temperature is manipulated by use of Fig. 13b from the temperature reading obtained by the thermocouple inserted into the above hole. This step is necessary because if the actual test-piece contains a drilled hole just 0.04 inch below the top surface, it acts as a strong stress raiser and causes earlier cracking of the material. But the hole drilled 1/8 inch below the surface (being at a comparatively lower temperature) was not found to have any stress raising effect which was verified in all later tests. This method of temperature determination was found to be very reliable and accurate.

Many people record the temperature of surfaces by spot welding the thermocouple wires on the test-piece. It is possible for the welded junctions to be either hotter or colder than the surrounding surface, owing to induced currents or to thermal conduction along the wire. Induced currents tend to make the junction too hot if the welded junction is large, especially if it is elongated in the direction of current flow, whilst thermal conduction in

Fig. 13A-Temperature profile in radial direction of the
test-piece

Fig. 13B-Temperature profile in axial direction of the
test-piece

A.



B.

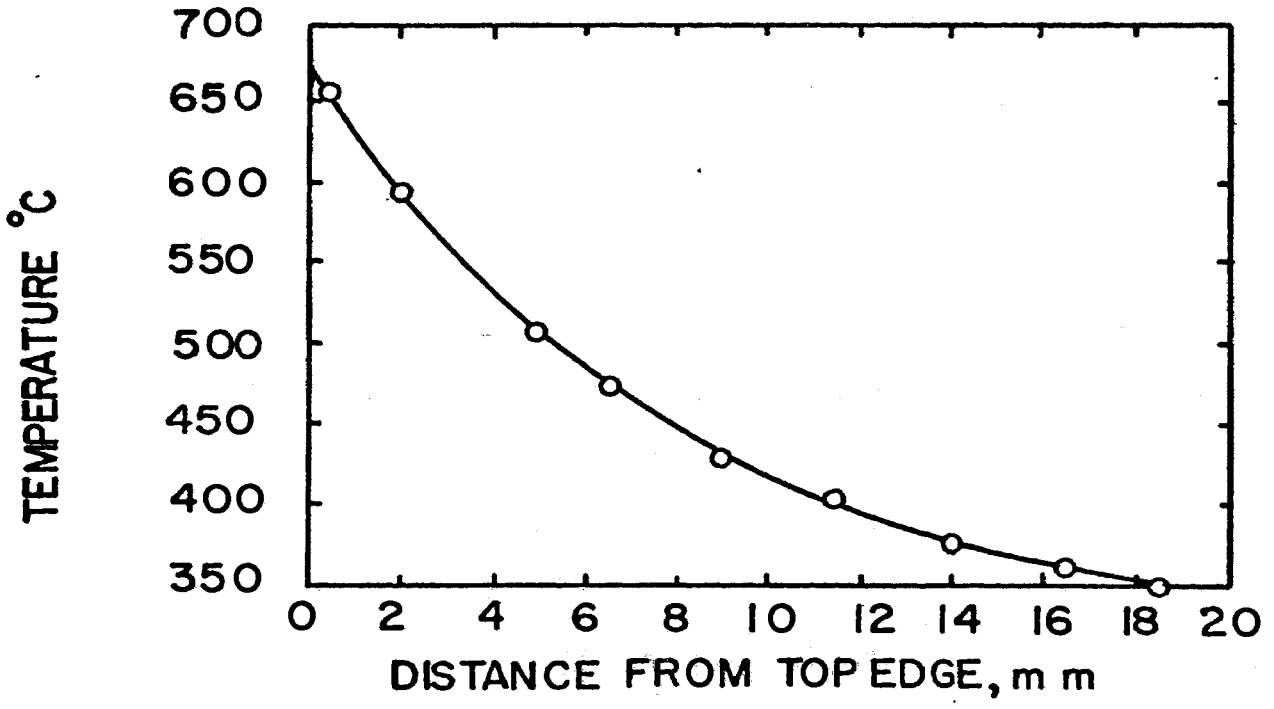


FIGURE 13

the wire can make the junction temperature too low if the wire is too heavy or if the area of the weld is small in relation to the cross-sectional area of the wire. A more serious error can arise in oxidizing atmospheres owing to gradual penetration of oxide into the welded junction. The area of contact can be greatly reduced and the temperature of the junction then falls owing to conduction of heat to the relatively large cold wire. The gradual oxidation of welded junction could lead to errors of 50°C or more.

The electrical resistance of the thermocouples and leads used in present experiments was 10 ohms and did not alter appreciably until the welded bead was on the point of breaking. The resistance of the wires and thermocouples was checked from time to time and the wires were rewelded in case of any doubt.

4. Heat Treatment

As the die steel dies are used in fully hardened and tempered condition, so as to have maximum resistance to thermal fatigue, it is essential to use the test samples under similar heat treated conditions. The die steels must not be exposed to oxidizing, carburizing or decarburizing atmospheres, as all such atmospheres tend to reduce the thermal fatigue resistance of die steels.

To overcome such difficulties, the specimens are sealed in stainless steel envelopes (0.002 inch thick). These

envelopes are of disposable type and they eliminate the need for having elaborate and costly gaseous atmospheres in heat treatment furnaces and are very useful for heat treatment of small samples. The samples are then austenitized at the required temperature and for required length of time (as indicated by the steel supplier), quenched and tempered. In present series of experiments, samples were heat treated to get hardness values of Rc 50 and 40 for each of the steels tested. The samples remain shining and bright after heat treatment in the stainless steel envelopes.

Muffle furnaces were used for all heat treatment operations in the present study.

5. Heating and Cooling Cycling

The specimen is first heated for one second in the beginning and when the whole piece is in equilibrium at 250°C (as indicated by the different thermocouples fitted on to the test-piece), heating is further carried out till 670°C temperature is obtained on the top surface. Once heating time is standardized, the induction unit automatically goes off after the set ON time and the solenoid operated air valve immediately supplies the pressurized air, through the nozzle fitted about $\frac{1}{2}$ inch above the specimen, for the required length of time till the sample cools to 250°C. The air supply then automatically stops after the fixed cooling time and the heating cycle starts again. Hence

after the first cycle, everything works automatically. Fig. 14 shows the complete apparatus set up for the present series of experiments.

The heating time for 4340 steel test-piece was standardized at 3.65 seconds and the cooling time at 17 seconds. The rate of heating is very rapid at first but then slows down slightly so that any error due to galvanometer lag is negligible.

Some time temperature graphs were drawn, as shown in Fig. 15. The heating rate is very fast while cooling rate which is very high in the beginning, slows down considerably after about 500°C. It should be noted here that a medium size die for casting an aluminum die casting, about 2 lbs. in weight, normally undergoes a similar time schedule on a 150 ton automatic pressure die casting machine (as per experience of the author in industry). Thus the above time-temperature cycle was considered to be a close simulation of the actual conditions experienced by a die surface in production.

The heat pattern experienced by the test-piece is shown in a 5X photograph (Fig. 16). The heat conduction can be observed as concentric isotherms going from the outer periphery towards the center and giving a severe temperature gradient radially as was shown earlier in Fig. 13a. Also, this heat pattern very closely resembles Nicolson's model (Fig. 2a) when points F and G are interchanged.

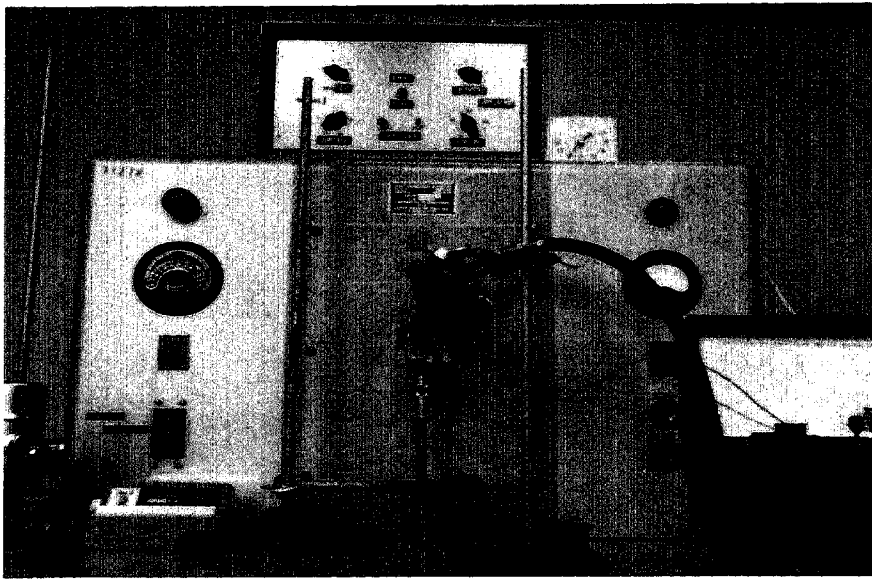


Fig.-14 Apparatus set up for thermal
fatigue testing of die steels

Fig. 15-Induction heating and air cooling cycle for thermal fatigue of die steels

INDUCTION HEATING AND COOLING CYCLE

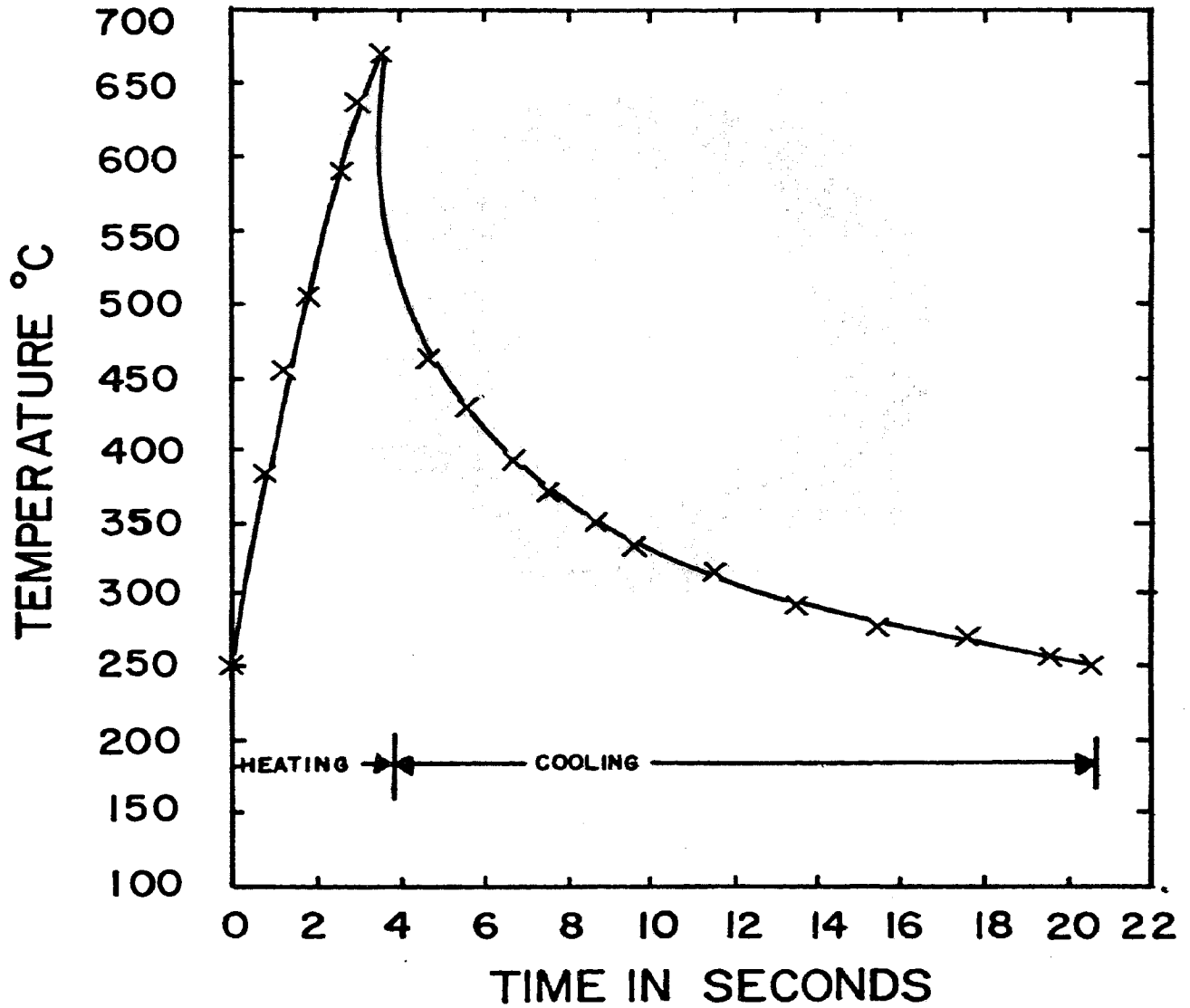


FIGURE 15

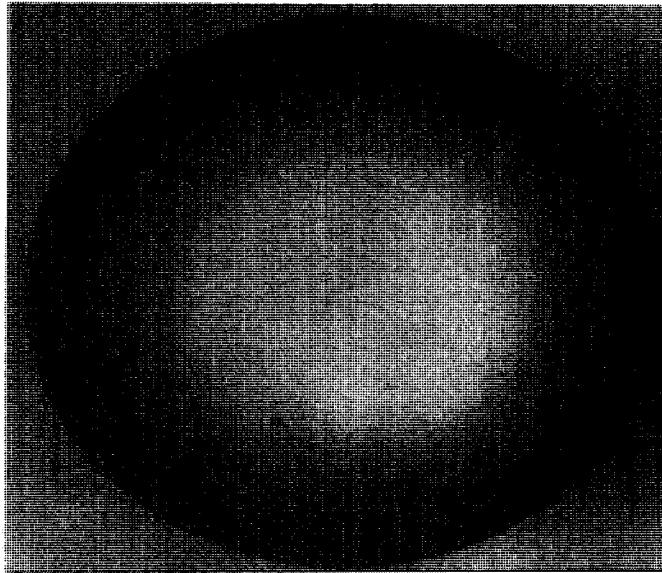


Fig. 16-Heat affected pattern on a thermal
fatigued specimen of 4340 steel after
100 cycles, in air, top face 5.5X

6. Experimental Procedure

To evaluate the effect of cyclic heating and cooling and to establish whether the cracks so developed resemble the fatigue cracks, the tests were first carried out on 4340H steel as per following testing conditions.

- a. Cylindrical test-piece of $\frac{1}{2}$ inch diameter and $\frac{3}{4}$ inch long was metallographically polished on the top surface with aluminum oxide, Linde B, 3 micron size or less.
- b. The polished sample was examined at 100X under microscope to make sure that the polished surface and edges were free from any micro-cracks.
- c. The test-piece was first brought up to 250°C in a manner indicated earlier and then heated for 3.65 seconds and cooled for 17 seconds. Dry and clean air at 60 psi pressure was used as cooling medium. The maximum temperatures attained during heating and cooling were 670 and 250°C respectively.
- d. Specimens were removed from the machine at intervals of 50 cycles during the early stages of testing. The surfaces were metallographically polished only on microcloth wheel using aluminum oxide. The progress of cracking was followed at a magnification of 100X, using parts from a travelling microscope fitted with a graduated eyepiece to enable the depths of the cracks to be measured.

First appearance of a crack at 100X was taken as the point of initiation of thermal fatigue. Three samples were tested up to the point of initiation and similar results were obtained, thereby showing the reproducibility of the results. Photographs were taken at magnifications between 5 to 9X.

One of the samples was then further cycled to study the rate of crack propagation with increased number of cycles. The sample was taken out at intervals of 100 or 200 cycles, metallographically polished and photographed. Lengths of the different cracks and their total number were recorded under a travelling microscope. These data were then plotted as shown later.

IV. EXPERIMENTAL RESULTS AND DISCUSSION

A. Observations and Results On 4340 Steel

1. Heat Treatment

Austenitized at 1550°F for $\frac{1}{2}$ hour.

Tempered at 800°F for 2 hours.

2. Hardness

Hardness of the samples as received - Rc 19

Hardness of the samples after above heat treatment - Rc40

3. Thermal Cycling

Heating time per cycle - 3.65 seconds

Cooling time per cycle - 17 seconds

4. Results

Number of cycles for crack initiation - 100

TABLE V

PROPAGATION OF THE LONGEST CRACK IN 4340 STEEL

Number of Cycles	Length of the longest crack, mm
100	0.22
150	0.26
290	0.62
400	0.90
510	1.17
610	1.36
800	1.60

5. Discussion of Results

After undergoing some cycles, an oxide coating is formed on the top edge and along the sides, forming a network of cracks developed in the brittle scale as shown in Figs. 17 and 27b. The metal surface is oxidized more rapidly beneath these cracks than in positions shielded by scale and hence the pattern is reproduced on the metal surface on further cycling. There exists a very close resemblance between Figs. 17 and 8a in the general appearance of thermal fatigue samples. The sharp edge of the sample acts as a further stress raiser in addition to the sharp temperature gradient existing from the outer edge towards the center and hence the fatigue cracks are seen to start from outer periphery and proceed radially inwards. (Figs. 20a-d).

The appearance of a single crack, as shown in Fig 18 at 133X, closely resembles an actual heat check in a die which was shown earlier in Fig.4c. This clearly established that the present thermal cycling method simulates the creation of actual fatigue cracks in die casting dies.

The crack propagation sequence can be nicely seen in this steel in the set of photographs shown in Figs. 20a-d. Fig. 20a shows two very sharp and fine cracks (few cycles after the crack initiation) at 150 cycles. On further cycling, these cracks propagate radially inwards, become wider at the edge and also some new cracks are developed



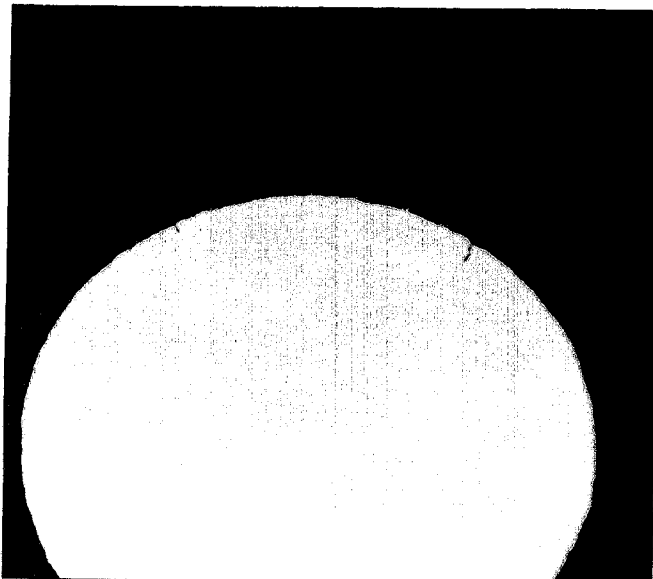
Fig. 17-Oxide scale and cracks formed on
the side of the cylindrical test-piece
of 4340 steel, in air, after 1200 cycles 7X



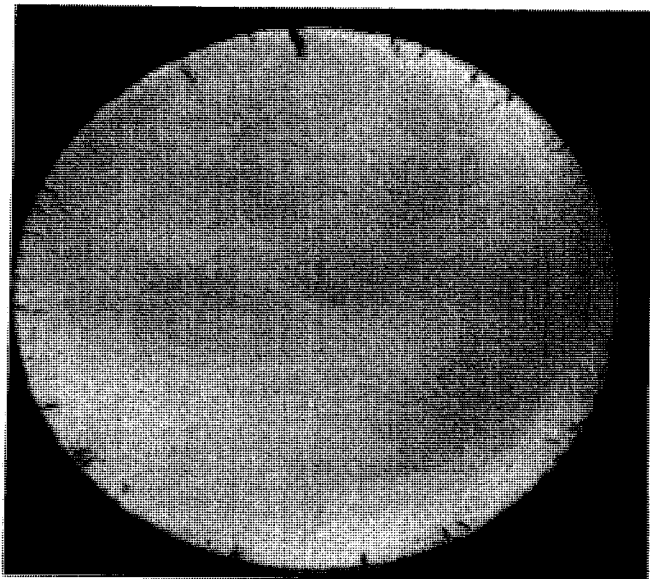
Fig. 18-An oxide filled
thermal fatigue
crack in 4340 steel
after 900 cycles 133X



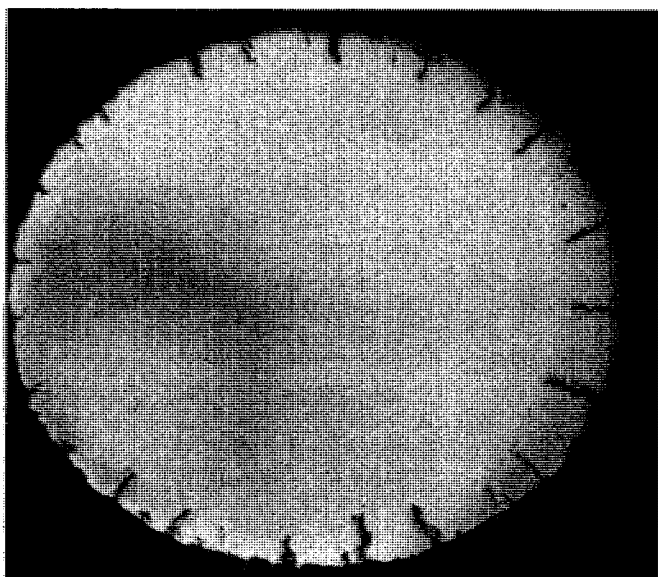
Fig. 19-Stress raising effect
of a thermocouple hole
only 0.04 inch below the
top surface; 4340 steel,
400 cycles 133X



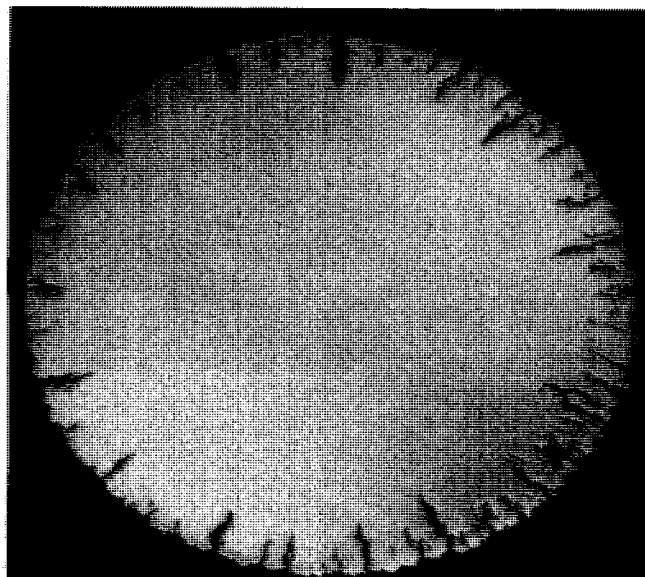
(a) 150 cycles 5X



(b) 290 cycles 5X



(c) 520 cycles 5X



(d) 800 cycles 5X

Fig. 20-Sequence of crack propagation in 4340 steel,
in air, 250-670°C

s can be seen in Figs. 20b-c. This steel seems to have failed very badly after 800 cycles (Fig. 20d) where cracks of 0.2 mm width and 1.6 mm depth can be seen. The severity and frequency of cracking clearly shows the unsuitability of such a steel for thermal fatigue resistance required of die steels.

The stress raising effect due to a thermocouple hole just 0.04 inch below the surface of a dummy sample can be seen in Fig. 19, where a large crack developed just above the hole at 400 cycles. Because of this reason, the thermocouple hole was made 1/8 inch below the surface in actual test-pieces which did not cause any stress raising effect in the cracking tendency as can be seen in Figs. 20b-d, where a uniform cracking developed all over the periphery and not preferentially at the location above the thermocouple hole.

The rate of cracking of this steel can be seen in Fig. 21. The cracking progresses at a very high rate up to a crack depth of about 1.2 mm and then the rate drops slightly. The reason for this drop in cracking rate is that the high temperature region (650-670°C) extends upto about 1.2 mm from the outer edge and the temperature drop is substantial beyond this region (Fig. 13a). Had there been a uniform high temperature region beyond 1.2 mm, the cracking would have progressed at almost the same rate in a linear manner.

Thus having established that the thermal fatigue test-

Fig. 21-Propagation of the longest crack with thermal cycling in AISI 4340 steel

AISI 4340 STEEL

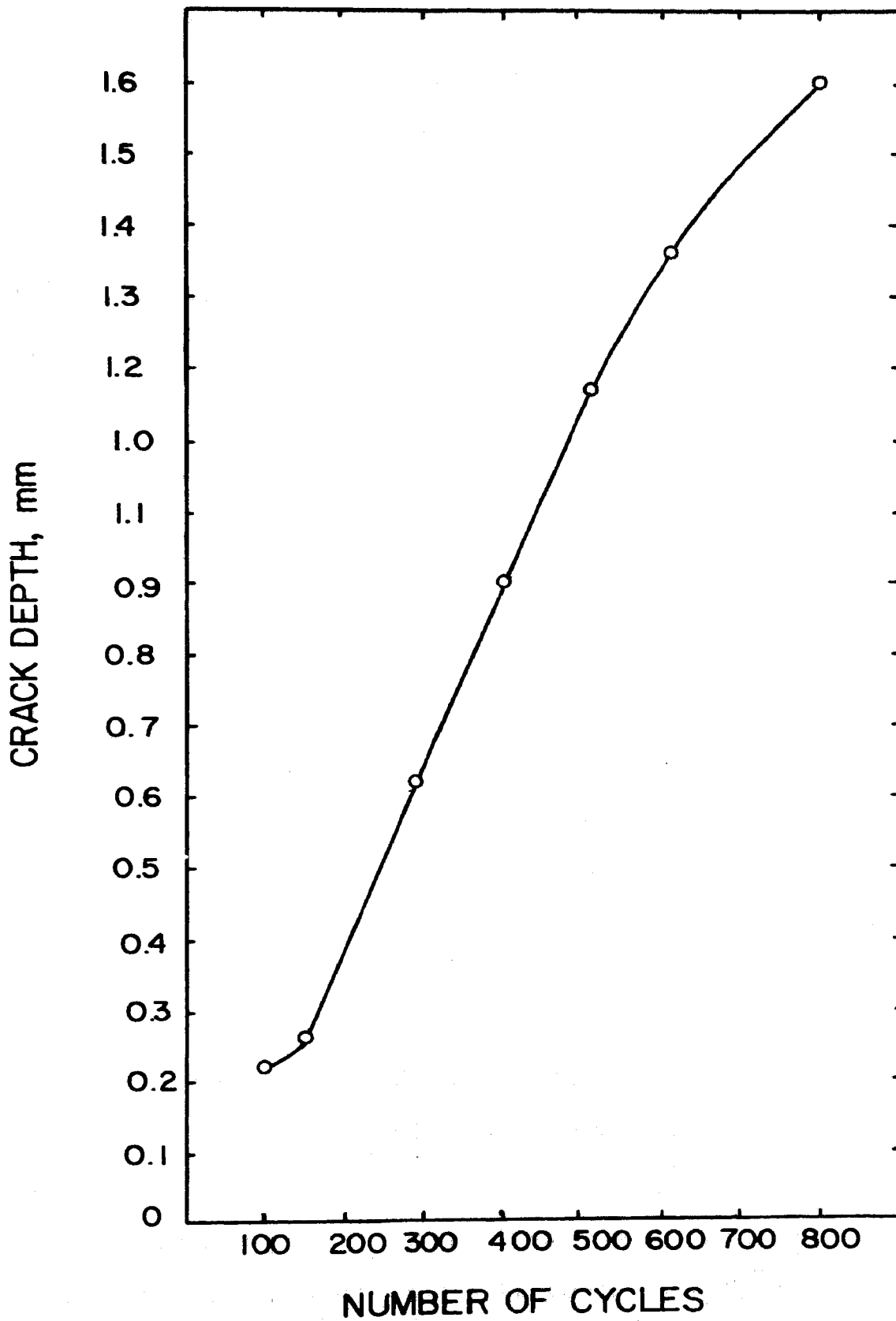


FIGURE 21

ing procedure carried out on 4340 steel reproduces the thermal fatigue behavior encountered in die casting dies, it was decided to continue the same testing technique on the commercially available and the potential candidate die steels to evaluate their resistance to thermal fatigue.

1. Ladish D-11 Steel

1. Heat Treatment

Group I: Austenitized at 1800°F for $\frac{1}{2}$ hour, air quenched and double tempered for 4+4 hours at 1100°F.

Group:II: Austenitized at 1800°F for $\frac{1}{2}$ hour, air quenched and double tempered for 4+4 hours at 1200°F.

2. Hardness

Hardness of samples as received - Rc 29

Hardness of samples of Group I after heat treatment -

Rc 48

Hardness of samples of Group II after heat treatment -

Rc 40

3. Thermal Cycling

Heating time per cycle - 3.3 seconds

Cooling time per cycle - 20.1 seconds

4. Results

Crack initiation of Group I samples - 125 cycles

Crack initiation of Group II samples - 75 cycles

TABLE VI

CRACK PROPAGATION WITH THERMAL CYCLING IN LADISH D-11 STEEL

Group I		Group II	
Number of Cycles	Crack length, mm	Number of Cycles	Crack length, mm
125	.46, .43, .41, .40, .38 (2)*, .35, .31 (2), .30, .25(2), .18, .17	75	.40, .39, .38, .33, .18, .17, .15, .13 (2), .10
300	.71, .68, .64 (2), .58 (2), .50, .49, .44 (2), .42, .29, .28 (2), .27, .24	300	.84, .79, .78, .77, .69, .68, .65, .64, .62 (2), .59, .58, .56, .55, .54, .53, .47 (2), .45, .37, .33, .30, .25
500	.99 (2), .89, .88, .83, .80, .75, .71 (2), .69, .65, .64, .63, .62, .61, .58, .56, .55, .52, .40, .38 (2)	500	1.20, 1.18, .92 (2), .90, .86 (2), .82 (2), .78, .76 (2), .72, .71, .66, .62, .60 (2), .54
700	1.17, 1.06, 1.03, .98, .97, .96, .95, .92 (2), .84, .78(2) .77, .76, .70 (3), .68, .66, .60, .55, .53, .47, .40, .38	700	1.47, 1.30, 1.28, 1.27, 1.25, 1.08, 1.06 (2), 1.03 (2), .98, .97, .95, .90, .86, .85 (2), .80 (2), .75, .66, .60, .56, .55, .54, .35, .34
900	1.31, 1.23, 1.22 (2) 1.12, 1.10, 1.08, 1.05, 1.04, 1.03, 1.02, .97, .96, .95, .94 (2), .90 (2), .88, .80, .77, .72 (2), .65, .63, .62, .47, .40	900	1.62, 1.43, 1.27, 1.24, 1.20 (3), 1.18, 1.15, 1.10, 1.08, 1.07 (2), 1.02, 1.00 (2), .98, .96, .88, .87, .85, .80, .76, .68, .47, .35, .26

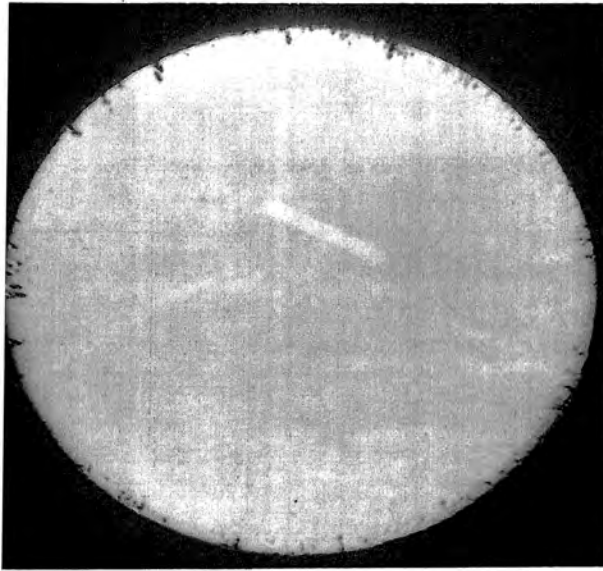
* Number within parenthesis indicates the number of cracks of same length. Same notation is followed in all later tables.

. Discussion of Results

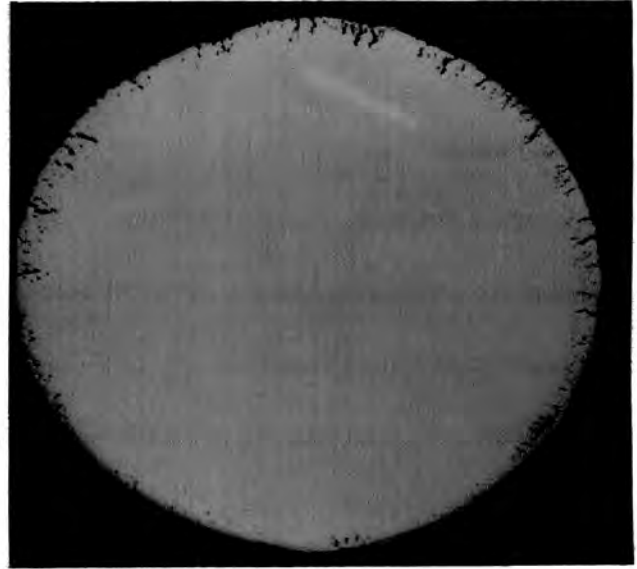
This steel was found to get oxidized badly within few cycles. The sequence of crack propagation in samples of hardness Rc 48 is shown in Figs. 22a-d while for samples of hardness Rc 40 is shown in Figs. 23a-d. The cracks are longer and wider for the lower hardness samples and at 900 cycles, both groups of samples show severe cracking, comparable with 4340 steel samples (Figs. 20c-d). The crack widths are upto 0.15 mm.

The fast rate of crack propagation can be seen in Fig. 24. The crack length varies almost linearly with the number of cycles upto high temperature region of 1.2 mm depth and then the cracking rate drops due to low temperature region beyond this depth. Cracking rates are 0.00191 and 0.00132 mm/ cycle for Rc 40 and Rc 48 hardness samples respectively, as calculated from the slope of curves in the linear region. It clearly indicates low resistance of steel to thermal fatigue at lower hardness levels. The shape of the curves drawn are almost similar for both hardness levels.

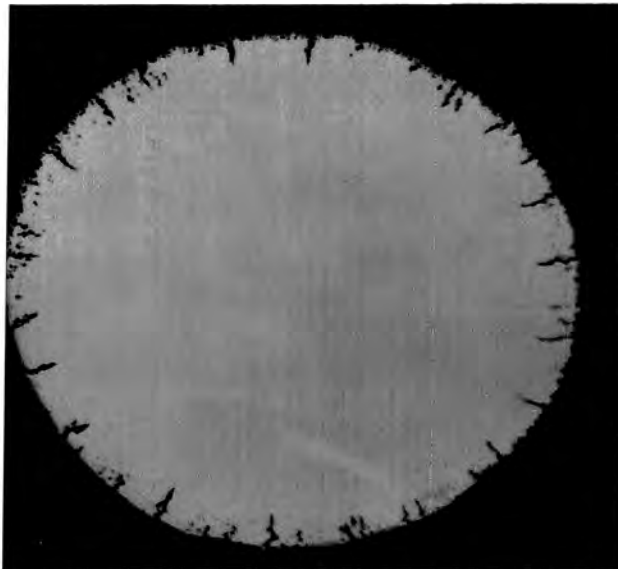
Curves have also been drawn for cumulative number of cracks vs crack lengths in Figs. 25 and 26. These curves indicate that the cumulative number of cracks increase with the increase in crack lengths for fixed number of cycles. Further, at larger number of cycles, number of cracks of smaller lengths is less while the larger cracks



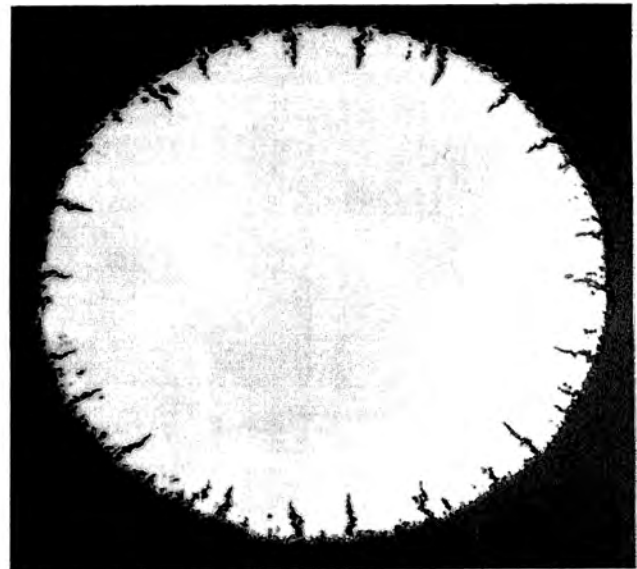
(a) 125 cycles 5X



(b) 300 cycles 5X

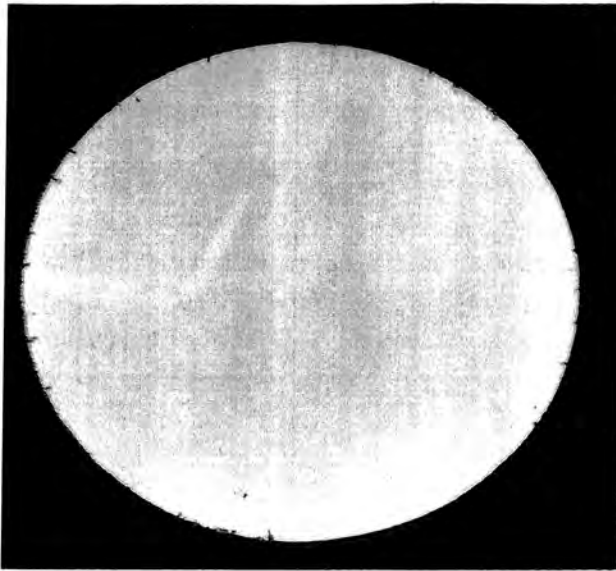


(c) 700 cycles 5X

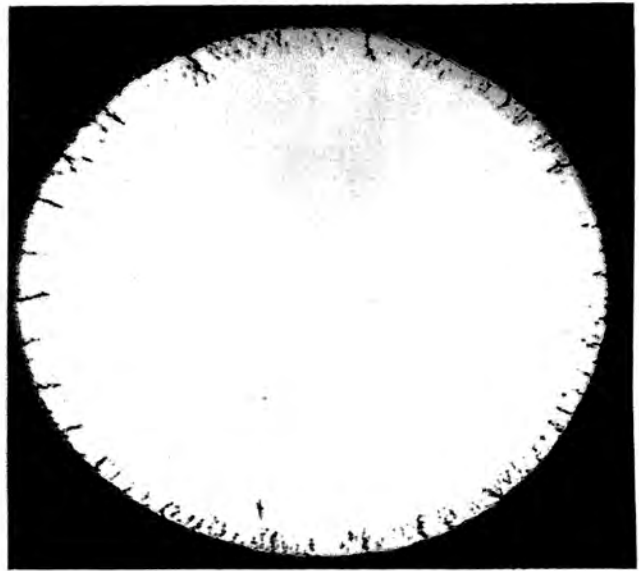


(d) 900 cycles 5X

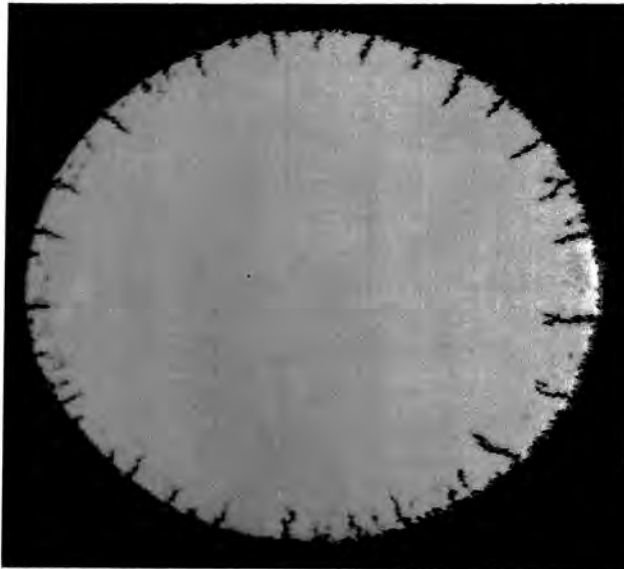
Fig. 22-Crack propagation in Ladish D-11 steel
samples of hardness Rc. 48



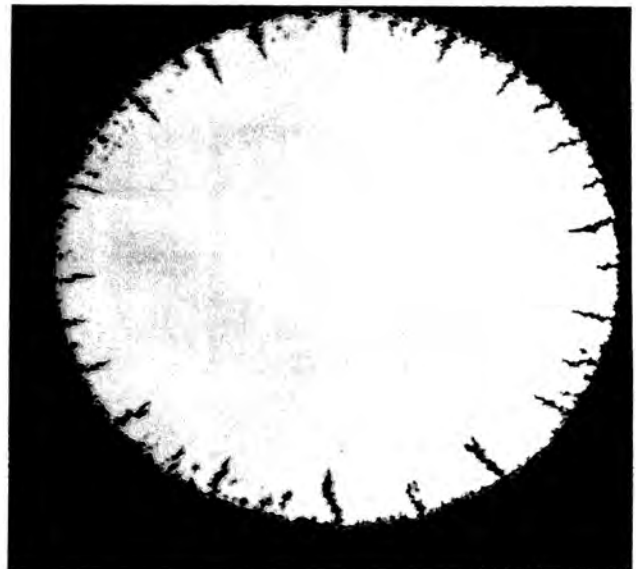
(a) 100 cycles 5X



(b) 300 cycles 5X



(c) 700 cycles 5X



(d) 900 cycles 5X

Fig. 23-Crack propagation in Ladish D-11 steel samples of hardness Rc. 40

ig. 24-Propagation of the longest crack with thermal cycling in Ladish D-11 steel samples of hardness Rc 48 and 40

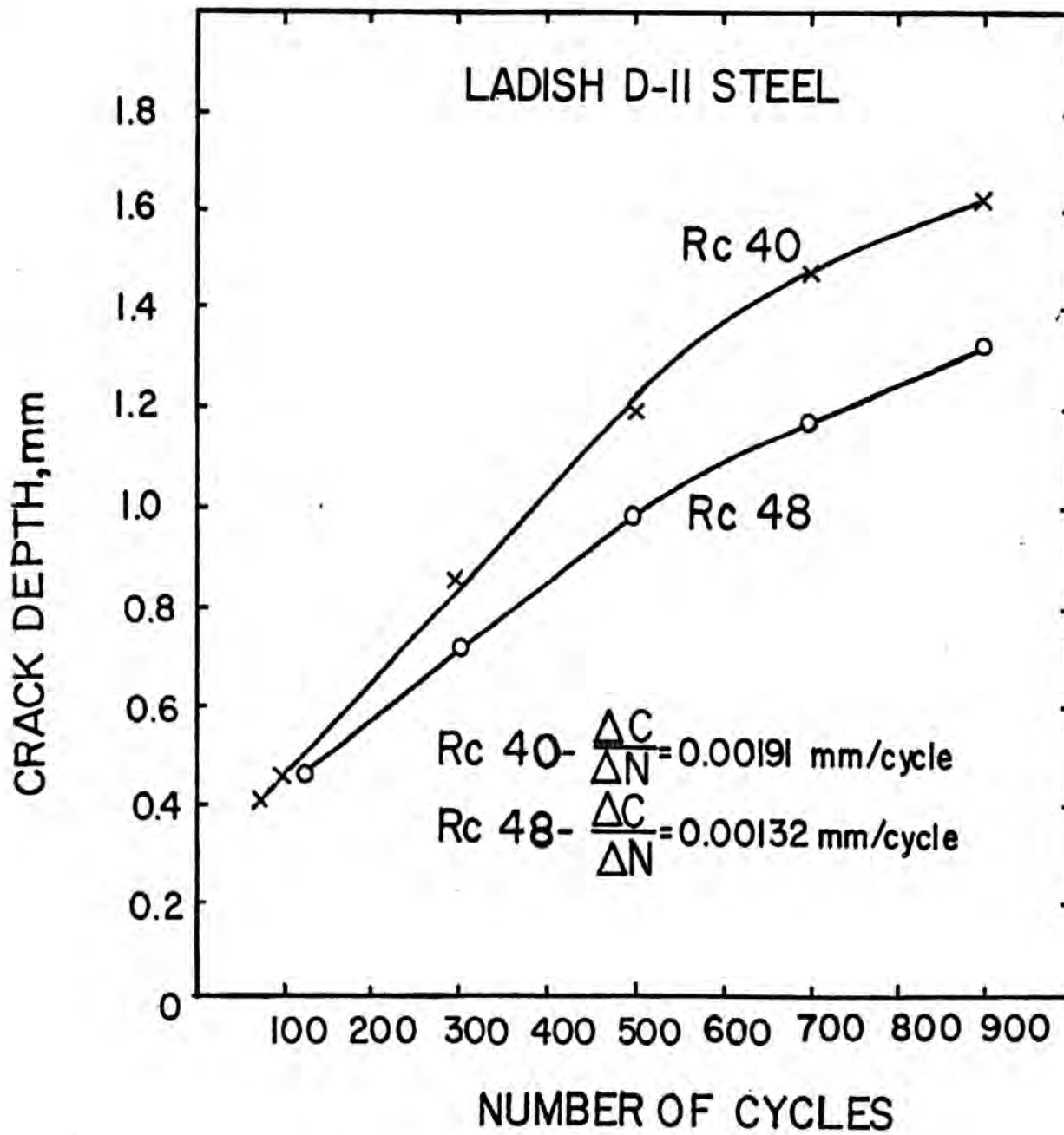


Fig. 25-Cumulative number of cracks versus crack length
at different stages of thermal cycling in Ladish
D-11 samples of hardness Rc 48

LADISH D-II STEEL Rc. 48

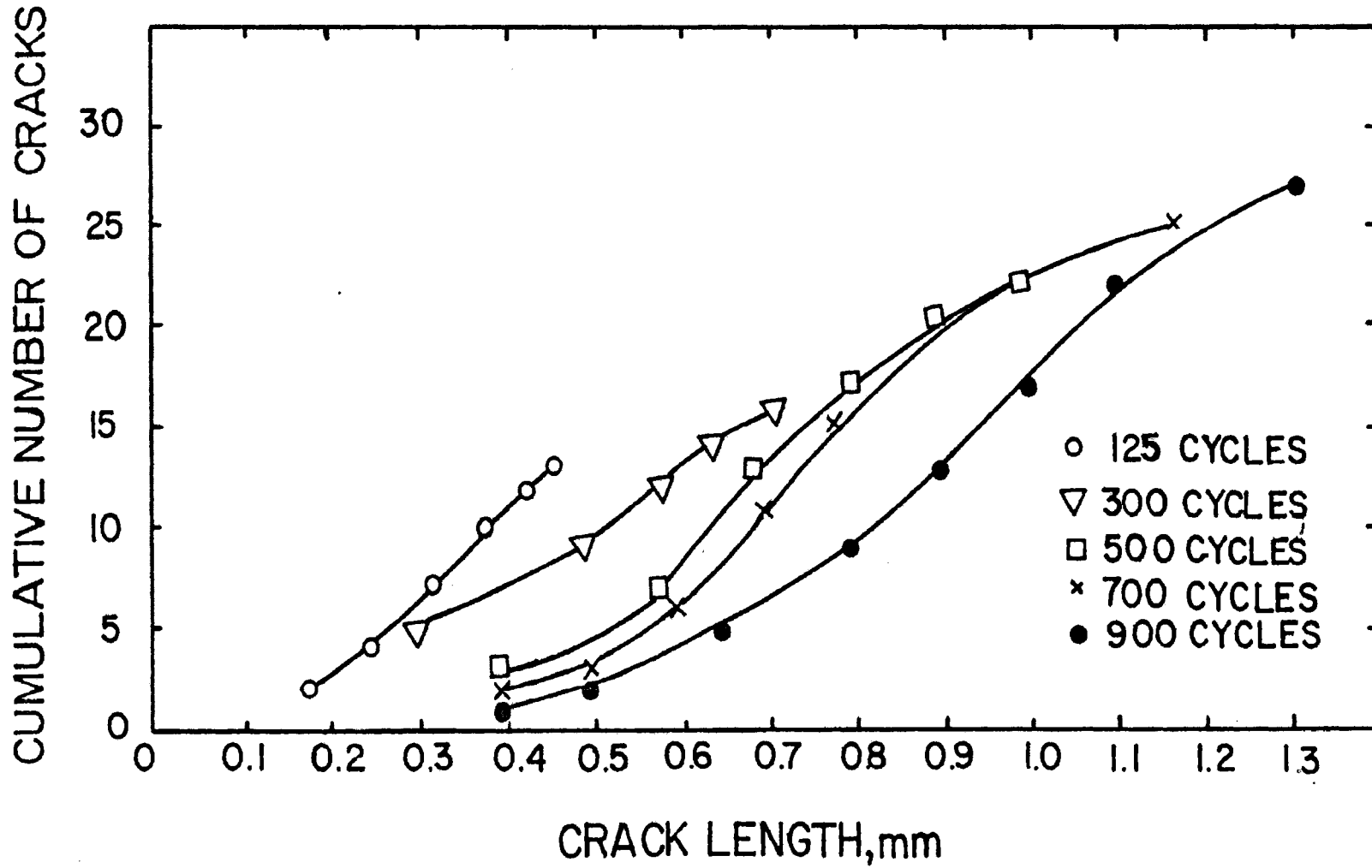
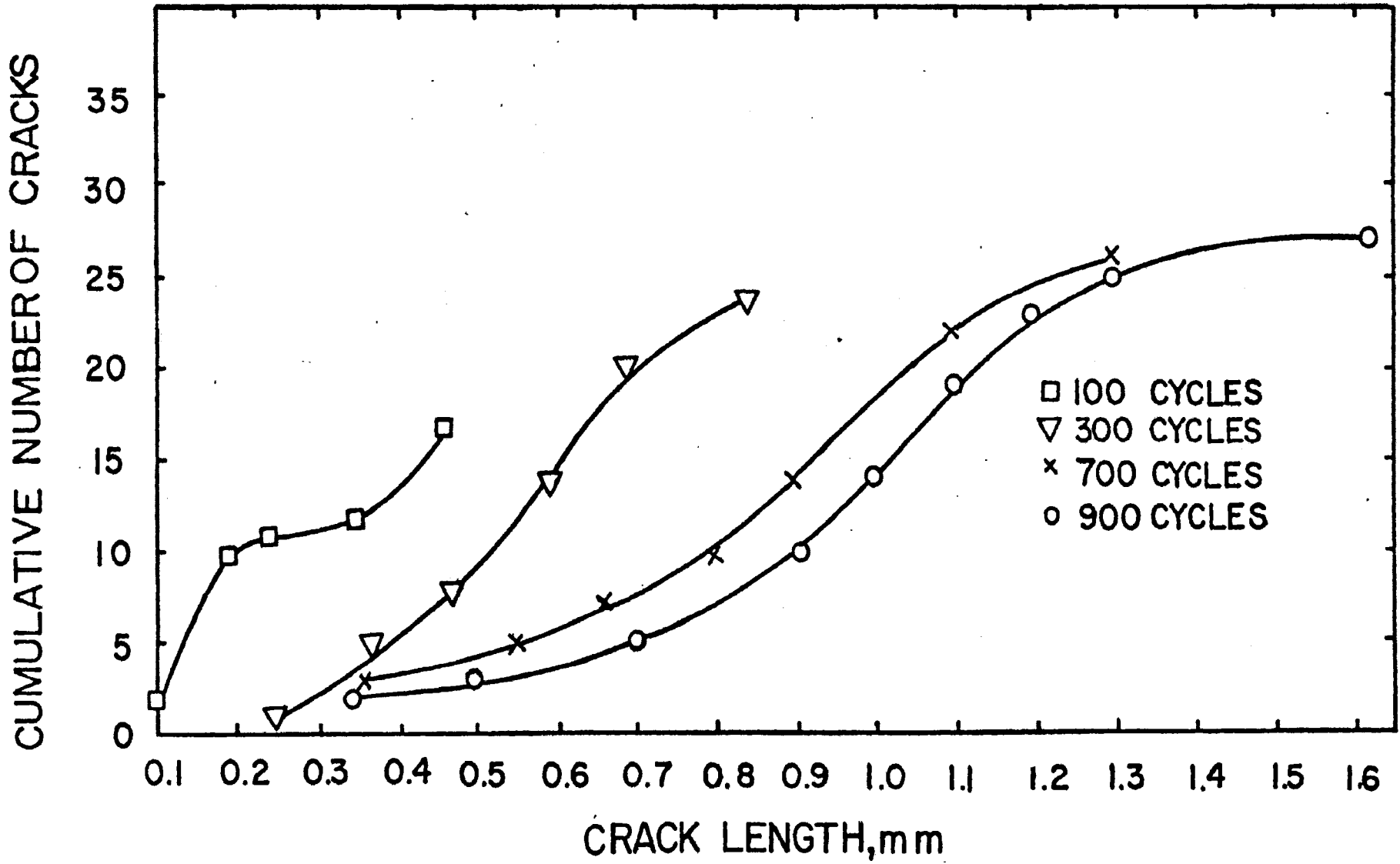


FIGURE 25

Fig. 26-Cumulative number of cracks versus crack length
at different stages of thermal cycling in Ladish
D-11 samples of hardness Rc 40

LADISH D-II STEEL R_c. 40



are more (Figs. 22 and 23). It brings out the fact that during earlier stages of cycling, more and more new cracks are initiated while during the later stages, earlier existing cracks are propagated and fewer number of new cracks are initiated.

Because of unexpectedly low number of cycles to failure and severe cracking rates, as compared to other die steels tested (see later sections), Ladish Company was requested to supply a new lot of D-11 steel bars. The latter lot was properly machined, heat treated to the Rc 48 and Rc 40 hardness levels and tested for thermal fatigue as before. But again, all the samples showed the same results as shown by the earlier lot, thereby indicating the reproducibility of the results by the present testing technique.

3. H-11 Die Steel

1. Heat Treatment

Austenitized at 1825°F for $\frac{1}{2}$ hour and air quenched.

Double tempered for 2 + 2 hours at 1025°F.

2. Hardness

Hardness of hot rolled and annealed samples - Rc 22

Hardness of heat treated samples - Rc 49

3. Thermal Cycling

Heating time per cycle - 3.0 seconds

Cooling time per cycle - 19.8 seconds

. Results

Number of cycles for crack initiation - 1100

TABLE VII

CRACK PROPAGATION WITH THERMAL CYCLING IN H-11 STEEL

umber of Cycles	Crack length, mm	Number of Cycles	Crack length, mm
1100	.06, .05, .045, .04(2)	3400	.62, .55, .54, .53, .48, .47, .45, .42, .40, .39, .38,
1300	.10, .09, .08, .075, .05, .04		.31(2), .29, .28, .27, .26(2), .25, .21(2), .20(3),
1600	.12, .11(2), .10(2), .09(3), .08, .07(4), .06, .05		.19, .18(2), .17, .15(3), .14, .13, .12(2), .11, .10(2), .06, .03
1900	.18(2), .16(5), .14, .12(2), .08, .06, .05(2), .02	3800	.80, .75, .68, .66, .65, .62, .60(4), .52, .50, .47(2), .40, .36, .35(2), .30, .28, .27(2), .24(2), .21, .20(2), .19, .18, .16, .15, .14(2), .13, .12(5), .10, .08
2200	.24, .23, .21, .20, .18(5), .15, .14, .13, .12(3), .11(2), .10(2), .08, .06(4), .05, .04, .03(2), .02(2)		
2600	.35, .31(2), .28, .26(2), .25(4), .24(2)	4200	.98, .94, .85, .80, .77, .75(2), .71, .70, .68, .63, .60(2), .55, .53, .45, .42, .40, .38, .36, .34, .30, .28(2), .24, .23, .22, .21, .19, .18, .13(4), .11, .10(2), .08
3000	.23(2), .21, .20(2), .19, .18(3), .16, .15(3), .14, .13, .12(2), .11(2), .10, .08, .07, .05, .04		
	.48, .47, .42, .39, .38, .37(2), .36, .35, .34(2), .30, .29, .27(3), .26, .25, .24, .23, .21, .20(2), .19, .18(2), .17(3), .16, .14, .13, .12, .11, .10(2), .09, .06(2)		

Discussion of Results

H-11 was found to form a thin but adherent and impervious oxide layer due to the presence of large amount of chromium. The cracking tendency is therefore reduced due to presence of this protective oxide layer. A comparison of the resistance of this steel to thermal cycling and oxidation can be seen in Figs. 27a-b. A sample of H-11 (Fig. 27a) showed very little oxidation near the outer periphery (high temperature zone) after 200 cycles whereas a test-piece of 4340 steel was found to have oxidized and cracked badly after only 800 cycles (Fig. 27b). It is because of this higher resistance to thermal fatigue that H-11 is used for hot work die steels.

Crack initiation in this steel is found to start with the formation of oxide lined sharp microcracks as shown in Fig. 28a. This microcrack then propagates with further cycling as in Fig. 28b and finally forms a macrocrack in the metal as shown in Fig. 28c. The sharp tip of the crack can be seen in all the three photographs.

Crack propagation on macroscale is depicted in Figs. 29a-d for the sample cycled between 2200 to 4200 cycles. The cracks seem to open up at the edges with further cycling (Figs. 29c-d) and finally can become large enough to entrap the molten metal in actual die casting operations.

Fig. 30 shows a plot between the longest crack

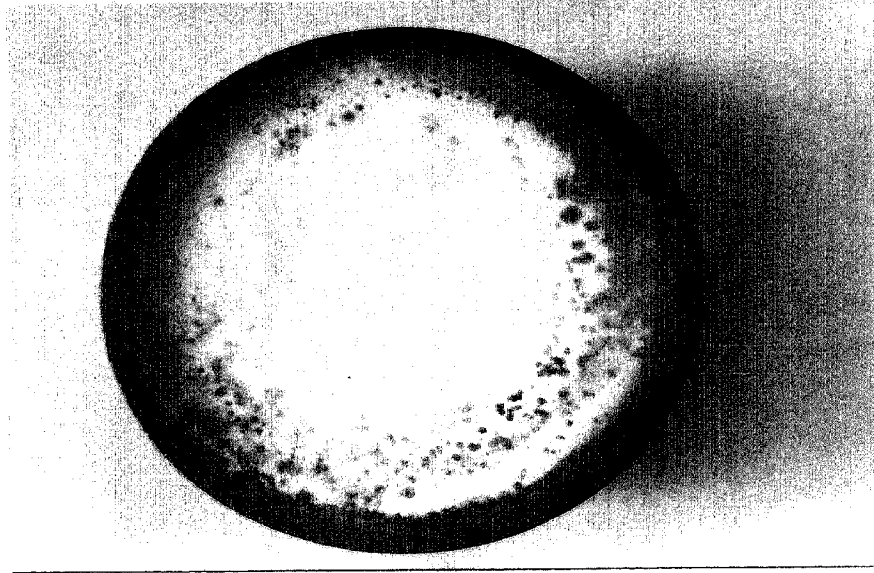
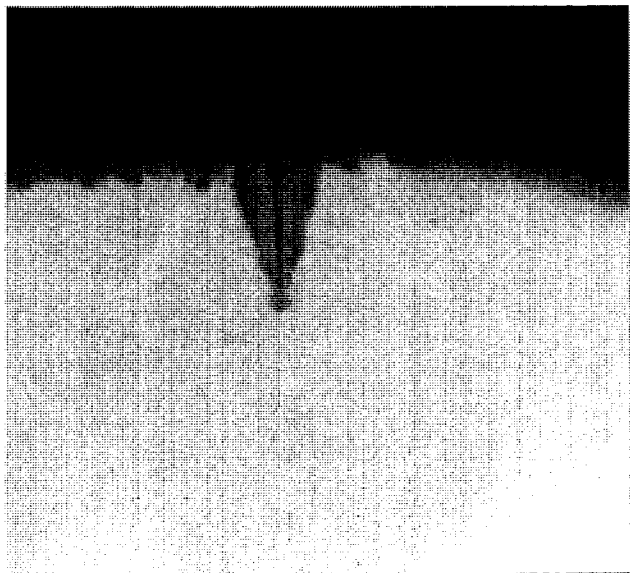


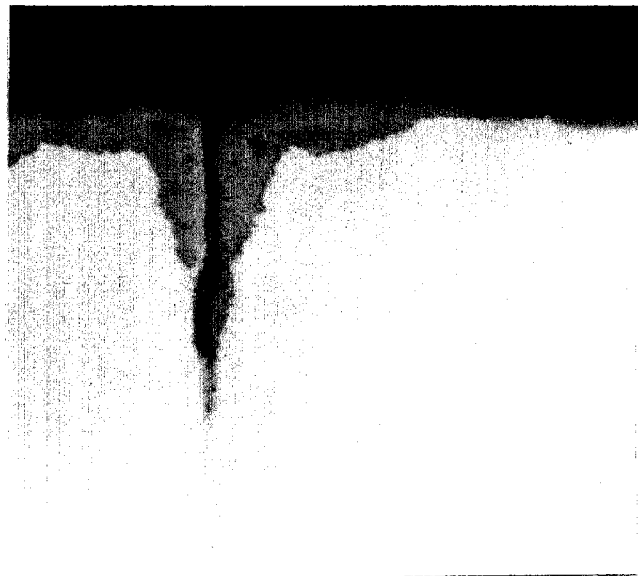
Fig. 27(a)-A thin, adherent oxide film formed
in H-11; unpolished surface, 1200 cycles 5X



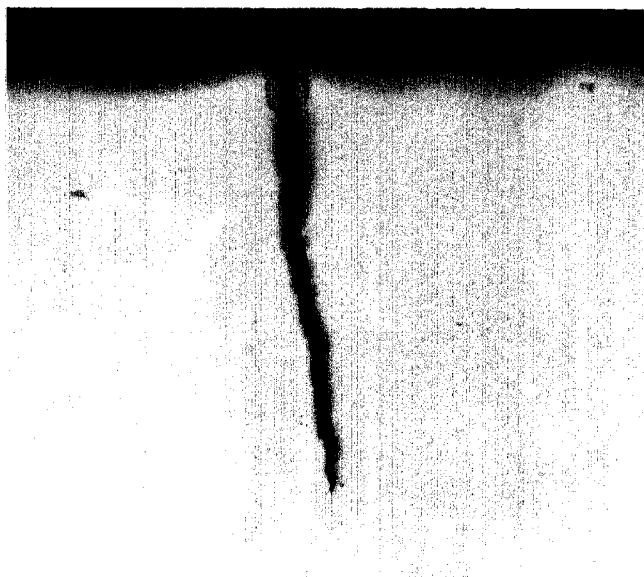
Fig. 27(b)-Brittle oxide scale and cracking in
4340 steel; unpolished sample, 800 cycles 8X



(a) 1125 cycles 266X

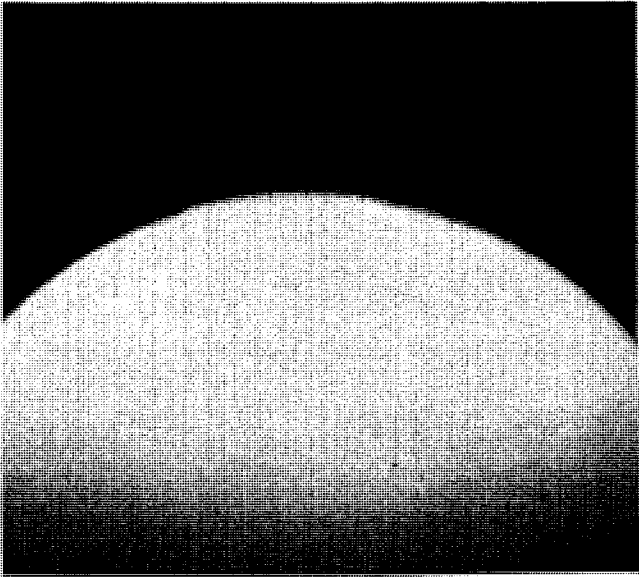


(b) 1250 cycles 266X

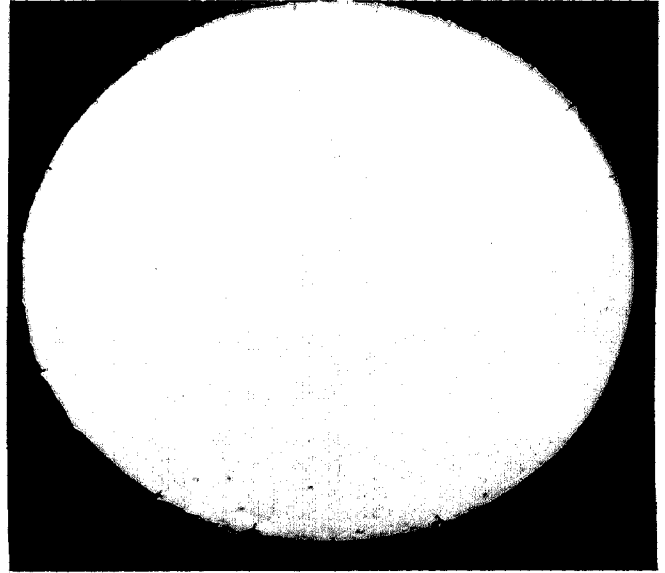


(c) 3000 cycles 133X

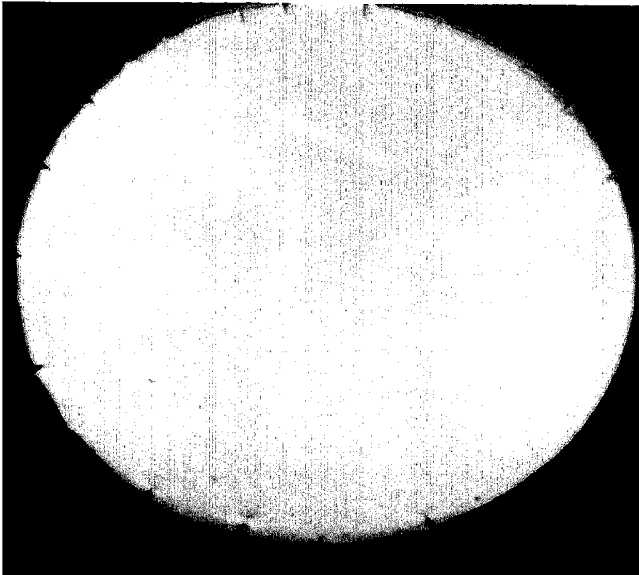
Fig. 28-(a) Initiation of a microcrack; (b) propagation of microcrack; (c) large macrocrack formed in H-11. Note the sharp tip of crack in (a)-(c). All these photographs are of the same crack after different number of cycles.



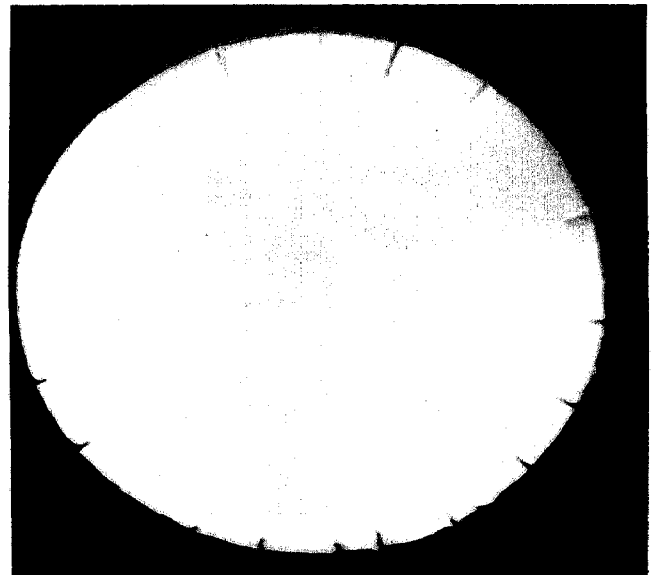
(a) 2200 cycles 7X



(b) 3000 cycles 5X



(c) 3400 cycles 5X



(d) 4200 cycles 5X

Fig. 29-Propagation of thermal fatigue cracks
with further cycling in H-11

Fig. 30-Propagation of the longest crack with thermal cycling in AISI H-11 steel

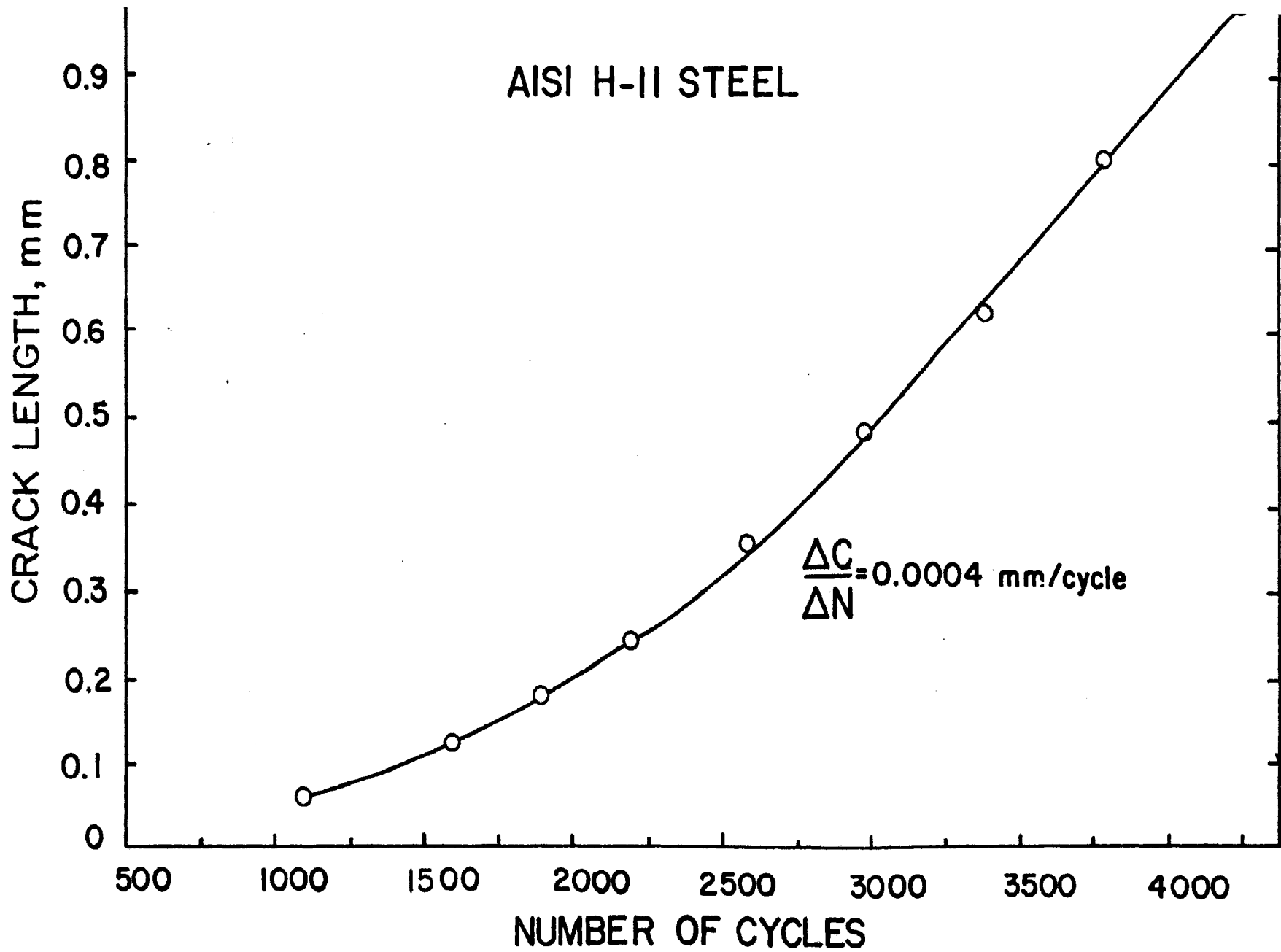


FIGURE 30

number of cycles. During the early stages, new cracks are created and also propagated while during the later stages of cycling mostly the earlier existing cracks are propagated. Hence slope of the curve is slightly lower initially while later it increases almost linearly. The crack propagation rate in the linear region of the curve is 0.0004 mm/ cycle.

Fig. 31 shows the cumulative distribution of all the cracks and the crack lengths for different number of cycles. The graph shows almost a linear relation between the cumulative number of cracks and crack length at larger number of cycles. At smaller number of cycles, the linear region is cut short probably as two phenomena, namely, the initiation and propagation of cracks, take place while only the latter phenomenon predominates at larger number of cycles.

H-13 Die Steel

Heat Treatment

Austenitized at 1850°F for $\frac{1}{2}$ hour and air quenched.

Double tempered at 1040°F for 4 + 4 hours.

Hardness

Hardness of samples received - Rc 22

Hardness after heat treatment - Rc 49

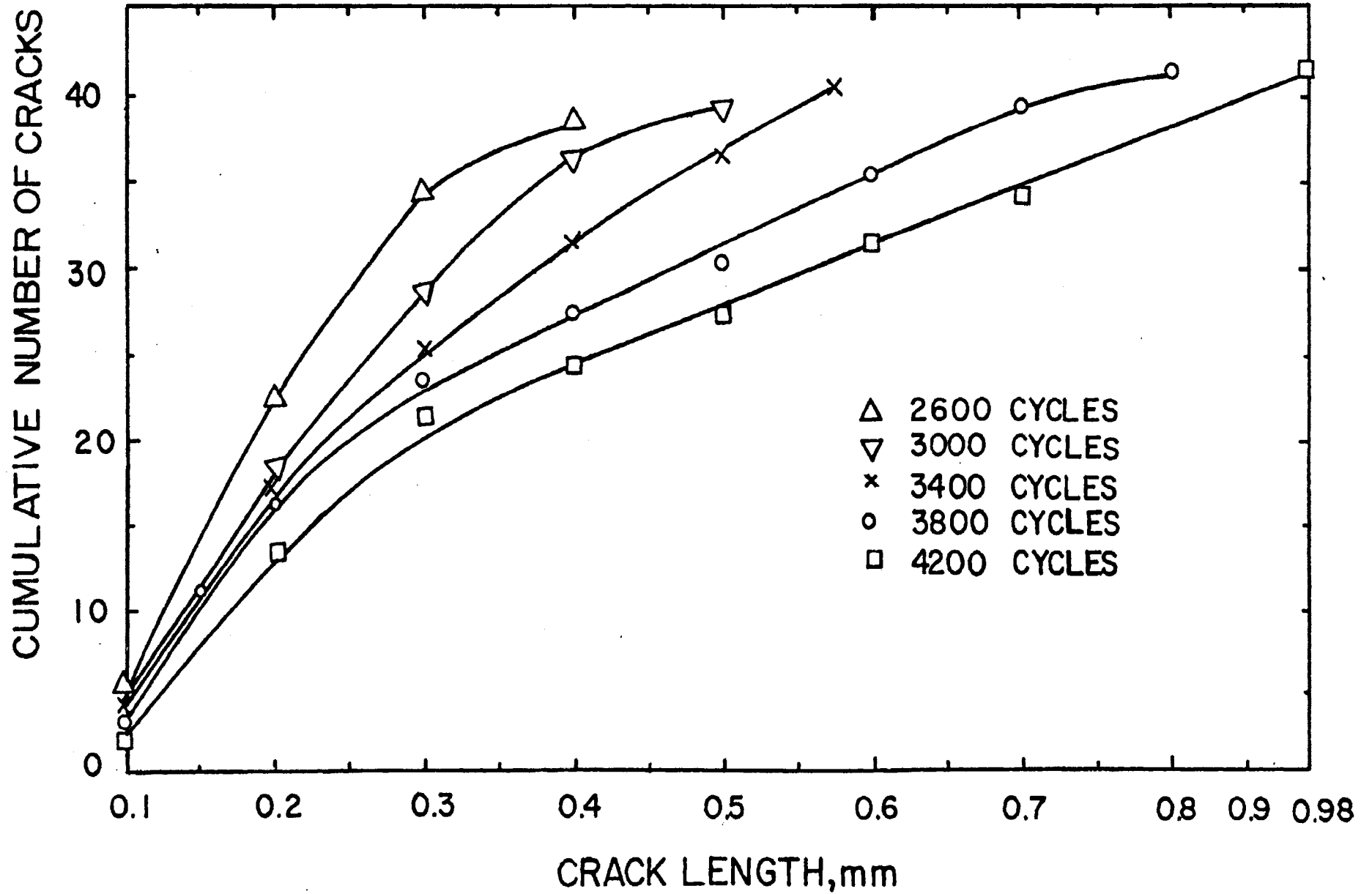
Thermal Cycling

Heating time per cycle - 3.0 seconds

Cooling time per cycle - 19.8 seconds

.g. 31-Cumulative number of cracks versus crack length
at different stages of thermal cycling in AISI
H-11 steel

AISI H-II STEEL



Results

Number of cycles for crack initiation - 1330

TABLE VIII

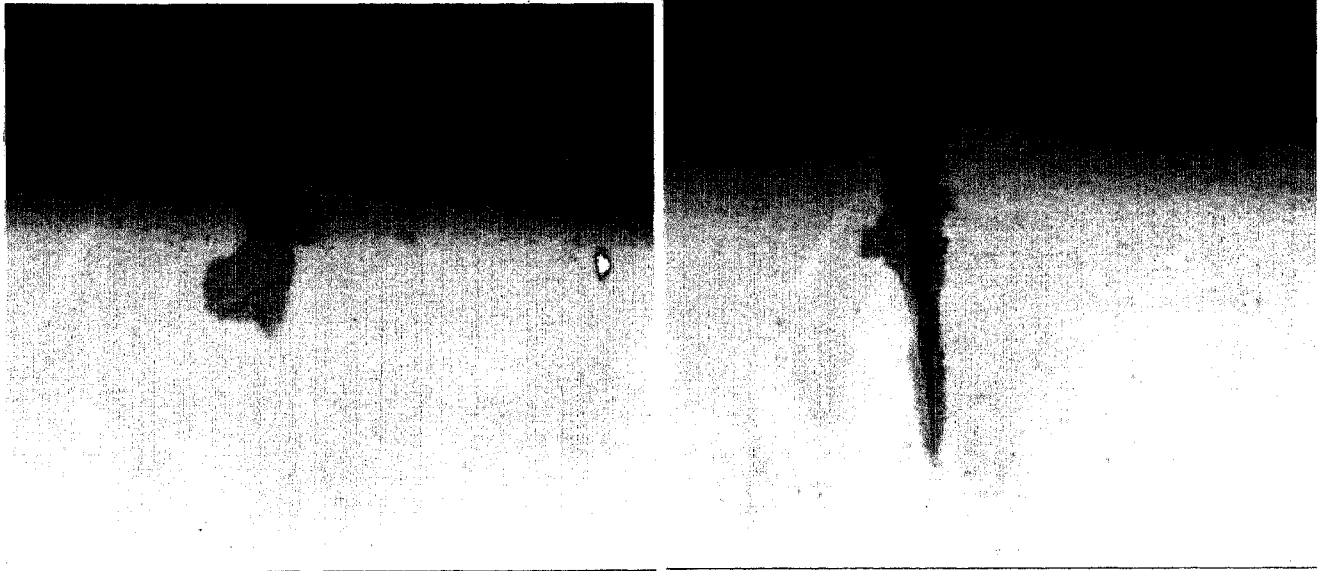
CRACK PROPAGATION WITH THERMAL CYCLING IN H-13 STEEL

Number of Cycles	Crack length, mm	Number of Cycles	Crack length, mm
1330	.07, .045	3400	.62, .365, .34, .30, .275, .26, .235,
1500	.082, .045, .02		.20, .18, .175,
1925	.19, .15, .06, .05, .04(2), .03		.17, .15, .13, .11, .10(2), .09(2), .08, .06, .05
2200	.24, .13, .12, .11, .08, .07(2), .06, .055, .04, .025, .02	3800	.79, .49, .48, .39, .36, .33, .30, .28, .25, .23, .22, .20, .18, .15(2), .13, .12, .08, .07, .05, .04, .03, .02
2600	.38, .175, .15, .14(2), .13, .10, .07(2), .065, .055, .05(2)	4200	.93, .58, .57, .48, .45, .44, .39, .38, .34, .30, .26, .24, .22, .20(2), .19, .16, .12, .10, .08(3), .05
3000	.50, .285, .26, .25, .22, .20, .17, .16, .15, .14, .13, .11, .10, .09, .06, .05, .05(2), .03		

Discussion of Results

This steel was also found to form a thin, adherent and protective oxide coating on the surface during cycling like H-11 but was more resistant to thermal fatigue cracking than H-11.

The cracking sequence on microscale is shown in Figs. a-c. As in H-11, initially very fine microcracks are formed



(a) 1330 cycles 400X

(b) 1600 cycles 400X



(c) 2700 cycles 133X

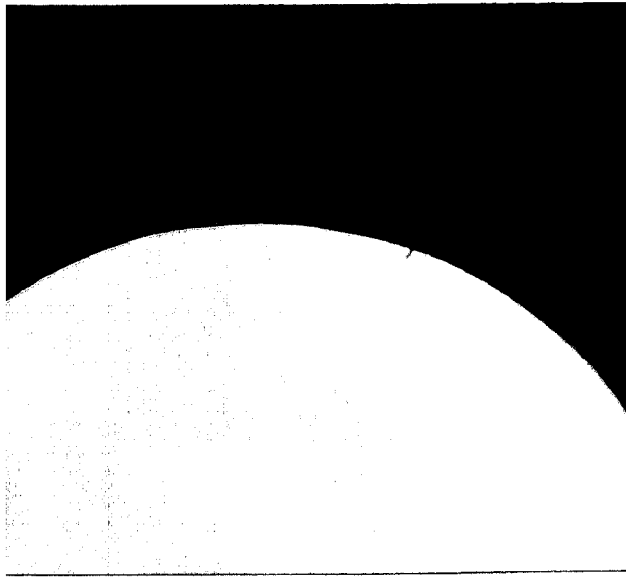
Fig. 32-(a) Initiation of a microcrack; (b) propagation of the microcrack; (c) a large macrocrack formation and its branching at an impurity or an inclusion in H-13

the edges (Fig. 32a), which propagate both radially and depth wise on further cycling (Fig. 32b). As the testing is being carried out in air, the walls of the crack are lined with oxide film (Fig. 32b). Further cycling causes the crack to propagate further and also opens up the width of the cracks (Fig. 32c). A branching of the crack at some inclusion or non-homogeneity in the steel can also be seen in Fig. 32c.

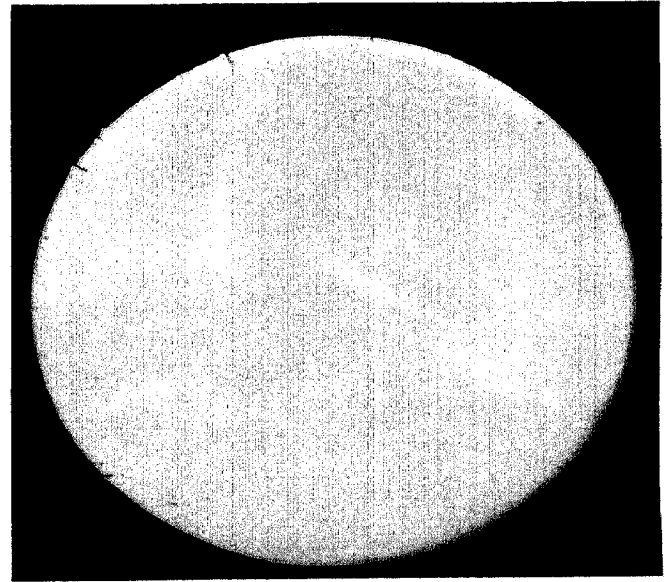
A macroview of the cracking on top surface is shown in Figs. 33a-d. Up to 3000 cycles, the cracks are comparatively smaller and fewer (Figs. 33a-b and Figs. 28a-b) than in H-11 steel. But the overall cracking sequence up to 4200 cycles is very much similar in the two steels. Some cracks, starting away from the edge can also be seen in Fig. 33d.

Progress of the longest crack with the increasing number of cycles is shown in Fig. 34. The initial region shows slightly smaller slope where both the crack initiation and crack propagation occurs. The later linear portion shows larger slope as the crack propagation phenomenon predominates at larger number of cycles. The crack propagation rate for this steel in the linear region is about $.000366\text{mm/cycle}$.

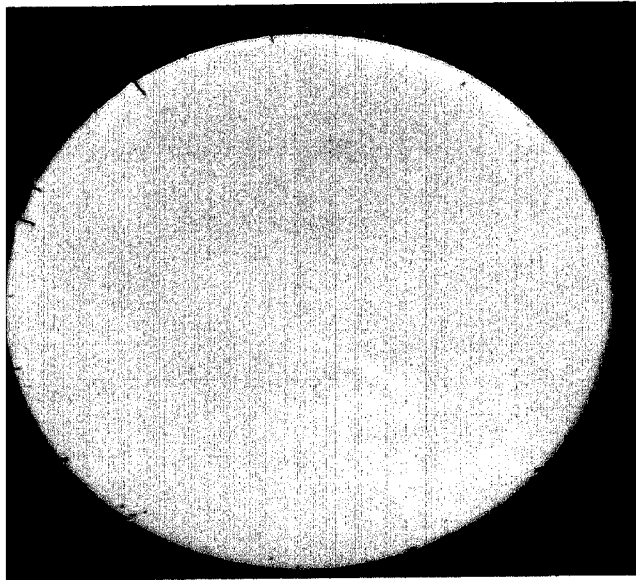
Fig. 35 shows the behavior of cumulative number of cracks at different cycles vs crack length for the region shown. These curves are very much similar to the one's shown for H-11 in Fig. 31.



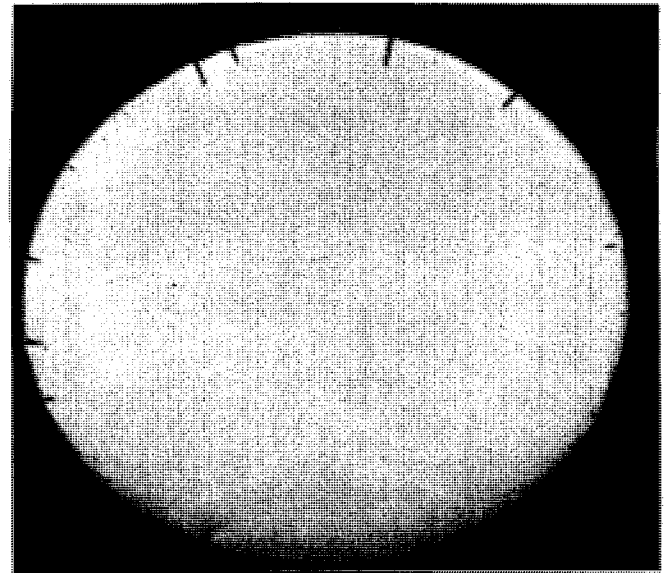
(a) 2200 cycles 7X



(b) 3000 cycles 5X



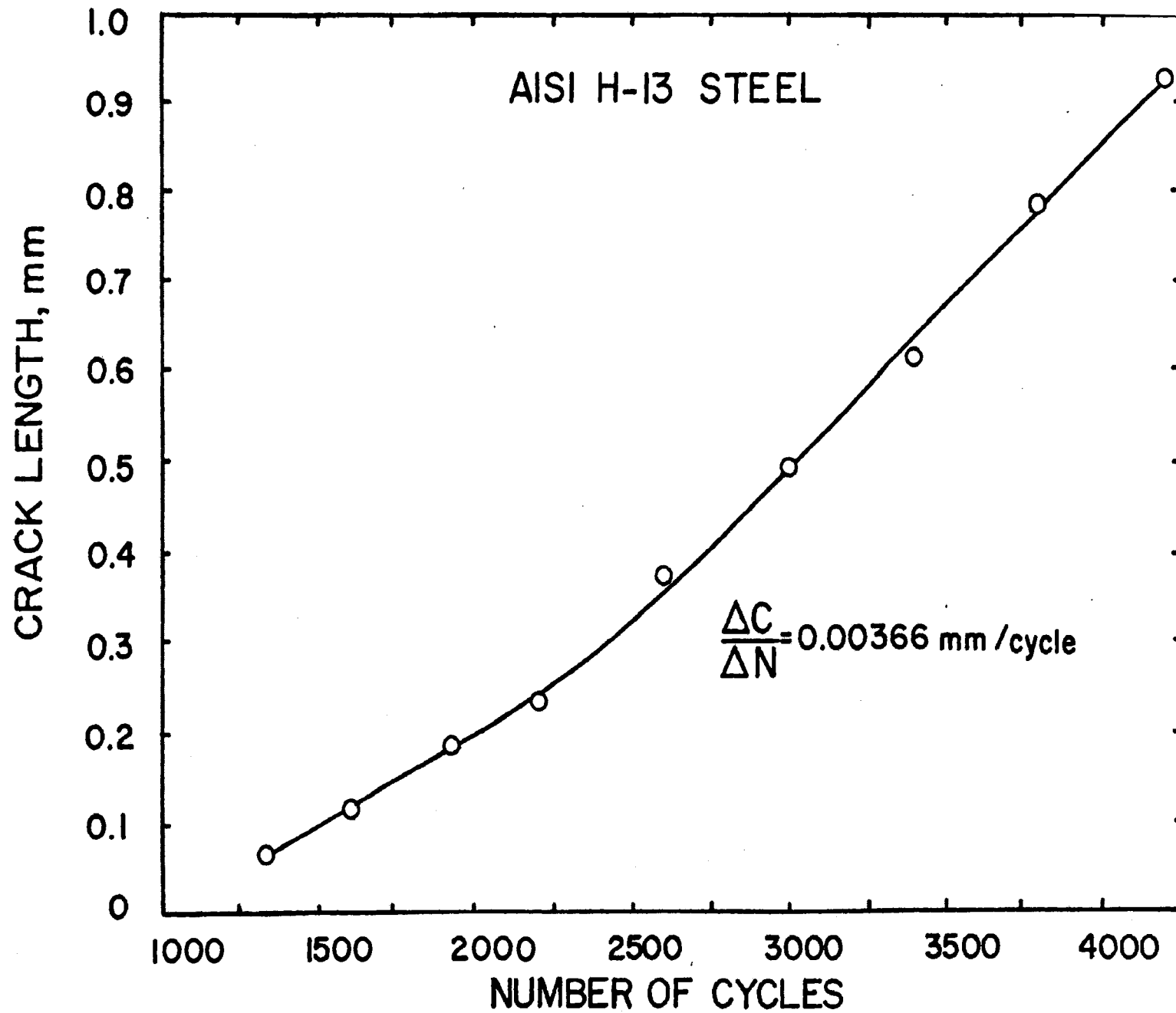
(c) 3400 cycles 5X



(d) 4200 cycles 5X

Fig. 33-A sequence of crack initiation and propagation on a macroscale in H-13. Note the cracks away from the edge in (c) and (d) which initiate at an inclusion or an impurity acting as a point of stress concentration.

g. 34-Propagation of the longest crack with thermal cycling in AISI H-13 steel



lg. 35-Cumulative number of cracks versus crack length
at different stages of thermal cycling in AISI H-13
steel

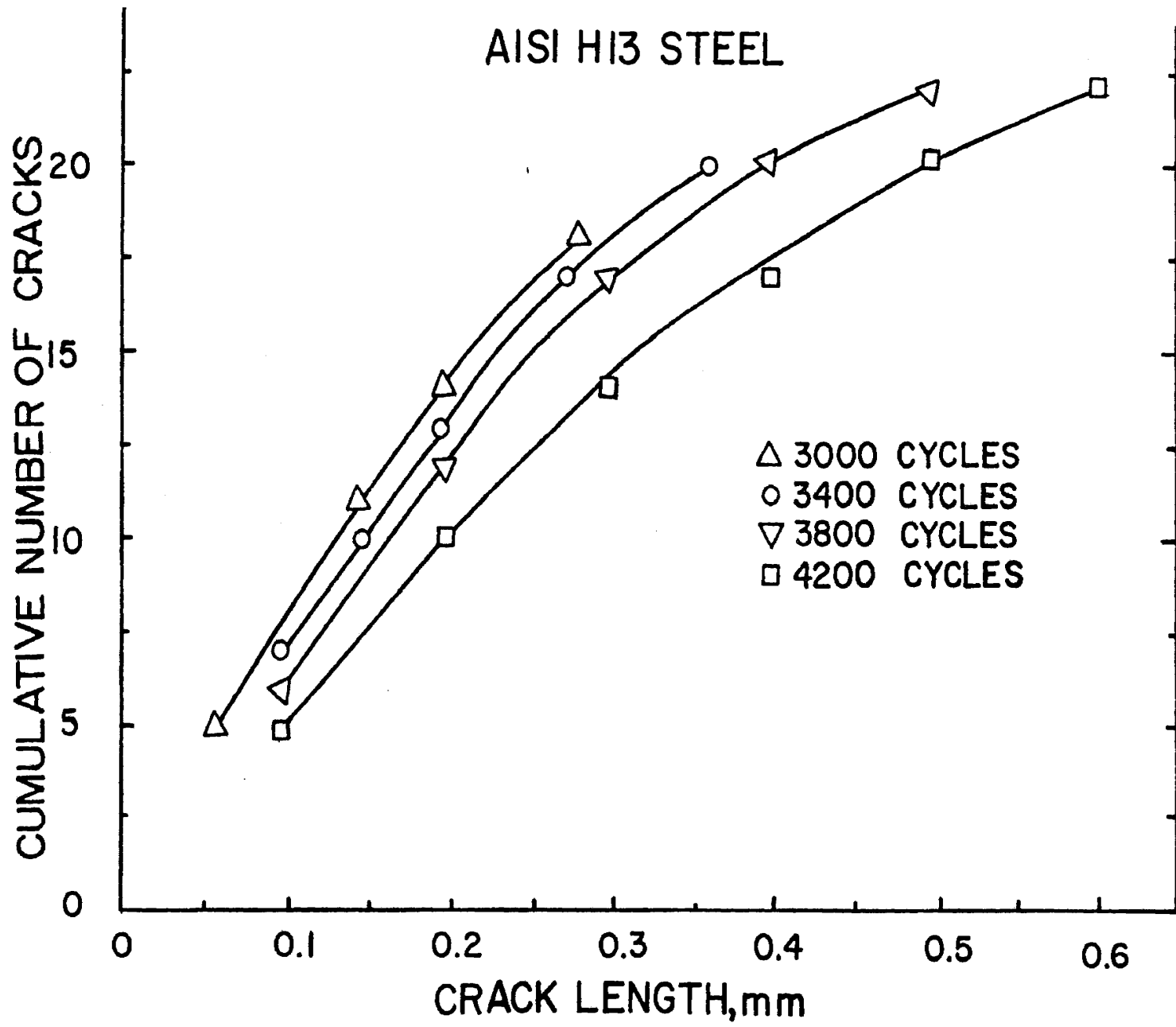


FIGURE 35

In general, H-11 and H-13 have the same composition except that vanadium is increased from 0.5 to 1.0 percent H-13. This increases the wear resistance of the steel. It is obvious from above data, H-13 gave slightly better resistance to thermal fatigue than H-11. The behavior of both steels was found to be very similar in all the experiments which is also borne out from similarity of photographs and graphs shown for both steels.

H-21 Die Steel

Heat Treatment

Austenitized at 2150°F for 15 minutes and air quenched.

Double tempered at 1120°F for 2 ± 2 hours.

Hardness

Hardness of the samples as received - Rc 22

Hardness after heat treatment - Rc 49

Thermal Cycling

Heating time per cycle - 2.6 seconds

Cooling time per cycle - 19 seconds

Results

Number of cycles for crack initiation - 1600

183271

TABLE IX

CRACK PROPAGATION WITH THERMAL CYCLING IN H-21 STEEL

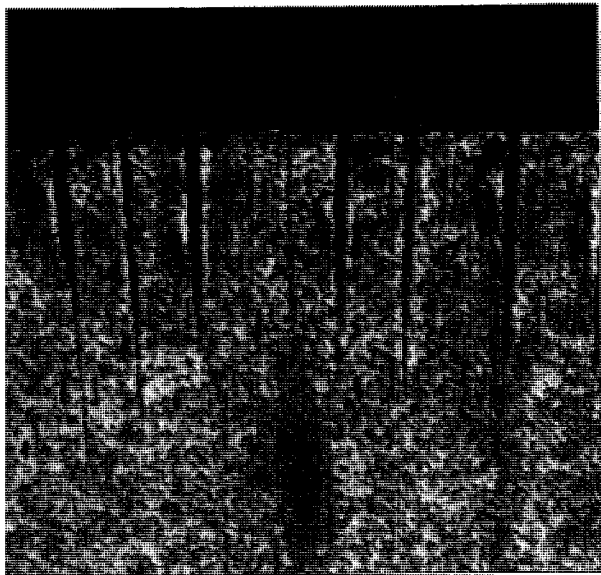
Number of Cycles	Crack length, mm	Number of Cycles	Crack length, mm
1600	.20	3400	.92, .73, .63, .61, .60, .57, .55, .53, .44(2), .43, .42, .39, .38, .37, .36, .35, .30(2), .28, .26, .25, .23, .20(2), .17, .16, .15(2), .12(2), .10(2), .08(3)
1725	.21		
1925	.30, .15, .10(4), .08, .07		
2100	.32, .18, .12(2), .11(2), .10(2), .08, .07, .06(5), .05(2), .04(2)	3800	1.07, .80, .73, .70, .69, .68, .60, .59, .55, .51, .50, .49, .45, .43, .40, .38(2), .37, .35(2), .30(2), .29(2), .28, .27, .25, .20(2), .19(2), .18, .17, .16, .10(2)
2400	.45, .33, .25, .22(2), .20(2), .19(2), .18, .17, .14(2), .12(2), .09(2), .08, .05(2), .04, .03(2), .02(2)		
2600	.54, .42, .38, .35, .34, .32, .30, .27, .26, .25, .24, .23, .22(2), .21, .20, .19(2), .18(4), .17, .15, .12(2), .10(4), .08, .06, .05(2), .04	4200	1.26, .85, .80, .79, .70, .69, .67, .58, .55, .53, .51, .49(2), .47, .46, .45, .44, .43, .40, .37, .36, .35, .34, .33, .32, .30(3), .29, .28, .25, .20(2), .19, .16, .14
3000	.72, .57, .52, .48, .47, .46, .43, .42, .38(2), .35, .33, .32(2), .30, .28(2), .27(2), .26, .25, .23, .21, .20(2), .16, .15, .14, .13, .10(2), .09, .08(2), .05(2)		

Discussion of Results

An oxide coating, thicker than in the case of H-11 and H-13 steels, is formed in this steel within first few hundred cycles. A typical phenomenon in the oxidation characteristics of this steel was observed which the author decided to investigate in great detail and came up with the following conclusions.

Long, thin, crack-like streaks are formed in the oxide coating during initial cycling (Fig. 36a). But when the sample is polished on the fine wheel, no cracks are observed on the metal surface. These superfluous cracks in the top oxide layer are observed even up to 1525 cycles, with no resultant cracking in the metal, as can be seen in Figs. 36b-c. The cracking in the metal starts only about 1600 cycles and then the crack propagation in the metal proceeds in a manner observed in H-11, H-13 and other steels tested. The crack propagation on the microscopic scale is clearly obvious from Figs. 36d-e. It is therefore the author's conclusion that if the oxide layer is not removed from the top, this steel shows better resistance to thermal fatigue cracking than H-11 and H-13 steels. Caution must be taken in not interpreting the initial superfluous cracks in the oxide layer as the cracks in the metal.

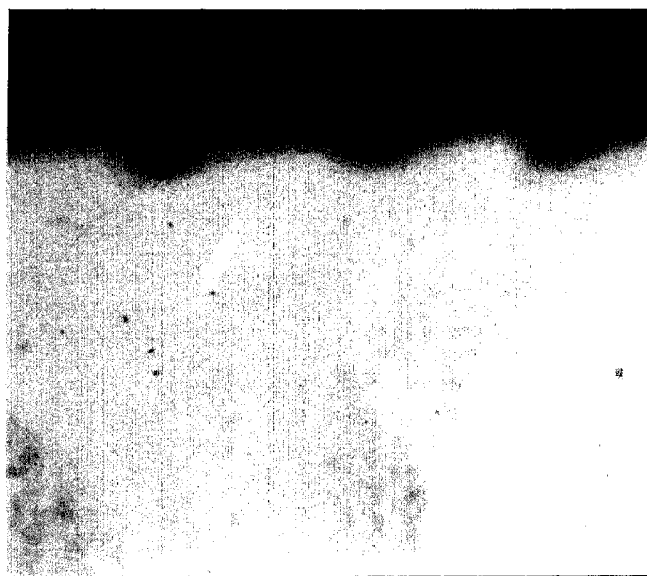
Crack propagation with further cycling on a macroscale is illustrated in Fig. 37a-d. Very sharp tipped and thin



(a) 450 cycles, unpolished
65X



(b) 1525 cycles, partly
polished 266X

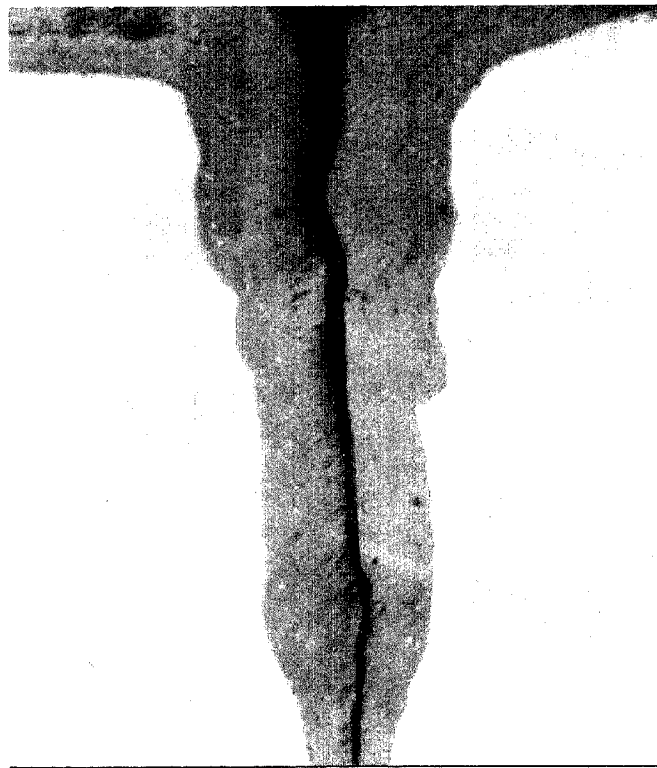


(c) 1525 cycles, fully polished 133X

See next page for caption

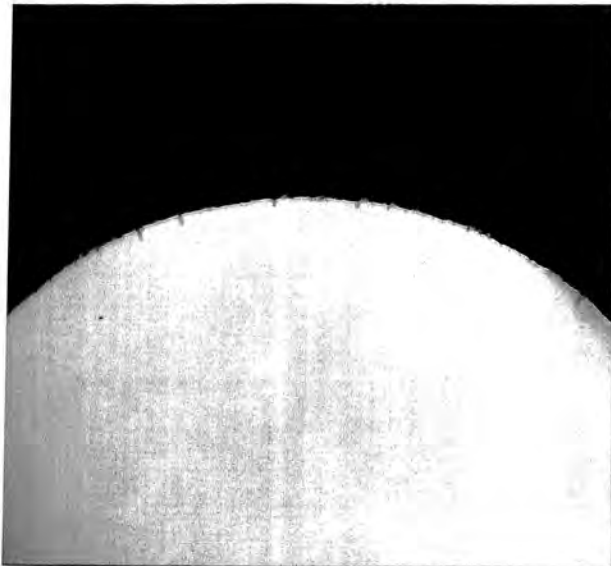


(d) 1725 cycles 266X

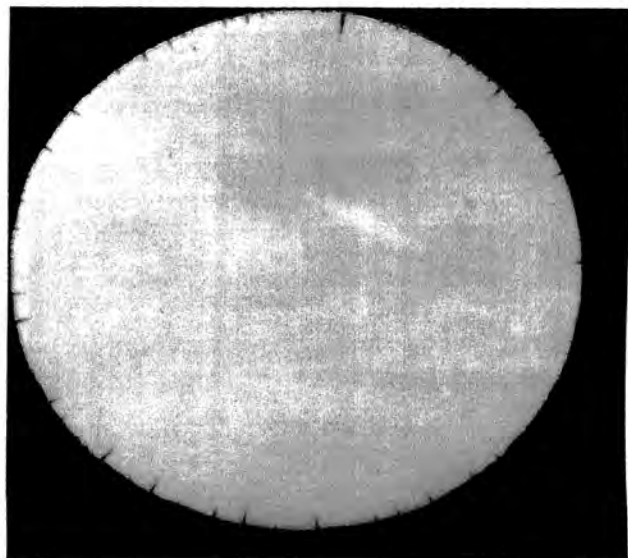


(e) 2100 cycles 266X

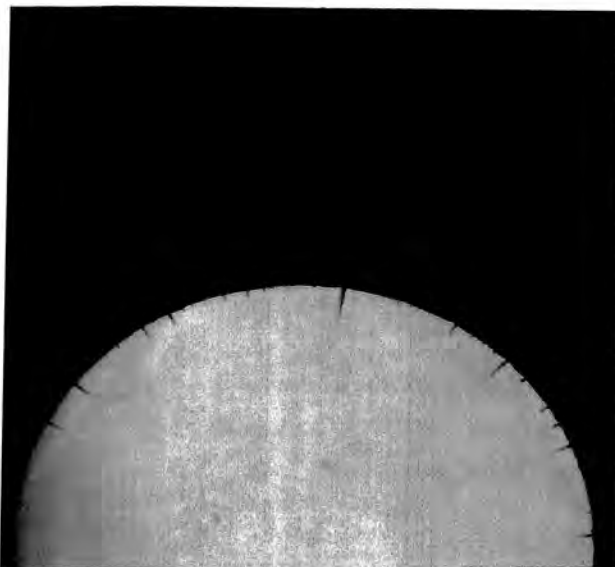
g. 36 (a)-(c) Crack-like streaks are formed in oxide film during early stages of cycling in H-21 but disappear on polishing; (d) shows the actual crack formed in the metal which propagates on further cycling as in (e).



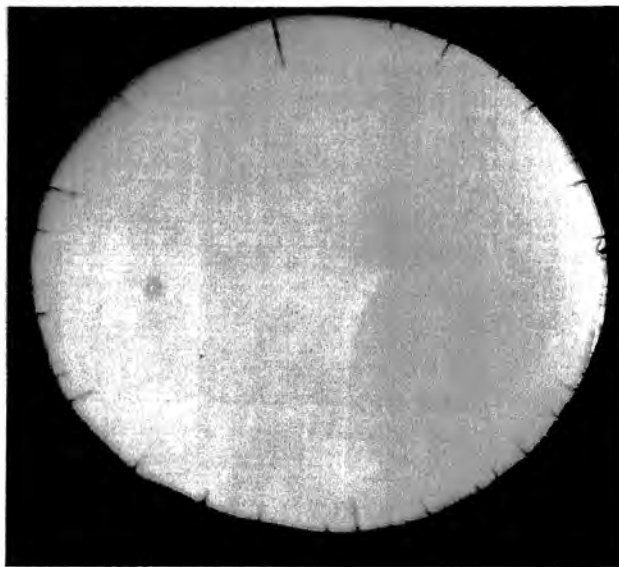
(a) 2100 cycles 7X



(b) 3000 cycles 5X



(c) 3400 cycles 5X



(d) 4200 cycles 5X

Fig. 37-Propagation of thermal fatigue cracks in H-21. Cracks are sharp tipped and their width near the edge is smaller than in H-11 and H-13.

cracks are formed up to 3000 cycles and then these cracks propagate radially inwards and also open up in width near specimen edge. A comparison of these photographs with those of H-11 and H-13 steels (Figs. 29, 33) clearly indicates that cracks are comparatively narrower in this steel.

The rate of propagation of the longest crack has been plotted in Fig. 38. Immediately after appearance of the first crack, at 1600 cycles, more cracks appear and also existing cracks propagate up to about 2400 cycles (see also Table IX). After 2400 cycles, not many new cracks are created but all the previously created cracks propagate in a linear manner. Because of both crack creation and propagation between 1600-2600 cycles, the curve shows a slightly smaller slope than the later linear region after 2600 cycles. The crack propagation rate in the linear region is about 0.000450mm per cycle.

Fig. 39 shows the graph between cumulative number of cracks and crack lengths at different stages of cycling. The graph clearly points out that all the cracks at different stages of cycling behave in an identical manner and that the crack lengths increase continuously with further cycling.

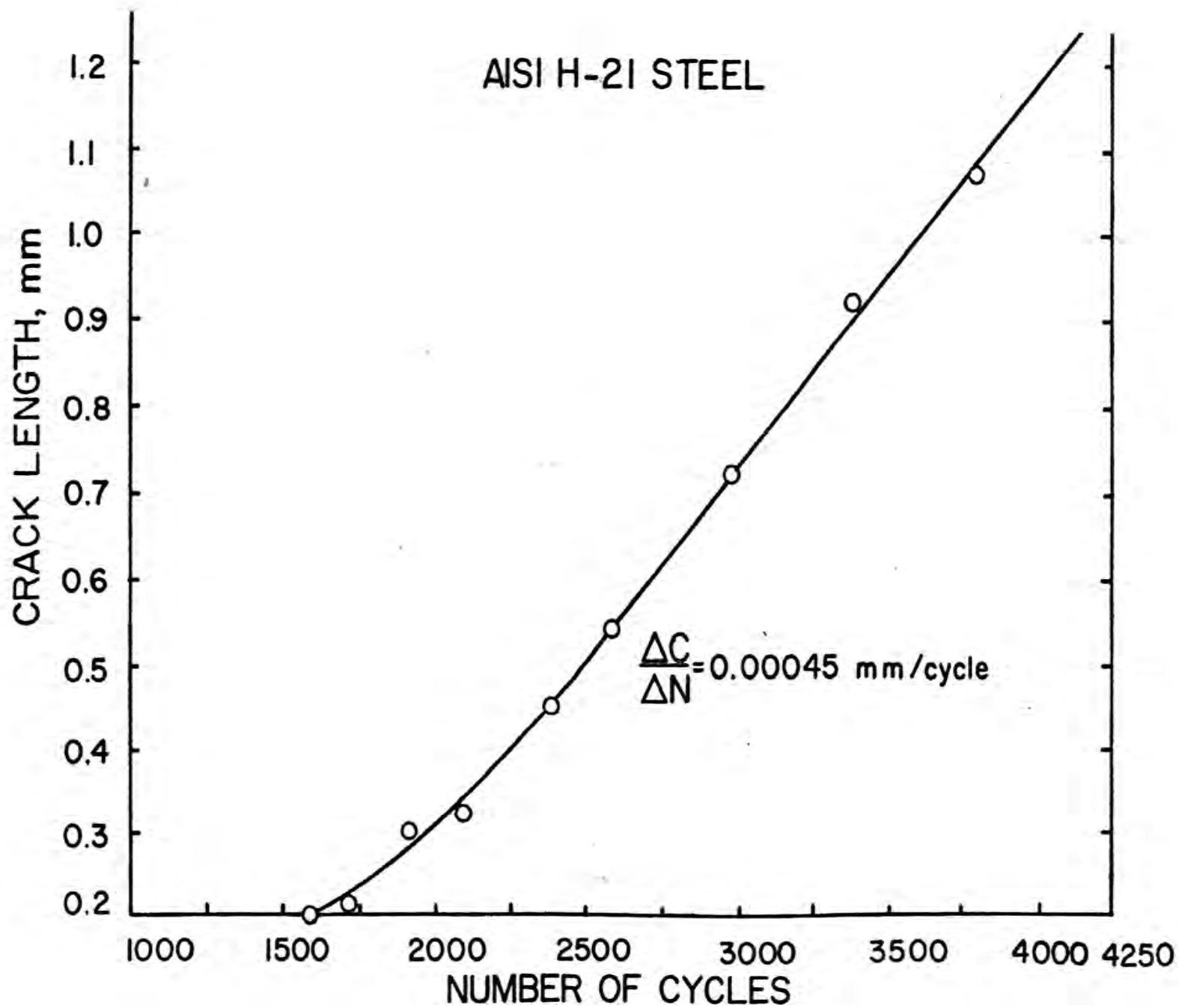
Maraging Steel

Heat Treatment

Aged at 900°F for 3 hours

5. 38-Propagation of the longest crack with thermal cycling in AISI H-21 steel

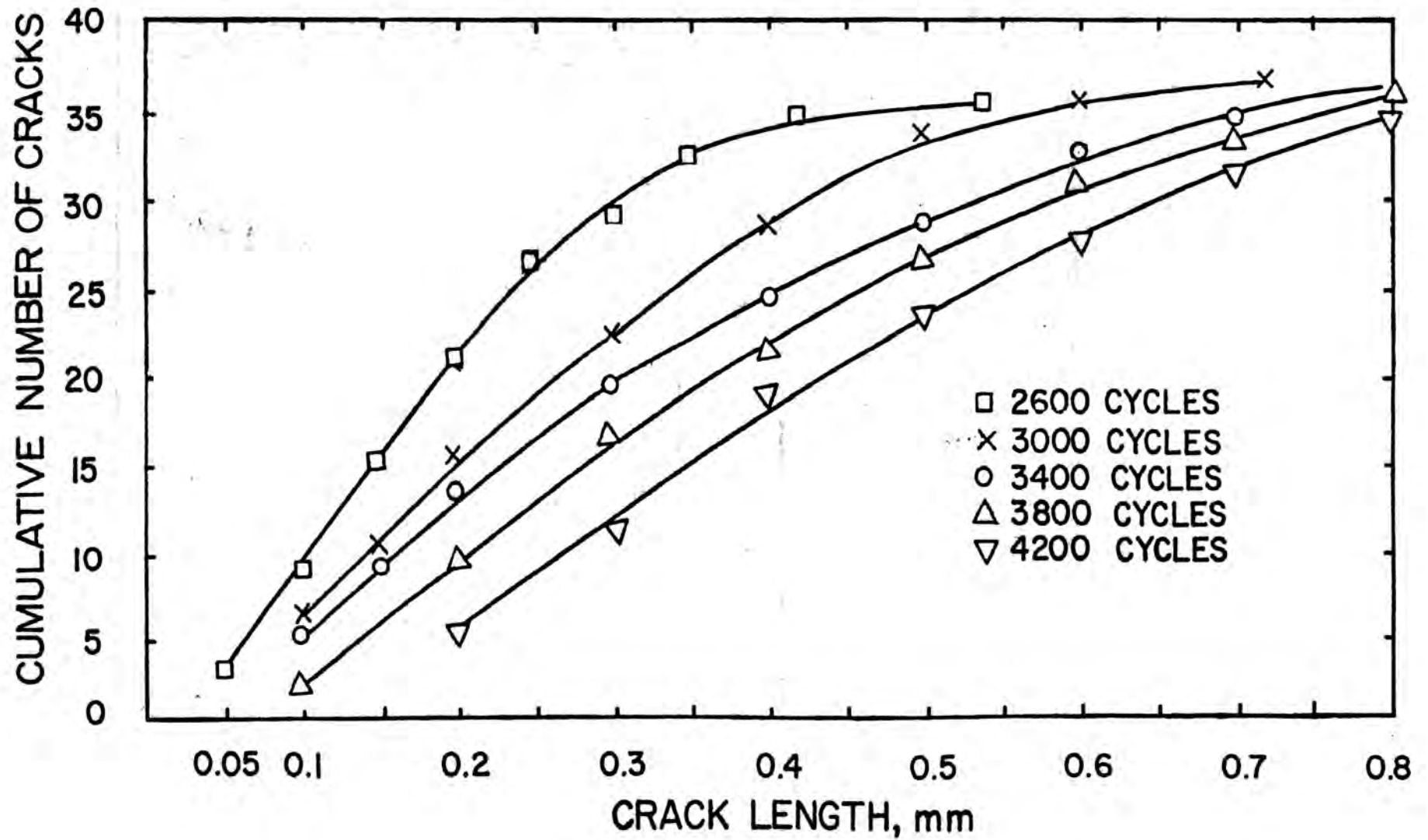
FIGURE 38



s. 39-Cumulative number of cracks versus crack length
at different stages of thermal cycling in AISI H-21
steel

FIGURE 27

AISI H-21 STEEL



Hardness

Hardness of the samples as received (Annealed at 1500°F at the mill) - Rc 34

Hardness after aging - Rc 53

Thermal Cycling

Heating time per cycle - 2.9 seconds

Cooling time per cycle - 17.4 seconds

Results

Number of cycles for crack initiation - 2000

TABLE X

CRACK PROPAGATION WITH THERMAL CYCLING IN MARAGING STEEL

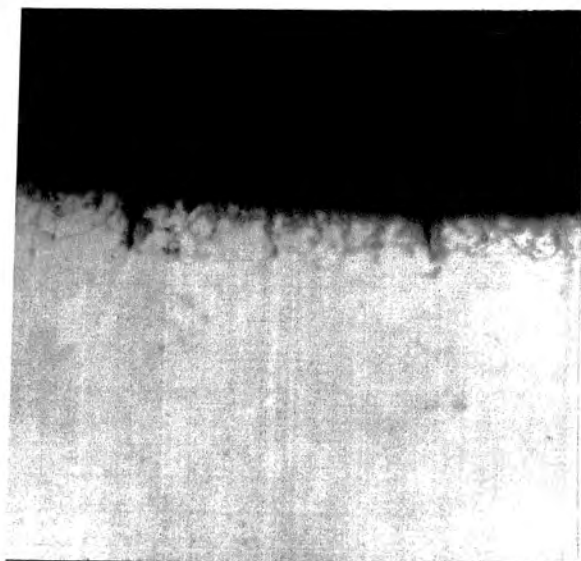
Number of cycles	Crack length, mm	Number of Cycles	Crack length, mm
2000	.02(3), .018, .015, .01(6)	3400	.40, .37(2), .28, .27, .24, .22, .21, .19, .18(3), .16(2)
2200	.03(2), .025, .02(2), .015(5), .0125(2), .01(5)		.155, .12(2), .11, .10, .09, .07(2), .055, .05, .04
2620	.10(2), .08, .064, .055(2), .04, .03(4), .025(3), .02(2), .015, .014, .012, .01(5), .005	3800	.62, .61, .60, .57, .47, .41, .40, .38(2), .31(2), .29, .28, .26, .22, .18, .17, .16, .14, .11, .08, .07(3), .06
3000	.24, .22, .195, .19, .16, .13, .125, .12, .11, .10, .09, .08, .06(4), .055, .05(2), .04, .03, .02, .017, .015, .01	4200	.80(2), .76, .63, .61, .59, .57, .55, .52, .48, .47, .43, .40, .37, .35, .27, .25, .21, .20(2), .19, .17, .16, .10(2)

Discussion of Results

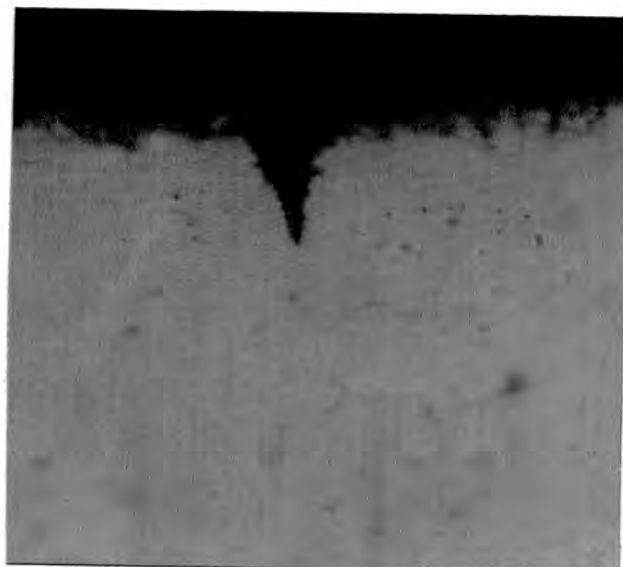
A thin, tight and adherent oxide scale is formed on surface of the test-piece during initial stages of cycling. The oxide scale formed is much less than in case of the other die steels tested earlier in present series of experiments. This steel was found to be most resistant to the crack initiation and the first cracks were observed only at 2000 cycles. Very fine microcracks were initially formed at 2000 cycles which were visible under 500X magnification (Fig. 40a). These microcracks propagate radially inwards with further cycling as can be seen in Figs. 40b-c.

A macroview of the crack propagation is illustrative in Figs. 41a to d. A comparison of these macrocracks in H-11, H-13 and H-21 steels, for the same number of cycles, clearly indicates that the cracks in maraging steel are much finer and they do not open up much at the specimen edge. Also, the frequency of occurrence of cracks is comparable to that of H-13 and is much lower than in H-11 and H-21 steels.

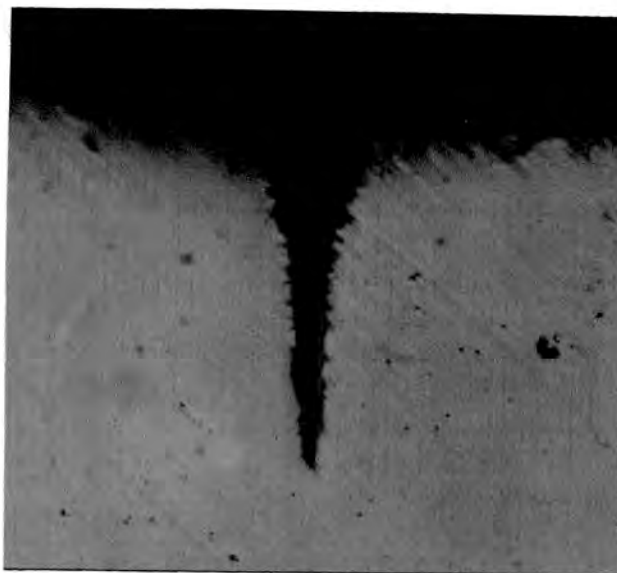
The propagation of the longest crack with higher number of cycles follows a trend very similar to that observed in the other steels tested earlier. The crack propagation rate in the linear region was observed to be 0.00047mm per cycle (Fig. 42). The maximum length of the longest crack after 4200 cycles was observed to be the lowest among all the



(a) 2000 cycles 520X

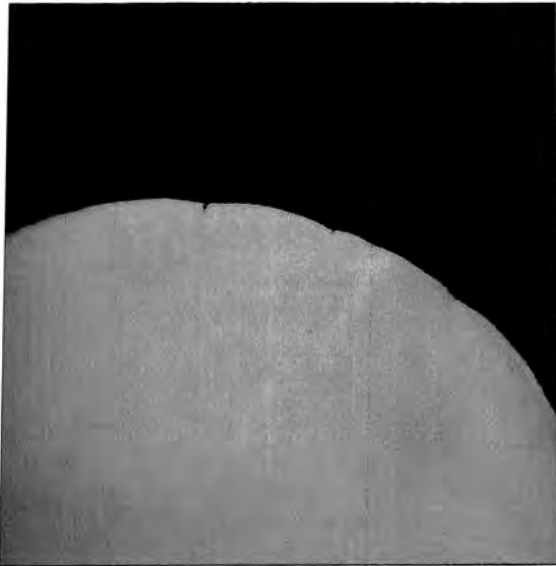


(b) 2200 cycles 520X

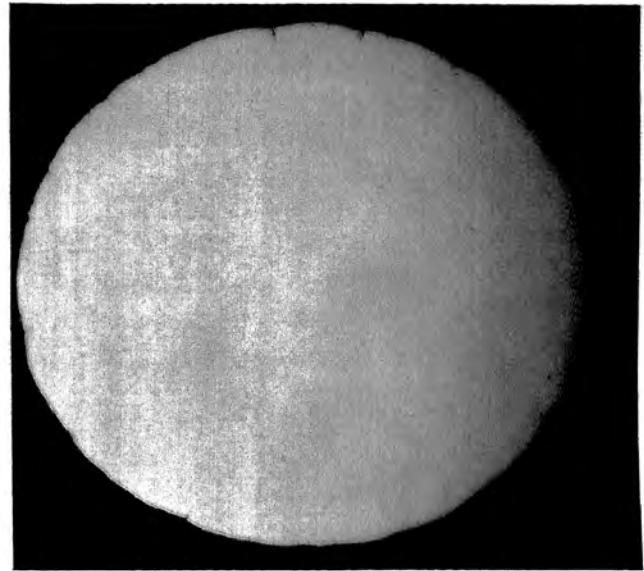


(c) 2620 cycles 400X

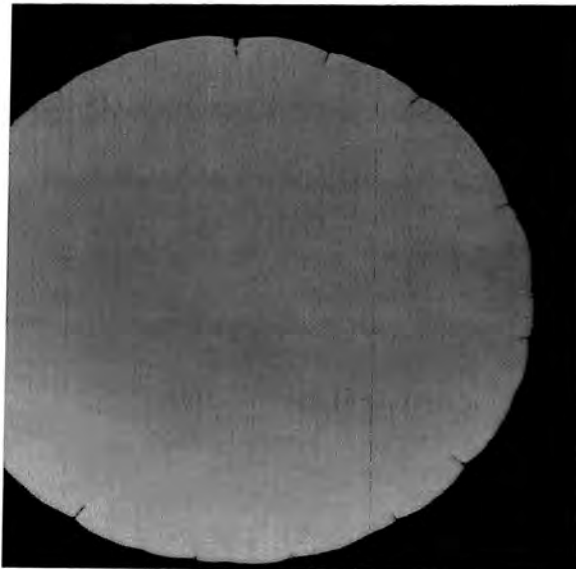
Fig. 40-(a) Initiation of microcracks near the specimen edge; (b)-(c) propagation of the same microcrack with further thermal cycling in 18% nickel maraging steel



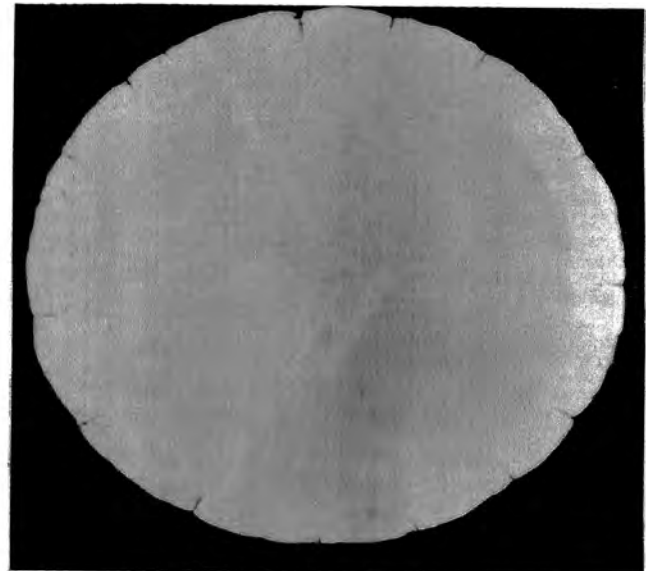
(a) 3000 cycles 7X



(b) 3400 cycles 5X



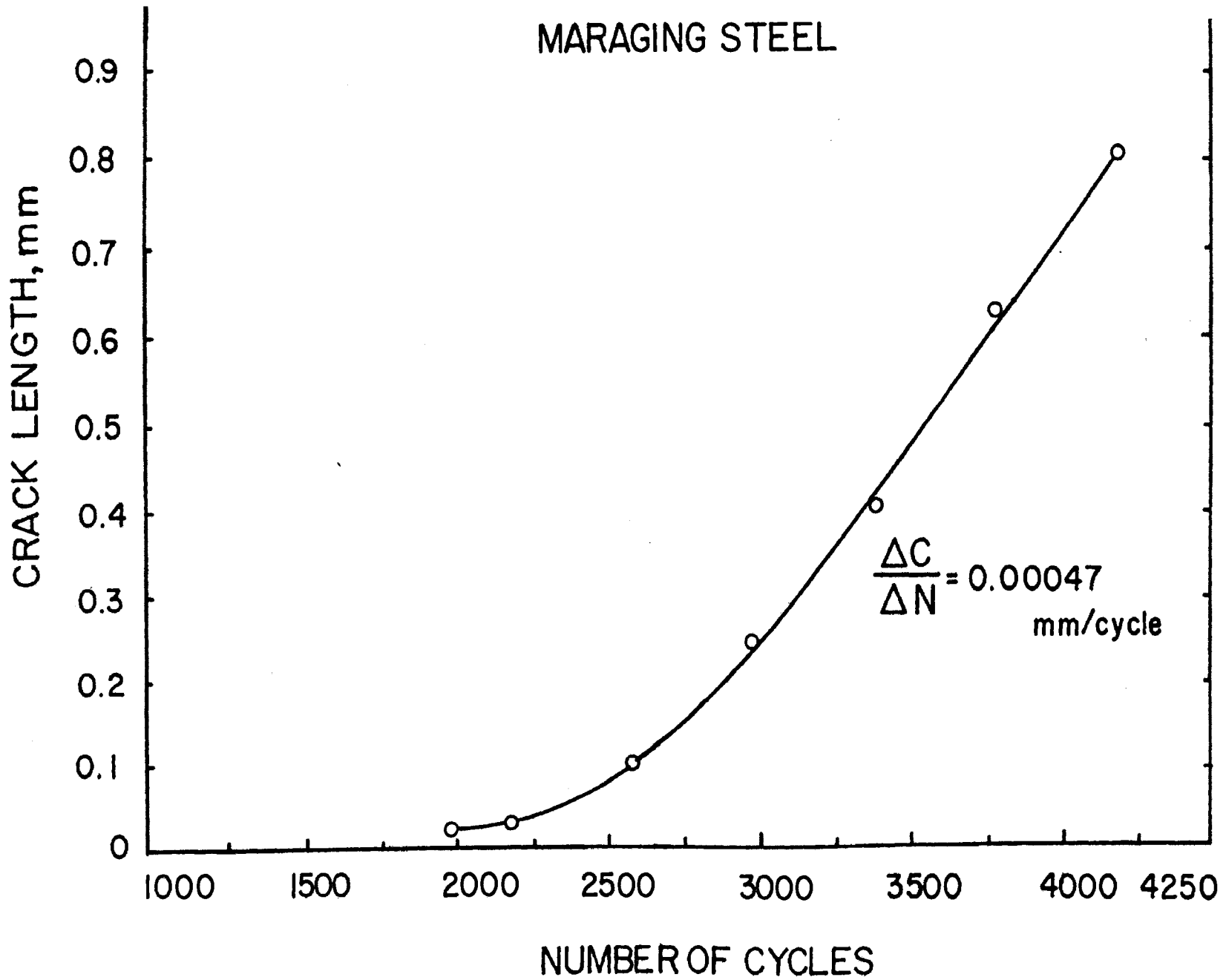
(c) 3800 cycles 5X



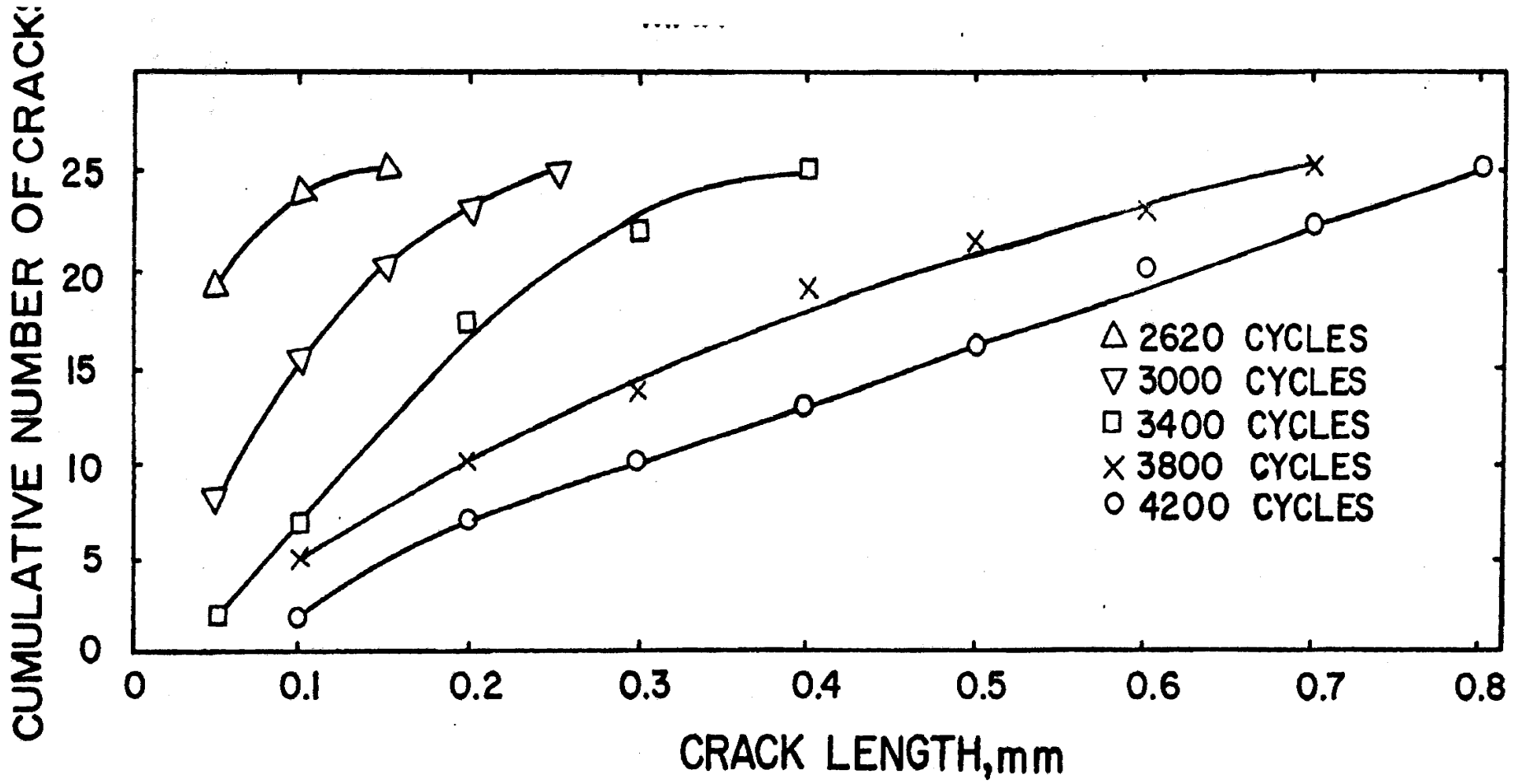
(d) 4200 cycles 5X

Fig. 41-Propagation of macrocracks with thermal cycling in maraging steel. Cracks are very narrow and straight and their width near the edge is the smallest among all the steels tested in the present investigation.

42-Propagation of the longest crack with thermal cycling in 18% nickel maraging steel



43-Cumulative number of cracks versus crack length
at different stages of thermal cycling in 18%
nickel maraging steel

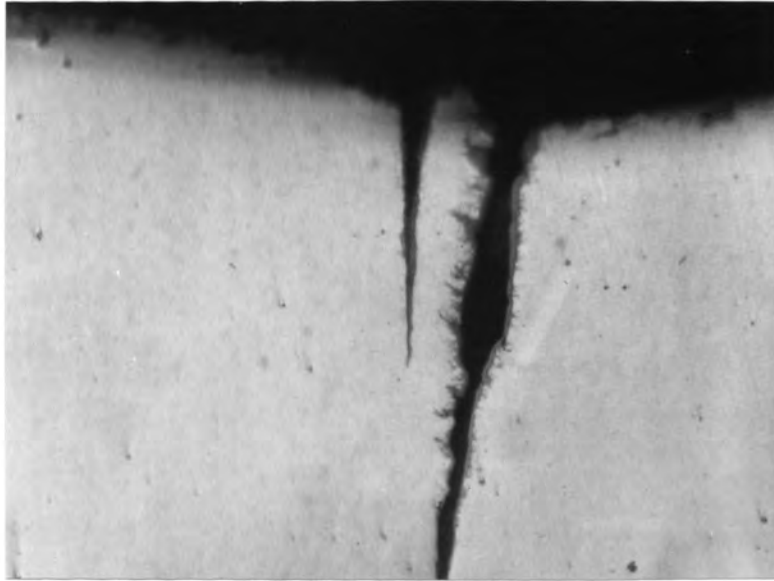


steels tested earlier. The propagation behavior of all the cracks observed can be seen in Fig. 43. All the cracks seem to behave in an identical manner and the crack lengths continuously increase with higher number of cycles.

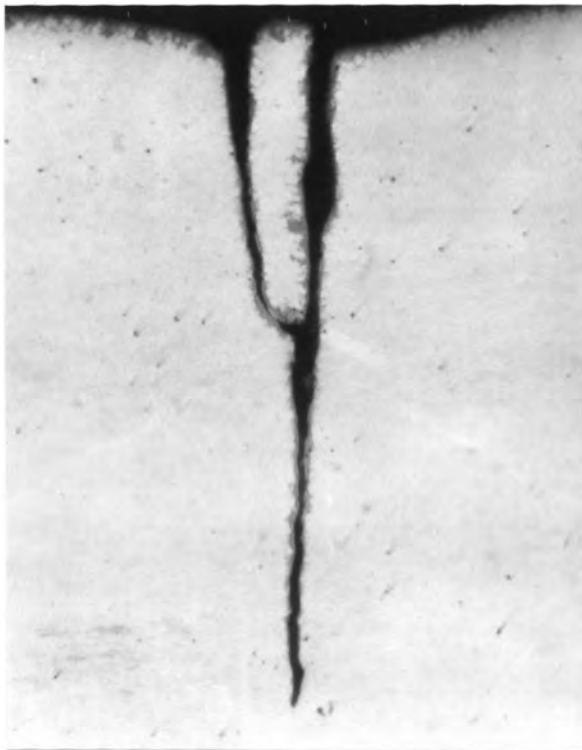
All the results clearly point out to the fact that for an equivalent hardness, the maraging steels are tougher than the conventional die steels. They showed a better resistance to gross cracking created due to thermal fatigue failure.

G. Some General Features of Cracks Observed

In all the steels tested, it was observed that cracking invariably started at the edges of the circular specimen or at some inclusions away from the edge. The sharp edge of the specimen and the surface inclusions act as points of stress concentration, thereby leading to an earlier cracking. At certain locations, where two or more cracks were initiated close by, further cycling caused the propagation and joining of the adjacent cracks. A sequence of two such adjacent cracks and their propagation in maraging steel is well depicted in Figs. 44a-c. Joining of such multiple cracks leads to the network of cracks frequently observed in die casting dies (Fig. 4a). Fig. 44c shows a complete collapse of a chunk of die steel, leading to the formation of a large pit at the edge which is in close contrast to such a phenomenon observed in actual dies (shown in Fig. 4c).



(a) 3000 cycles 266X



(b) 3400 cycles 195X



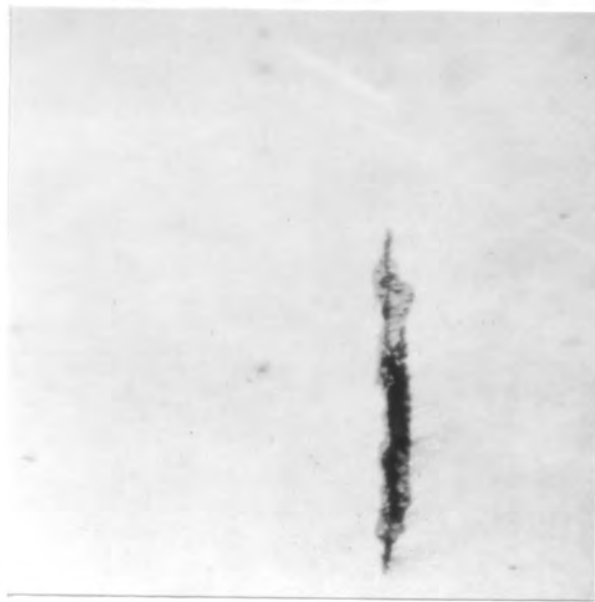
(c) 3800 cycles 133X

Fig. 44-Two adjacent cracks propagate simultaneously and finally join together on further cycling, causing the small chunk of metal to drop off and form a pit or heat check in maraging steel.

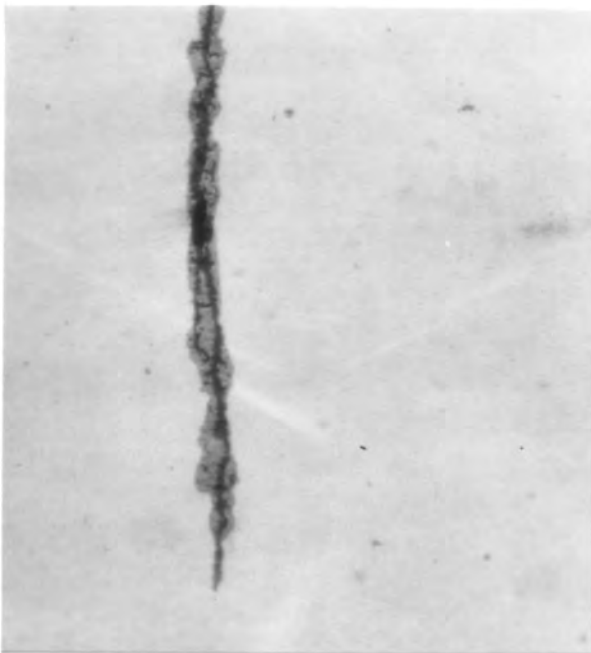
Initiation of a crack at an inclusion away from the edge of specimen is shown in Fig. 45a. On further cycling this crack propagated on both sides (Fig. 45b). Fig. 45c shows the joining of a crack propagating from the edge with another crack which originally started from an inclusion away from the edge. A sequence of the initiation and propagation of these two cracks was studied by the author and the two were found to have joined at the point A shown in the photograph.

All the thermal fatigue cracks observed propagated radially inwards and also axially downwards. Fig. 46a shows a crack on the top surface after 4200 cycles in H-21 steel. Figs. 46b and c show the same crack at a depth of 0.014 and 0.050 inch respectively at the same magnification. All the features in the appearance of the crack at the different depth levels appear to be similar except that the crack is more opened up at the top surface than at larger depths below the surface.

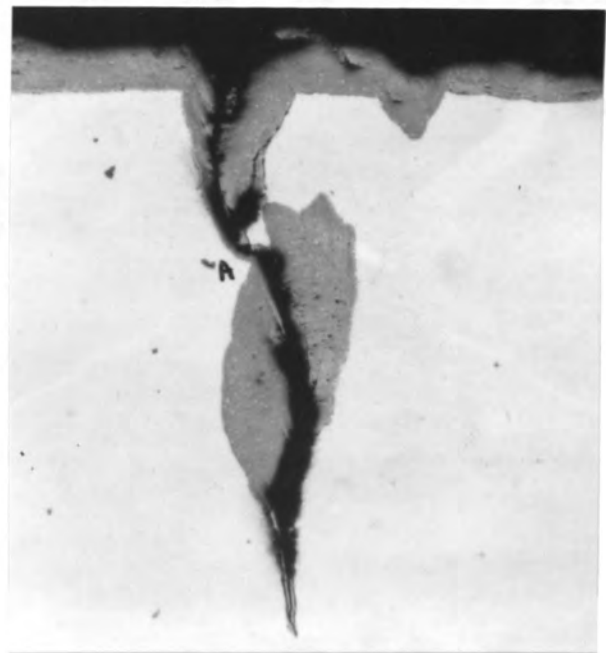
An investigation of microstructures of the different steels was carried out to understand the nature of cracking. It was found that in all the steels tested, the cracks were straight, oxide lined and transcrystalline. Fig. 47a shows a heavily oxide lined crack in H-21 steel at the top surface after 4200 cycles while Fig. 47b shows a crack 0.050 inch below the surface. The subsurface portion of the crack has comparatively less oxide lining. A similar trend



(a) 3000 cycles, 266X



(b) 4200 cycles 266X

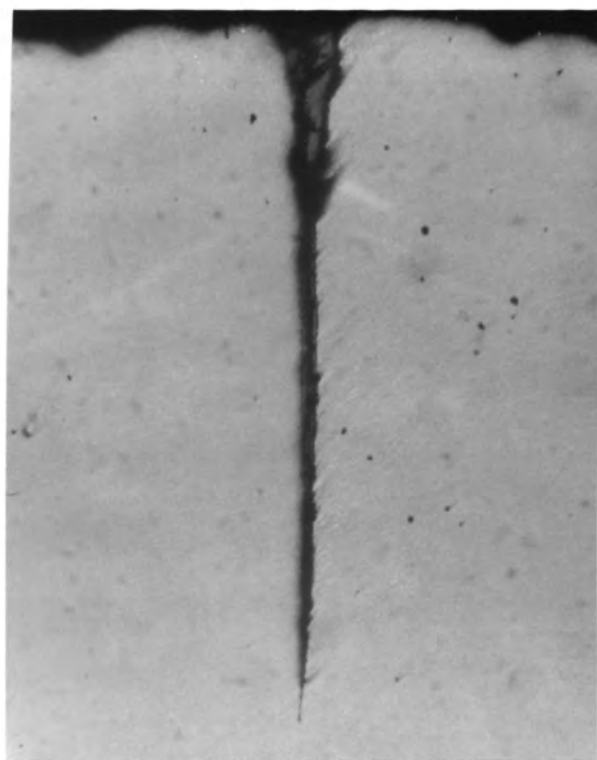


(c) 2200 cycles 133X

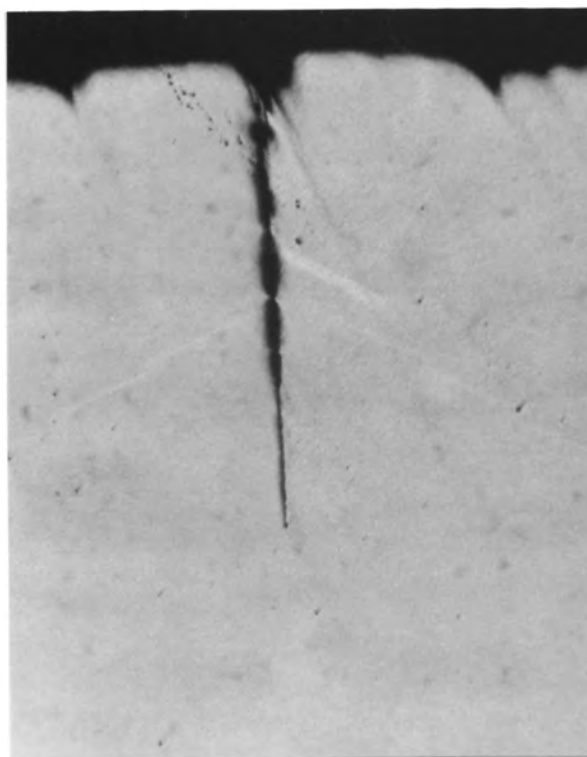
Fig. 45 (a)-(b) Initiation of a crack at an inclusion or an impurity, away from the specimen edge and its propagation in both directions in H-13; (c) a crack started at an inclusion away from the specimen edge and on further cycling it joined with a crack (initiated at the edge) at the point A.



(a) 4200 cycles,
top surface

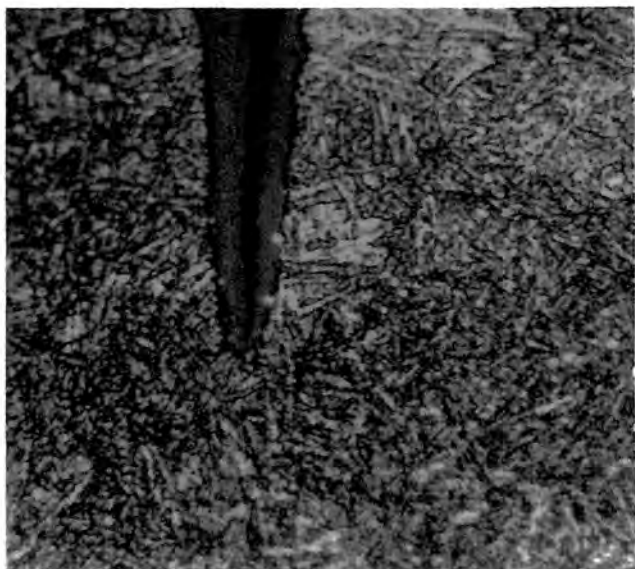


(b) 4200 cycles, 0.014 inch
below the surface

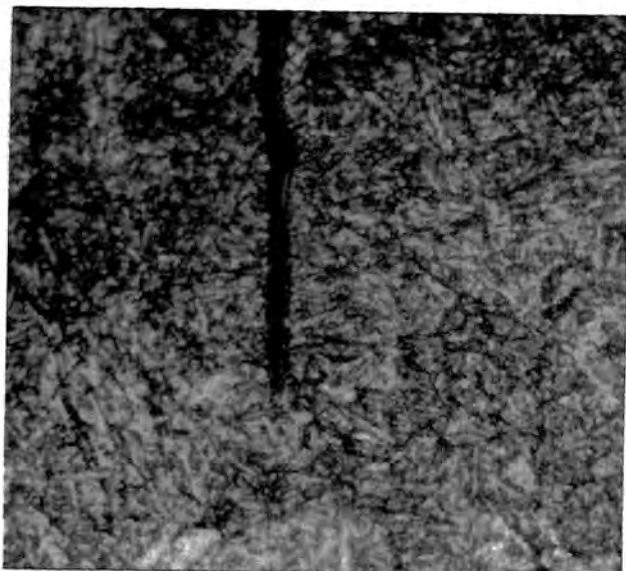


(c) 4200 cycles, 0.050 inch below the surface

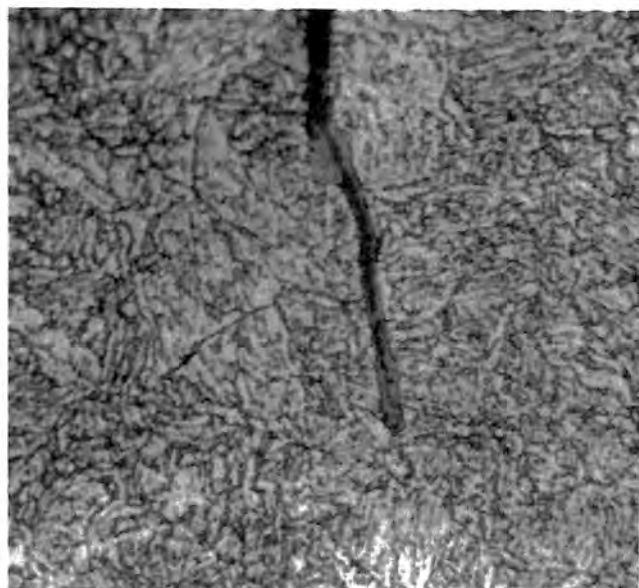
Fig. 46-Appearance of a thermal fatigue crack at
different depths from the top surface in H-21



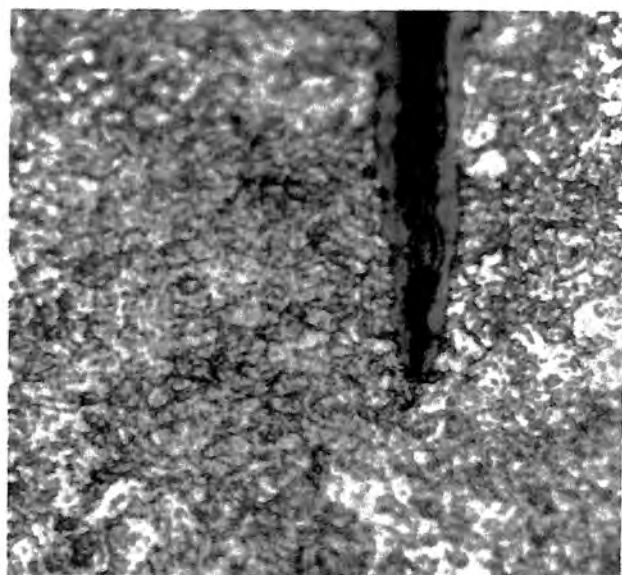
(a) H-21, 4200 cycles, top surface, Etch. Picral 800X



(b) H-21, 4200 cycles, 0.05 inch below the surface, Etch. Picral 800X



(c) H-11, 4200 cycles, Etch. Picral 800X



(d) H-13, 4200 cycles Etch. Picral 800X

Fig. 47-Microstructures of die steels after thermal cycling. The fatigue cracks in all the steels are oxide filled and transcrystalline in nature.

was observed in H-11, H-13 and Maraging steels (Figs. 47c-d). The appearance of microstructures and cracks is in quite close agreement with Fig. 9 shown in the literature review section.

The appearance of oxide filled crack in Fig. 47a appears to indicate that these cracks have ceased to propagate, or are propagating very slowly. During the test the more pronounced cracks can be seen to close in the heating stage of the cycle, and open on cooling, and it is clear that the oxide can not fill these cracks completely. Progressive oxidation of the walls of the cracks must occur, and this oxide will tend to give a wedge action on heating.

V. CONCLUSIONS

. It has proved feasible to develop a testing technique whereby the thermal conditions experienced by die steels in aluminum die casting dies can be simulated very closely in a time cycle comparable to the actual production time. The use of the cyclic thermal fatigue setup to alternately heat and cool, in a controlled manner, a surface area which is small in comparison to the mass of the test specimen, materials have been tested for their tendency to heat check.

. The induction heating technique adopted is very simple, comprehensive and efficient as compared to other heating methods and the whole equipment setup is very inexpensive. Because of the very short time-cycles used, it is possible to evaluate a large number of materials in a relatively short period of time.

. Ladish D-11 steel samples were found to have very low oxidation and thermal fatigue resistance for the hardness and temperature range normally used in aluminum die casting dies. The crack initiation in samples of hardness Rc 48 started at 125 cycles while the rate of crack propagation and severity of cracking was found to be the highest among all the steels tested in the present study.

. The method of heating a small portion of the specimen by a gas flame and water quenching to check thermal

igue resistance, as developed by Ladish Company (and also
ig used by some other steel industries in U.S.A.), does
seem to follow the actual physical conditions encountered
lie steel dies in aluminum die casting industry. Water
nching can cause quench cracks and it can lead to erroneous
rmaal fatigue resistance results. This is probably the
n reason for the discrepancy in the results reported
Ladish Steel Company⁽¹³⁾ and the author's present investi-
ions.

a. For the same level of initial hardness of Rc 50,
it took maximum number of cycles to initiate thermal
fatigue cracks in maraging steel, followed by H-21,
H-13 and H-11 respectively in the decreasing order as
shown in the bar chart in Fig. 48.

b. The frequency of crack occurrence at the maximum
number of cycles run in the present series of tests
was the highest in H-11. H-21 showed smaller number
of cracks than H-11 while H-13 and maraging steel
showed comparable number of cracks which were less
than in H-11 and H-21.

c. The length of the longest crack after maximum
number of cycles run in the present series of tests
was minimum in maraging steel, followed by H-13, H-11
and H-21 respectively.

d. The rate of crack length propagation per cycle

Fig. 48-Bar chart showing the comparison of the number of cycles at the initiation of thermal fatigue cracking in different steels tested in the present investigation

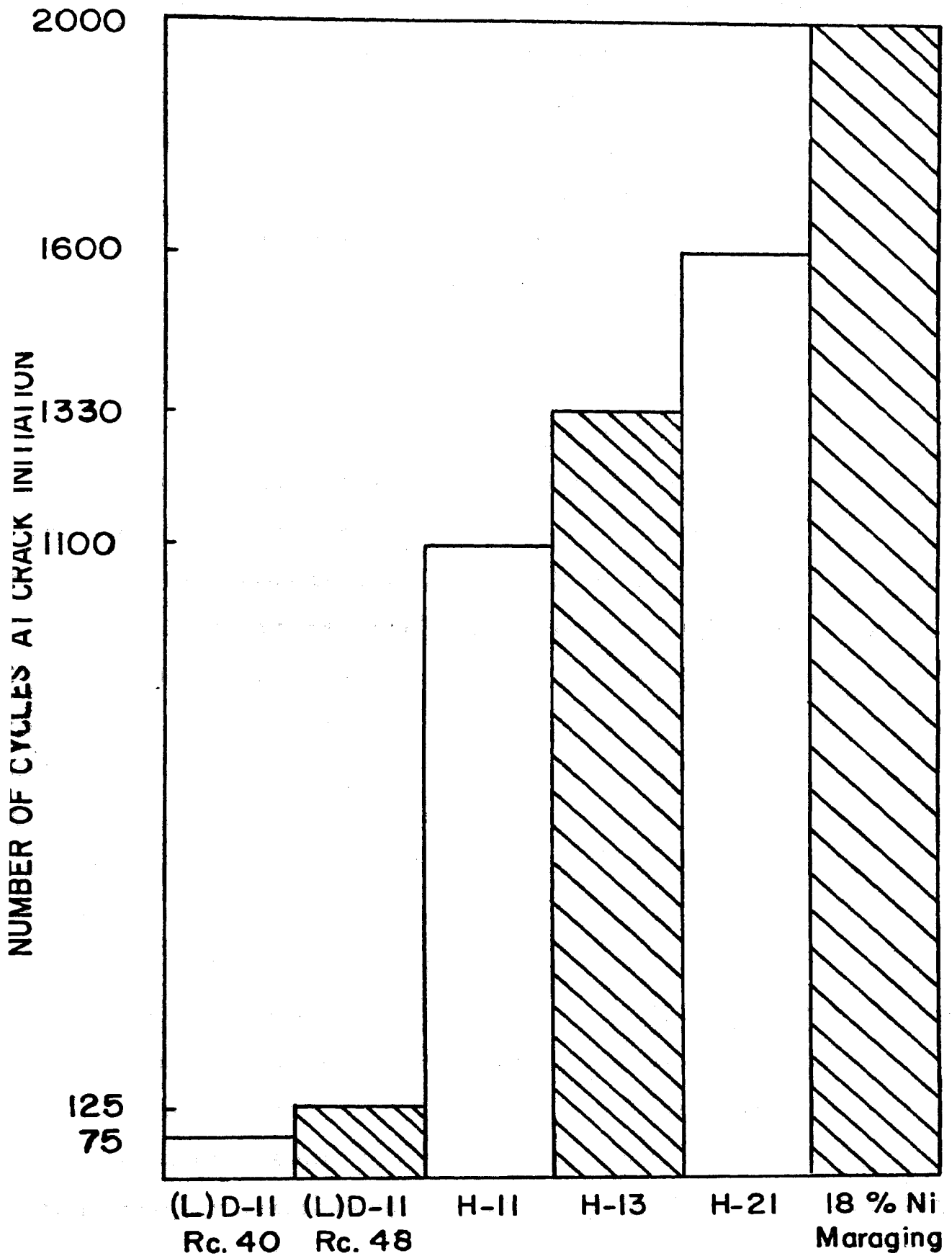


FIGURE 48

is comparable in H-11 and H-13 while it is slightly higher in H-21 and 18% nickel maraging steel. A comparatively thicker oxide coating is formed in H-21 which has to be removed before measuring the crack length. If the oxide coating is not removed, it acts as a protective coating. H-21 will therefore give better service than H-11 or H-13 as crack initiation in the former case starts at appreciably larger number of cycles.

Although rate of crack propagation is slightly higher in maraging steel, crack width is the least in it as compared to all other steels tested which is evident from the series of photographs presented earlier.

From 5a-d, it is concluded that 18% nickel maraging steel can give the best service for aluminum die casting dies, followed by H-21, H-13 and H-11 respectively in that order. The suitability of maraging steel for aluminum die casting is supplemented by the results of its use in some of the industries in the U.S.A. (19) In private communication with the author, Ladish Company indicated failure of 18% nickel maraging steel (in their thermal fatigue testing machine using water quench) earlier than H-11 or H-13. But it is the author's conclusion (on the basis of the present experimental techniques) that 18% nickel maraging steel shows the best combination of thermal fatigue properties needed for aluminum die casting temperature

range.

The results of the above four steels indicate that steels with better physical and mechanical properties at elevated temperatures show higher resistance to thermal fatigue.

6. Experimental investigations on samples of (L) D-11 of hardness Rc 48 and Rc 40 revealed that the crack initiation started earlier and the rate of crack propagation was higher in samples of lower hardness values. The general behavior of crack initiation and propagation was quite similar. It can thus be concluded that in general, the lower initial hardness gives lower thermal fatigue resistance.

7. The thermal fatigue cracks initiate at the points of maximum stress concentration caused by alternate heating and cooling cycles and at any inclusion present on the specimen surface. The cracks propagate radially inwards and axially downwards in the cylindrical test specimen with increasing number of cycles. During the initial stages of cycling, new cracks are initiated at more and more places while the prior existing cracks continue to propagate. But after a certain number of cycles, depending on the characteristic properties of the steel under investigation, crack initiation becomes negligibly small while the crack propagation proceeds almost linearly at a higher rate. Also, branching and intersection of cracks occur, leading to formation of heat checks and pits. A still further cycling

of the steel would lead to a catastrophic failure.

Almost all the cracks look straight, having a sharp tip and slightly larger width near the specimen edge. The walls of the cracks are oxide lined because of the tests being carried out in air. Progressive oxidation of the walls of the cracks occurs with further cycling and the oxide tends to give a wedge action on heating and causes further propagation.

Microstructural study of all the steels tested revealed that the thermal fatigue cracks were transcrystalline in nature as evidenced by the photographs presented earlier.

The appearance of thermal fatigue cracks and their mechanism of propagation seem to have confirmed the work of some earlier authors in this field. (4,8,9,13,18,19)

8. The series of photographs presented in the present work act as a clear evidence of behavior of various steels when subjected to different stages of thermal cycling. The photomicrographs show the mechanism of thermal fatigue crack initiation and propagation of individual cracks. The photomacrographs indicate a general trend of cracking which acts as a better guide for comparison of thermal fatigue resistance of steels under investigation for all practical purposes.

VI. SUGGESTED FURTHER RESEARCH

The presently developed technique for evaluating thermal fatigue of die steels for aluminum die casting can be used very effectively for testing other materials of interest.

It is suggested that the potential die materials for zinc, magnesium, brass and the presently being talked about ferrous die casting be studied essentially on the similar lines as in the present study. Also, thermal fatigue testing of stainless steels and other widely used materials under temperature conditions different from those used in the present investigation, is another possible area of further research.

Present induction heating technique will also prove very helpful for investigating the thermal fatigue failure of materials under controlled atmospheres and under different cooling media.

VII. BIBLIOGRAPHY

1. Metals Handbook, A.S.M., 8th Edition, p. 39, (1961).
2. Smith, D.G., "A New Approach to an Old Problem - Die Erosion", Trans. S.D.C.E., Paper No. 25, p. 3, (1964).
3. Sharp, H.J., Metal Industry, Vol. 83, p. 121-123, (1953).
4. Williams, D.N., Kohn, M.L., Evans, R.M., and Jaffee, R.I., "Corrosion-Fatigue in Two Hot Work Die Steels", Trans. A.F.S., 68, (1960).
5. Noeson, Stanley J. and Williams, Hervey A., Trans S.D.C.E., Paper No. 801, p. 1, (1966).
6. Nicolson, A.H., "Recording Die Temperatures", Metal Industry (London), Vol. 66, No. 20, p. 306, May 18, 1945.
7. Mickel, E., "Die Stresses", Metal Industry (London), Vol. 66, No. 18, May 4, 1945, p. 276.
8. Roberts, G.A., and Grobe, A.H., "Service Failures of Aluminum Die Casting Dies", Metal Progress, Feb. 1956, p. 58.
9. Northcott, L., and Baron, H.G., "The Craze-Cracking of Metals", Journal of the Iron and Steel Institute, Dec. 1956, p. 402.
10. Coffin, L.F., Jr., Trans A.S.M.E., 76, p. 267 (1954).
11. Glenny, E., Northwood, J.E., Shaw, S.W.K., and Taylor, T.A., "A Technique for Thermal-Shock and Thermal-Fatigue Testing Based on the Use of Fluidized Beds", Journal of Institute of Metals, Vol. 8, p. 294, (1958-59).

12. Glenny, E., and Taylor, T.A., " A Study of the Thermal Fatigue Behavior of Metals", Journal of Institute of Metals, Vol. 8, p. 449, (1959-60).
13. Wollering, W.R., and Oertle, L.C., Trans. S.D.C.E., Paper No. 804, (1966).
14. Coffin, L.F., and Wesley, R.P., A.S.M.E., Paper No. 53-A-77.
15. Coffin, L.F., A.S.M.E., Paper No. 53-A-76.
16. Coffin, L.F., A.S.T.M., 1954, Preprint No. 100a.
17. Northcott, L., and Baron, H.G., Ibid., p. 385.
18. Metals Handbook, A.S.M., 1948, p. 674.
19. Hamaker, J.C., Jr., and Yates, D.H., "A Forward Look at the New Die Steels", Trans. S.D.C.E., Paper No. 1201, p. 3, (1966).
20. Furgusan, C.A., Personal Communication, Oct. 12, 1967, Ladish Company, Cudahy, Wisconsin.

VIII. VITA

Kulwant Singh Sabharwal was born on January 11, 1944, in Peshawar, India (now in West Pakistan). He received his primary and secondary education in New Delhi, India. He got his Bachelor of Technology (Honors) Degree in Metallurgical Engineering from Indian Institute of Technology, Kharagpur, India in January 1965. He worked as a metallurgical engineer in E.M.C. International, India from 11 August 1967.

He was selected as a Rotary Foundation Fellow and was sponsored by Rotary International to do graduate study at University of Missouri - Rolla in September, 1967. He has been enrolled in the graduate school of University of Missouri - Rolla since then.